EASA
European Aviation Safety Agency

Report EASA.2012.07

Research Project:

HELMGOP II
Helicopter Main Gearbox Loss of Oil Performance Optimisation

Appendix B

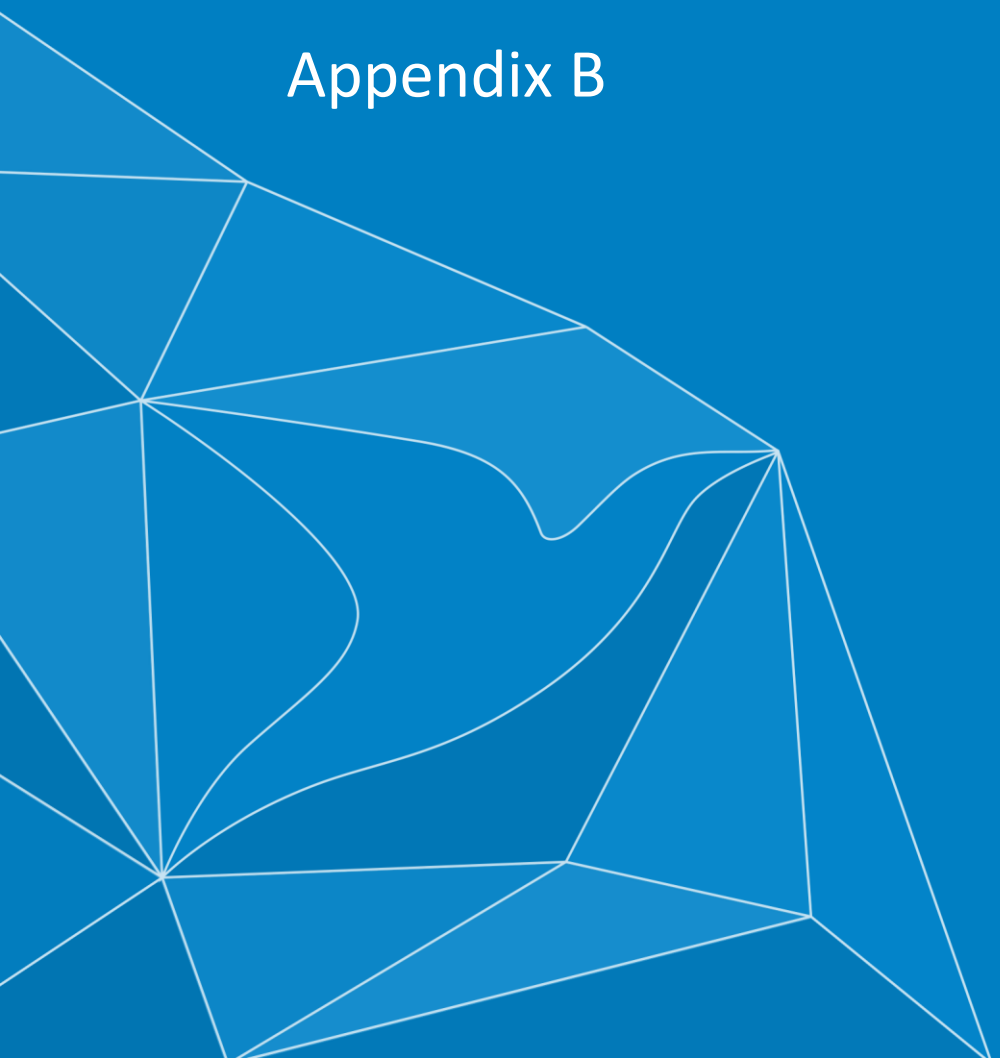

An agency of the European Union

Disclaimer

This study has been carried out for the European Aviation Safety Agency by an external organization and expresses the opinion of the organization undertaking the study. It is provided for information purposes only and the views expressed in the study have not been adopted, endorsed or in any way approved by the European Aviation Safety Agency. Consequently it should not be relied upon as a statement, as any form of warranty, representation, undertaking, contractual, or other commitment binding in law upon the European Aviation Safety Agency.

APPENDIX B – HELICOPTER MAIN GEARBOX TEST RIG DETAILS

B.1 Helicopter MGB System Description

The commercial helicopter gearbox used to investigate the performance of a mist lubrication system using commercially available thioether lubricant was a category “A” helicopter MGB as shown in Figures B.1 to B.4.

Figure B.1 Category “A” Helicopter MGB (Left) (Source: Author)

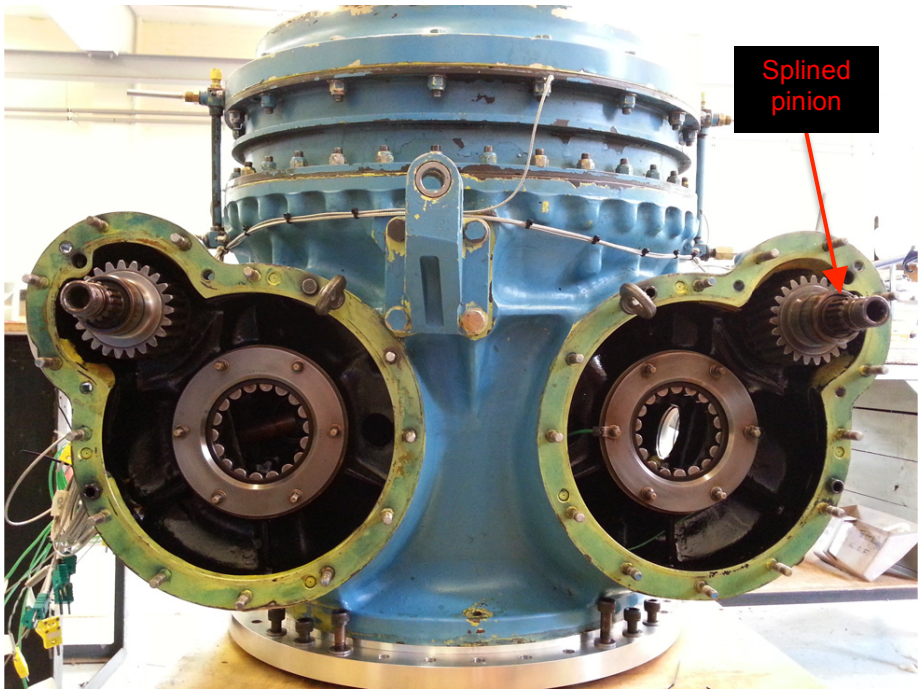

Figure B.2 Category “A” Helicopter MGB (Fwd) (Source: Author)

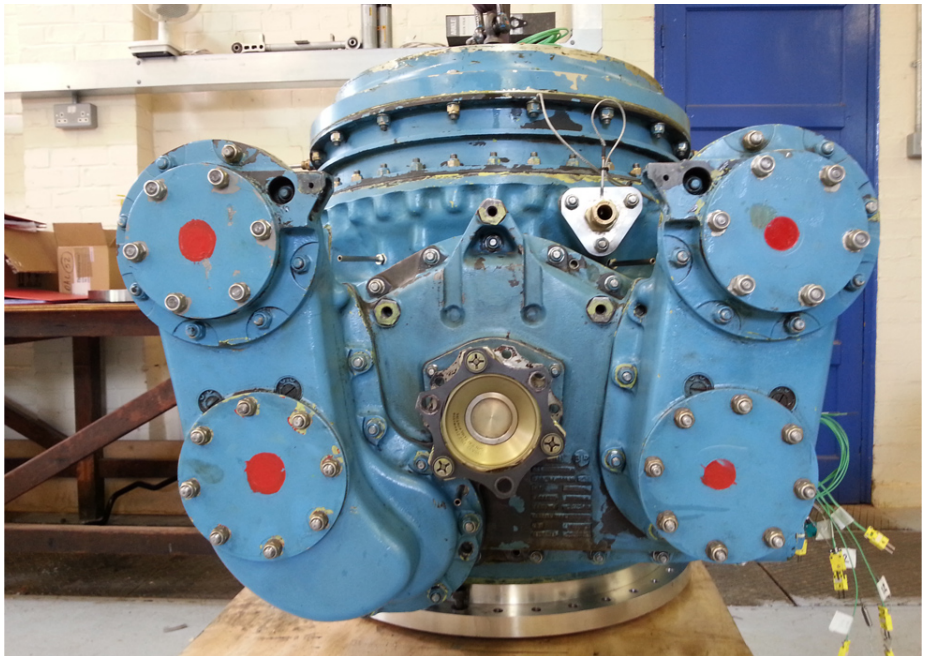

Figure B.3 Category “A” Helicopter MGB (Aft) (Source: Author)

Figure B.4 Category “A” Helicopter MGB Part Number (Source: Author)

According to the Category “A” Helicopter flight manual, the MGB is powered by two turboshaft engines and has a total input torque limit of 1560 Nm at maximum continuous power of 1300 kW (measured at the freewheel intermediate shafts). The design input and output drive speeds of the MGB are 22,841 RPM and 265 RPM respectively. The MGB is of modular design and comprises 5 reduction gear modules: LH and RH Fwd Reduction Gear Modules, Aft Reduction Gear Module, Main Reduction Gear Module and a 2-Stage Epicyclic Reduction Gear Module. The LH and RH Fwd Reduction Gear Modules (1:2.87 speed ratio) each has a splined pinion to mate with the high-speed drive shaft of the turboshaft engines (Figure B.2). The Aft Reduction Gear Module (1:1.63 speed ratio) is responsible for driving the tail rotor drive

train as well as the accessory drive systems such as the lubricating oil pump, hydraulic oil pumps and the electrical generators. It also houses the freewheel units that enable rotational movement only in the engine-to-rotor direction. Two freewheel intermediate shafts connect the Fwd Reduction Gear Modules to the Aft Reduction Gear Module. The Main Reduction Gear Module (1:2.05 speed ratio) incorporates a spiral bevel gear system to achieve a direction change in the driving torque. The 1st Stage (1:3.10 speed ratio) and the 2nd Stage (1:2.91 speed ratio) of the Epicyclic Reduction Gear Module utilises a 8-planetary gear and a 9-planetary gear system respectively to further step down the rotational speed to 265 RPM.

The lubrication oil system has a total capacity of 22 litres and operates using NATO O-155 type mineral oil. Lubrication of the MGB gears and bearings is achieved through nozzles positioned within the MGB casing to direct oil jets at the bearings and gear meshes (Figures B.5 to B.10). To lubricate the splined ends of each freewheel intermediate shaft, a nozzle assembly works in conjunction with the inner walls and drainage holes on the shaft to direct the lubrication oil (Figure B.11). An intricate series of internal oil galleries within the MGB casing serves to distribute the lubricating oil from the inlet port to all the oil nozzles. A gear-type positive displacement pump draws hot lubricating oil from the MGB sump and delivers it at 4.5 bars, 4000 LPH (67 LPM) to the external oil cooler assembly (heat exchanger) and subsequently to the oil filter assembly before supplying cooled oil to the MGB inlet port at 1.5 to 1.7 bars. The oil pump is mechanically driven by gears in the accessory drive at a speed of 2,733 RPM. At the external oil cooler, a fan driven by the MGB provides a continuous air circulation to extract heat from the hot lubricating oil. Figure B.12 illustrates the internal galleries of the MGB and a schematic of the lubrication oil system.

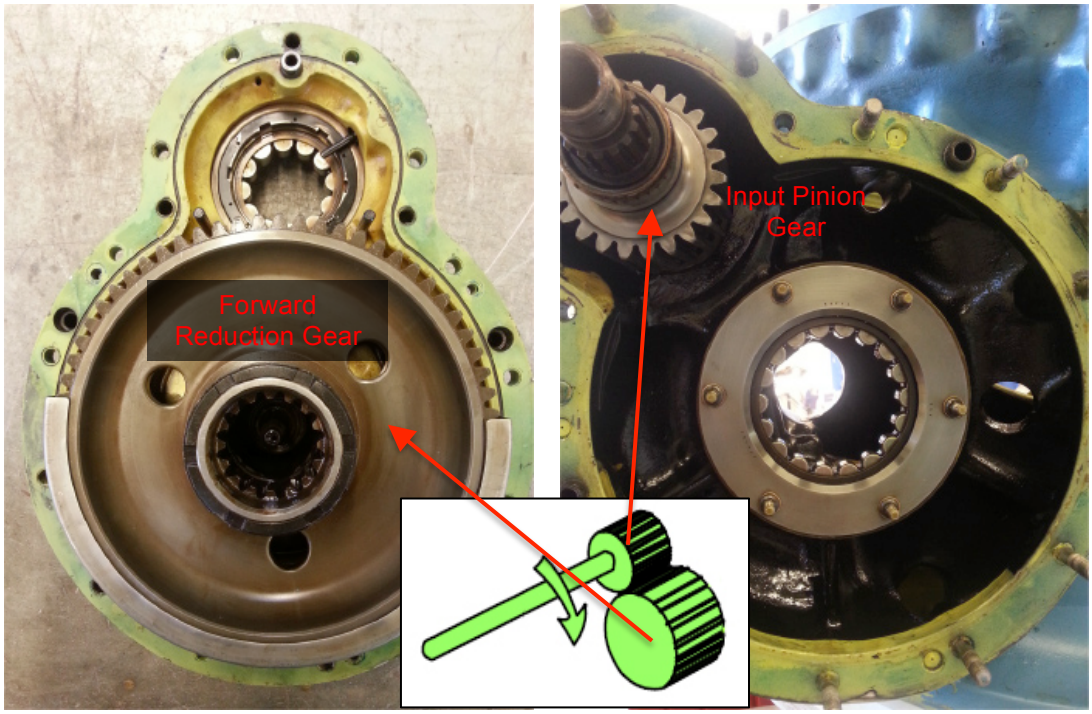

Figure B.5 Fwd Reduction Gear Module (Internal) (Source: Author)

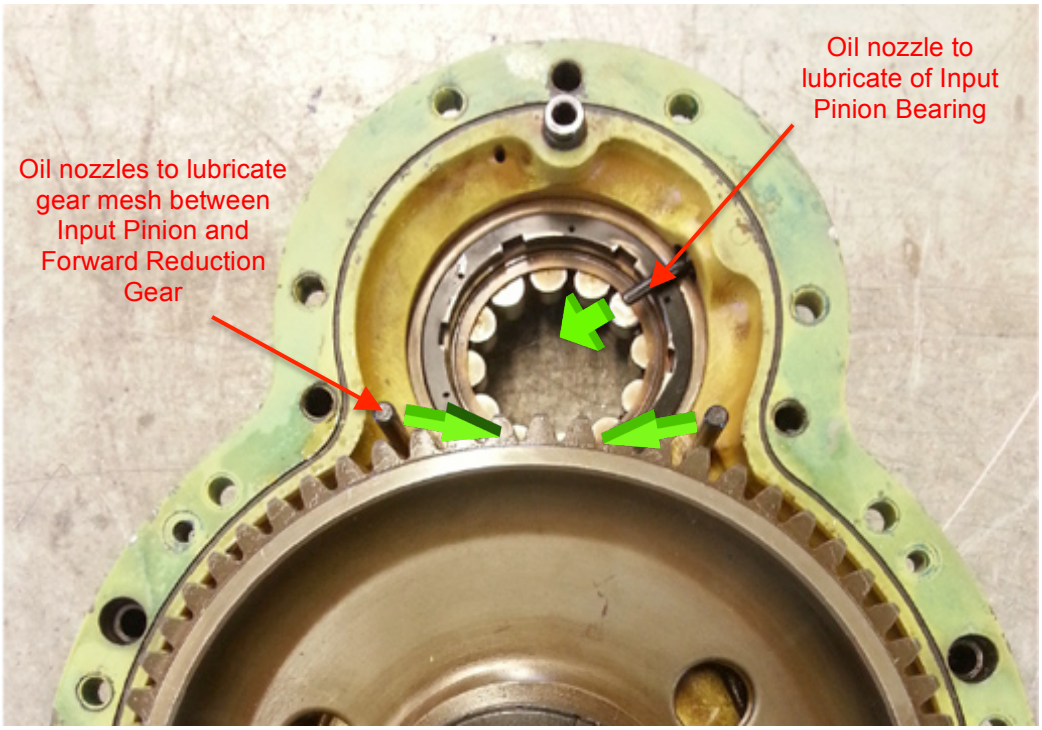

Figure B.6 Fwd Reduction Gear Module Lubrication (Source: Author)

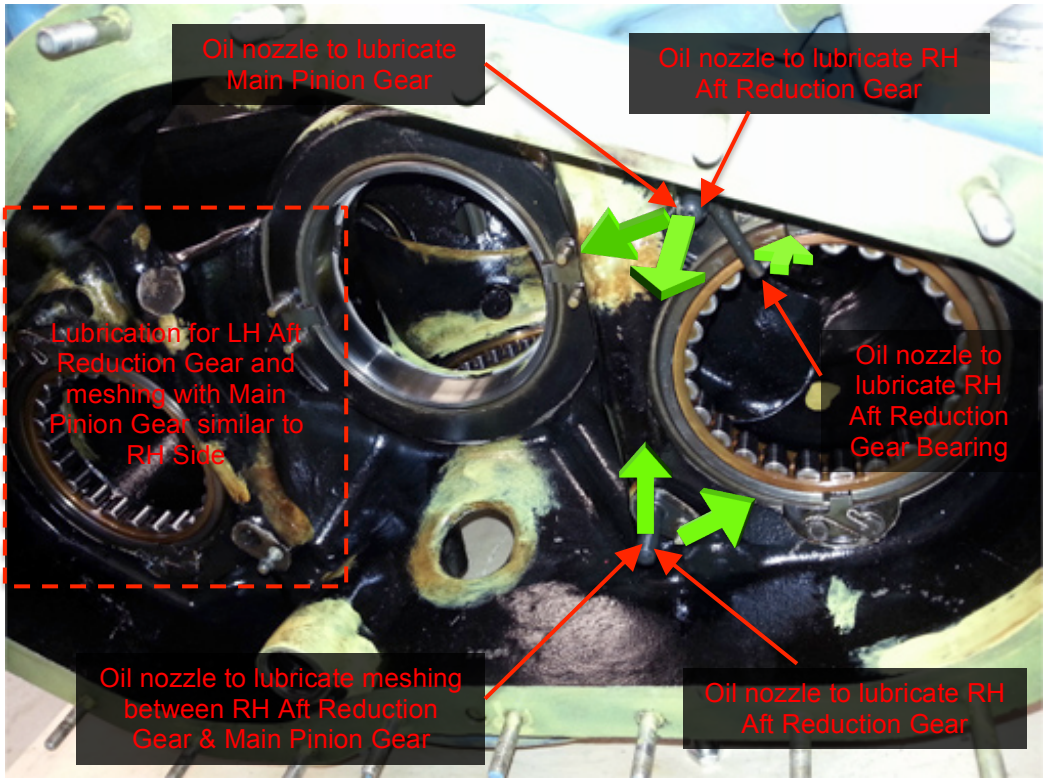

Figure B.7 Aft Reduction Gear Module Lubrication (Source: Author)

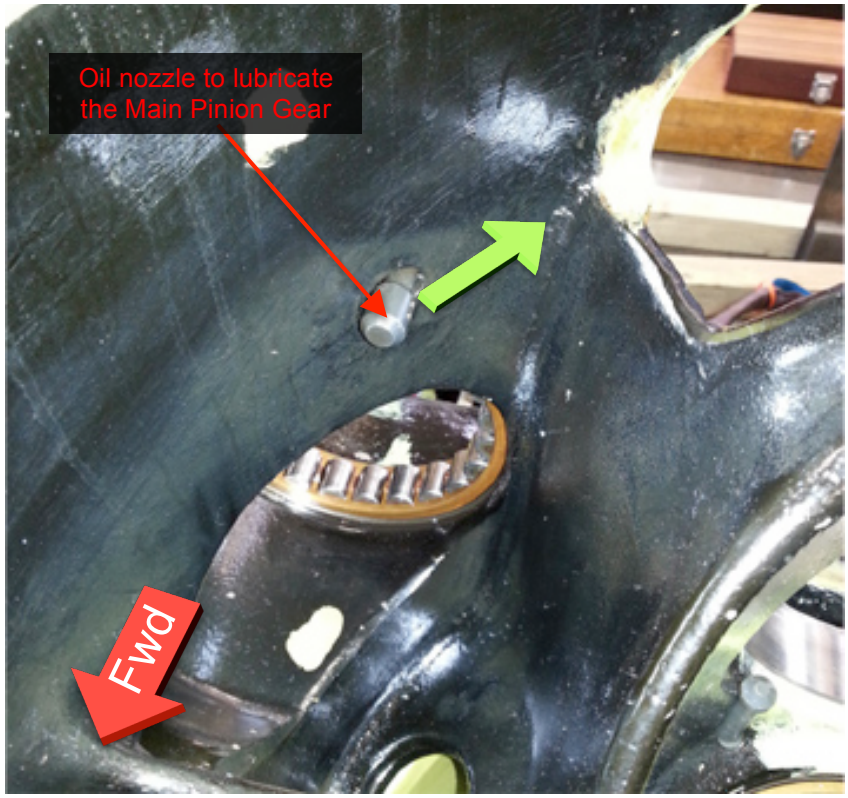

Figure B.8 Main Reduction Gear Module Lubrication (Source: Author)

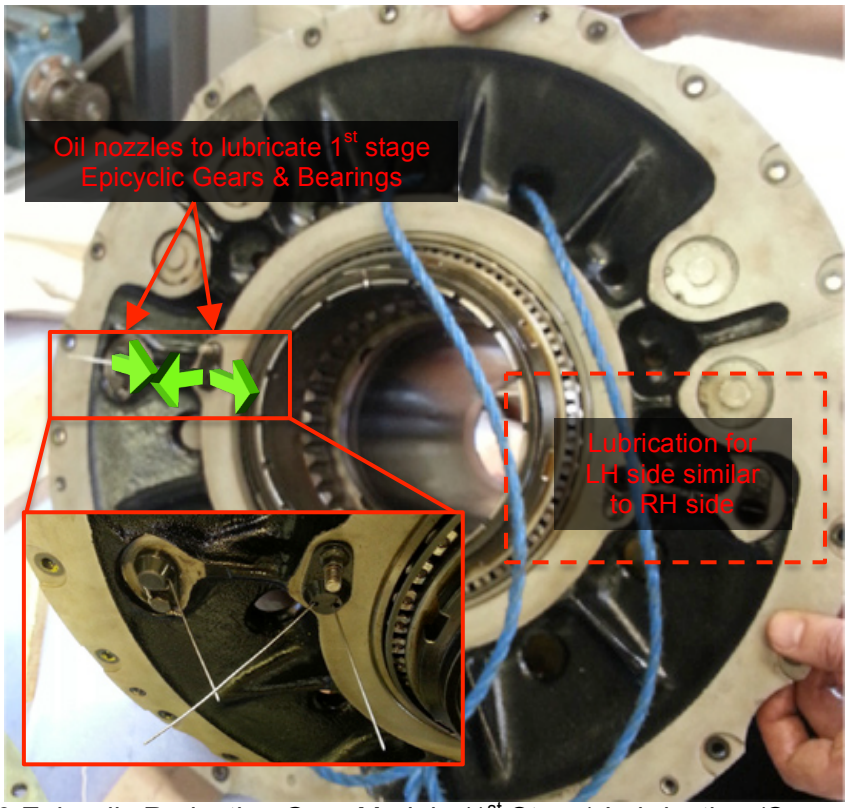

Figure B.9 Epicyclic Reduction Gear Module (1st Stage) Lubrication (Source: Author)

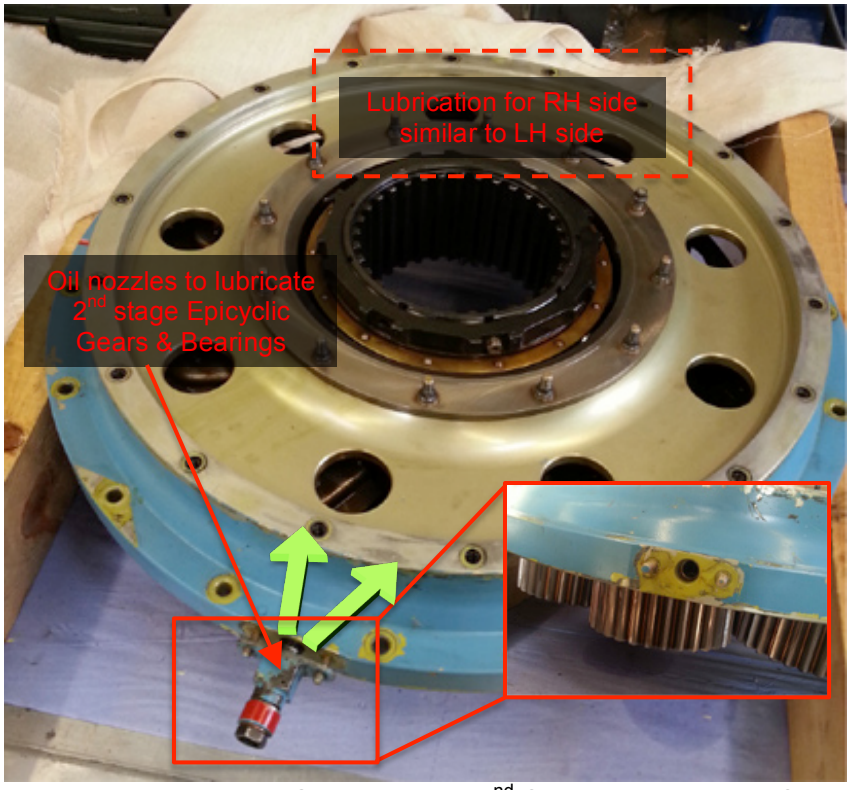

Figure B.10 Epicyclic Reduction Gear Module (2nd Stage) Lubrication (Source: Author)

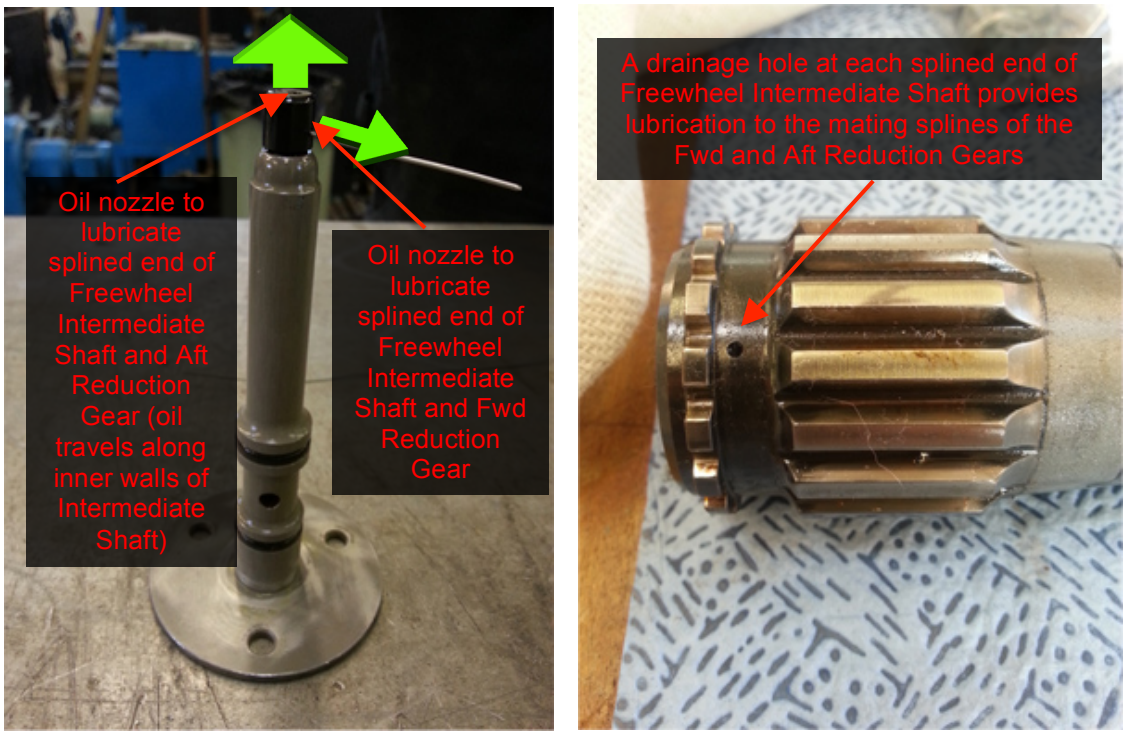

Figure B.11 Freewheel Intermediate Shaft Lubrication: Nozzle (Left) and Lubrication Hole (Right) (Source: Author)

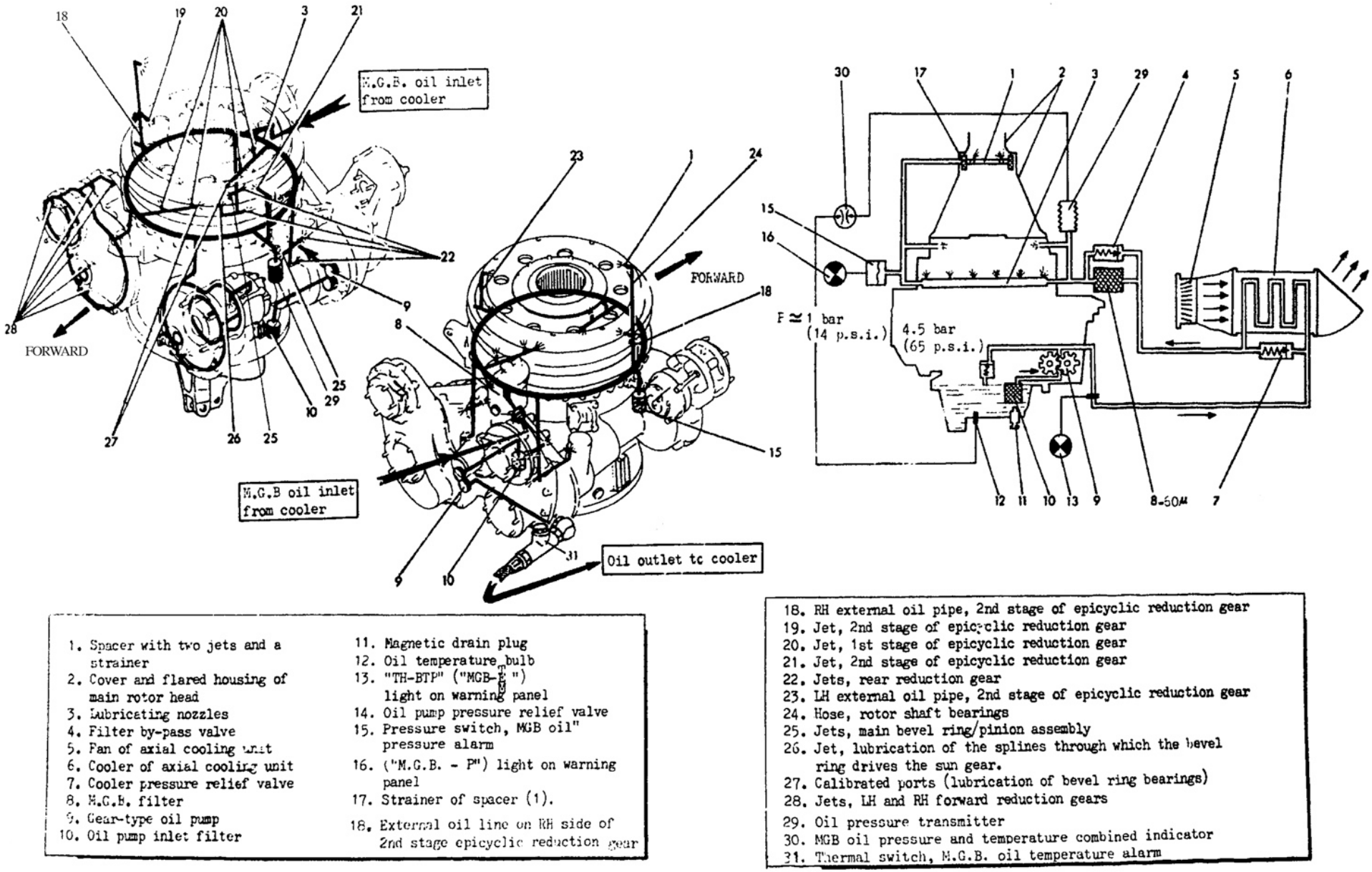

1. Spacer with two jets and a strainer
2. Cover and flared housing of main rotor head
3. Lubricating nozzles
4. Filter by-pass valve
5. Fan of axial cooling unit
6. Cooler of axial cooling unit
7. Cooler pressure relief valve
8. M.G.B. filter
9. Gear-type oil pump
10. Oil pump inlet filter
11. Magnetic drain plug
12. Oil temperature bulb
13. "TH-BTP" ("MGB-T°") light on warning panel
14. Oil pump pressure relief valve
15. Pressure switch, MGB oil" pressure alarm
16. ("M.G.B. - P") light on warning panel
17. Strainer of spacer (1).
18. External oil line on RH side of 2nd stage epicyclic reduction gear
18. RH external oil pipe, 2nd stage of epicyclic reduction gear
19. Jet, 2nd stage of epicyclic reduction gear
20. Jet, 1st stage of epicyclic reduction gear
21. Jet, 2nd stage of epicyclic reduction gear
22. Jets, rear reduction gear
23. LH external oil pipe, 2nd stage of epicyclic reduction gear
24. Hose, rotor shaft bearings
25. Jets, main bevel ring/pinion assembly
26. Jet, lubrication of the splines through which the bevel ring drives the sun gear.
27. Calibrated ports (lubrication of bevel ring bearings)
28. Jets, LH and RH forward reduction gears
29. Oil pressure transmitter
30. MGB oil pressure and temperature combined indicator
31. Thermal switch, M.G.B. oil temperature alarm

Figure B.12 MGB Lubrication System: Internal Galleries (Left) and Schematic (Right) (Source: Helicopter Technical Manual)

The MGB is designed to operate with an oil return temperature of up to 125°C[1] at the sump. Any oil return temperature above this value would trigger a warning to the pilots to indicate the risk of overheating of the internal bearings and gears. The helicopter manufacturer has stated that the MGB gears and bearings would sustain thermal damage if subjected to temperatures exceeding 340 °C. When the lubricating oil pressure drops below 1.0 bar, a warning would also be triggered to inform the pilots that the MGB is no longer lubricated ("oil-off" condition).

The MGB is mounted on the helicopter engine deck via a flexible mounting plate, which helps to counter the reaction torque loads generated by the MGB. The mounting plate has a forward incline angle of 2.0 degrees. The output shaft of the MGB is also inclined forward by 5.0 degrees from the vertical. This implies a total cant angle of 7.0 degrees for the main rotor system to facilitate flight. The mechanical coupling of the engine driveshaft to the high-speed input pinion of the Fwd Reduction Gear Module is made through a flexible coupling that is capable of handling slight misalignment between the engines and the MGB. The output drive of the MGB comes in the form of a splined rotor mast that is connected to the main rotor system comprising the swashplate assembly, rotor head and rotor blades (Figure B.13). The operating specifications of the MGB are summarised in Table B.1. It provides the necessary information for a good understanding of the MGB, which is critical for the design of an appropriate test rig system.

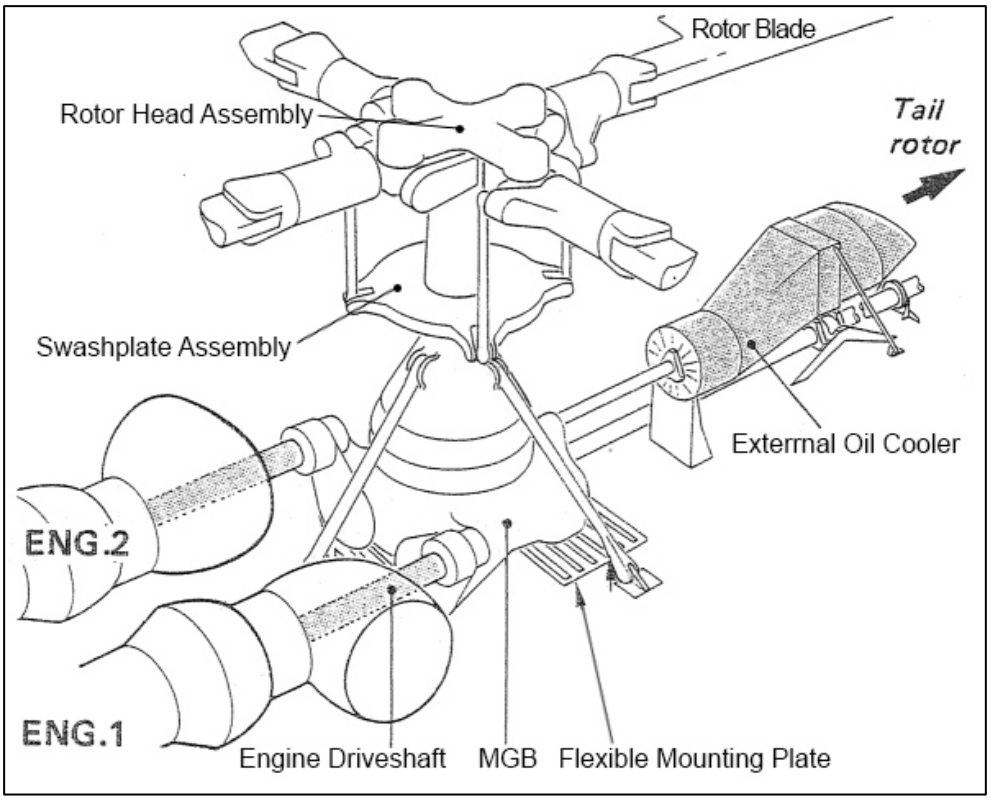

Figure B.13 Installation of MGB on the Helicopter (Source: Helicopter Manufacturer)

[1] Based on the category "A" helicopter flight manual

Category “A” Helicopter MGB	
Description	**Value (unit)**
Input Drive Speed (High-Speed Input)	22,841 (RPM)
Output Drive Speed	265 (RPM)
Maximum Continuous Power Rating	1300 (kW)
Maximum Torque Rating (Freewheel Intermediate Shaft)	1560 Nm @ 7960 RPM
Total Forward Inclination Angle (Cant Angle)	7.0 (degrees)
Lubricating Oil	Aeroshell 5M-A (NATO O-155)
Oil Supply Feed Pressure	1.5 to 1.7 (bars)
Oil Supply Pressure Limit	1.0 (bar)
Oil Supply Flow Rate	67 (LPM)
Oil Return Temperature Limit (Sump)	125 (°C)
Oil Capacity (including cooling system)	22 (Litres)
Bearing and Gears Temperature Limit	340 (°C)

Table B.1 Category “A” Helicopter MGB Operating Specifications (Source: Author)

B.2 Test Rig Drive & Load Systems

B.2.1 MGB Drive System

The driving unit for the MGB experiment is a tandem drive Direct Current (DC) electric motor from Sicmemotori (P/N: NP225 KS5 PVA/B3) that is capable of a combined maximum power output of 750 kW at a maximum speed of 3,000 RPM (Figures B.14 and B.15). The operating specifications of the tandem drive DC electric motor are summarised in Table B.2.

Figure B.14 Tandem Drive DC Electric Motor (Source: Author)

Figure B.15 DC Electric Motor Specifications (Source: Author)

SICMEMOTORI Tandem Drive DC Electric Motor (P/N: NP225 KS5 PVA/B3)	
Description	**Value (unit)**
Maximum Output Power	750 (kW) at Tandem Drive
Maximum Rotational Speed	3000[2] (RPM)
Max Continuous Torque (per motor)	1193 (Nm) at max speed
Voltage Drawn (per motor)	605 (V) at max speed
Current Drawn (per motor)	663 (A) at max speed
Armature Circuit Efficiency	93.5 (%) at max speed
Armature Circuit Inductance	0.19 (mH)
Armature Circuit Resistance	0.027 (ohm)
Lubrication Grease	Grade 3, Lithium
Type of Cooling	Forced Ventilation

Table B.2 DC Electric Motor Operating Characteristics (Source: Author)

A speed-increasing gearbox from Compact Orbital Gears Limited (P/N: F5030) with a speed ratio of 5.947:1 is used to attain an input drive speed that is close to the MGB design specification of 22,841 RPM. With an input speed of 3000 RPM, the gearbox is capable of an output speed 17,842 RPM, which is 78% of the MGB design input speed (Figure B.16). The operating specifications of the speed-increasing gearbox are summarised in Table B.3.

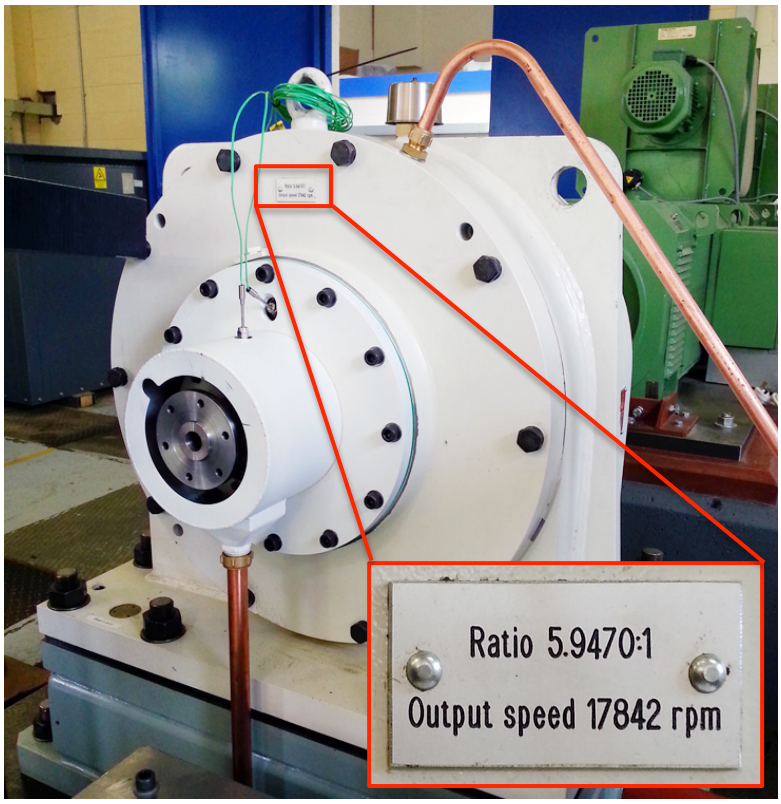

Figure B.16 Speed-Increasing Gearbox Assembly (Source: Author)

[2] The nominal speed of the electric motor is 2720 RPM, with a continuous torque of about 1316 Nm. Field weakening is used to “overclock” the motor to its maximum speed of 3000 rpm.

Speed-Increasing Gearbox (P/N: F5030)	
Description	**Value (unit)**
Speed Ratio	5.947:1
Maximum Input Rotational Speed	3000 (RPM)
Maximum Output Rotational Speed	17,842 (RPM)
Lubricating Oil	Aeroshell 500 (NATO O-156)
Oil Supply Feed Pressure	2.8 bars
Oil Supply Temperature Limit	40 (°C)

Table B.3 Speed Increasing Gearbox Operating Characteristics (Source: Author)

The power and speed limitations of the DC electric motor coupled with the single drive design of the speed-increasing gearbox meant that the MGB could only be powered by up to 750 kW at one input drive and at a speed of 17,842 RPM. It is important to note that according to CS 29-297(c), the requirement for 30 mins of MGB operation on a Category A aircraft, following a loss of primary oil lubrication, involves the setting of a minimum input torque that is necessary to sustain flight. The helicopter manufacturer has therefore advised that a sum of input power of 750 kW is required at the input drives of the MGB for an "oil-loss" situation or specifically 375 kW at each of the input drives. It was a coincidence that the DC electric motor is capable of delivering up to 750 kW for the dual drive of the MGB in an "oil-off" situation, but this requires an upgrade of the speed-increasing gearbox to one of a dual drive configuration in the near future. Hence for its current configuration, the power delivered by the DC electric motor was restricted to 375 kW at the input drive of the LH Reduction Gear Module.

The MGB input power information from the helicopter manufacturer is based on the designed input speed of 22,841 RPM. However, given the speed limitation of 17,842 RPM from the speed-increasing gearbox, the final power to be delivered to the MGB was de-rated to 293 kW in order to maintain a constant driving torque as per the designed input speed (Equations B.1 and B.2).

$$Power = Torque * \frac{RPM * 2\pi}{60} \qquad \text{Equation B.1}$$

$$If\ Torque = Constant,$$

$$Power_2 = Power_1 * \frac{RPM_2}{RPM_1} = 375 * \frac{17842}{22841} = 293kW \qquad \text{Equation B.2}$$

For the installation of the MGB onto the test rig, a steel box-like platform complete with a mounting flange that has a corresponding 2.0 degrees cant angle as the aircraft mounting plate, was designed and manufactured as shown in Figure B.17. The platform provides the necessary elevation and positioning of the MGB to enable the level coupling of the speed-increasing gearbox to the LH Reduction Gear Module. Holes below the mounting platform allow easy access to the MGB sump as well as instrumentation wiring. Flanges at either side of the platform support the mounting structure of the absorption dynamometer, which would serve as the load system for the test rig.

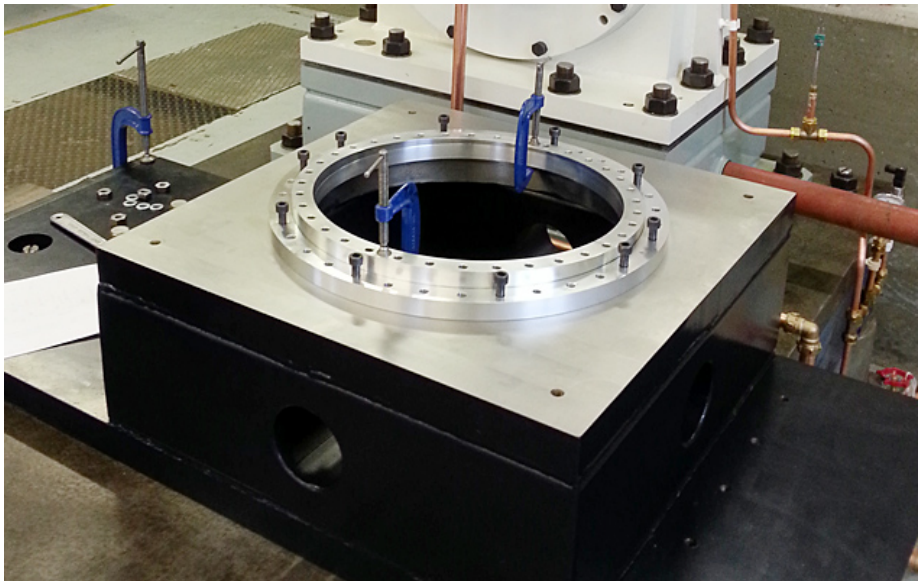

Figure B.17 MGB Installation Platform (Source: Author)

The mating of the speed-increasing gearbox to the MGB is achieved through a machined coupling flange (Figure B.18). One end of the coupling flange is bolted to the output drive of the speed-increasing gearbox while the other end is bolted to the flexible coupling of the MGB input drive. By incorporating the flexible coupling, the mechanical drive link between the speed-increasing gearbox and the MGB is able to accommodate slight misalignment between both assemblies, thereby minimising any fatigue stress damage.

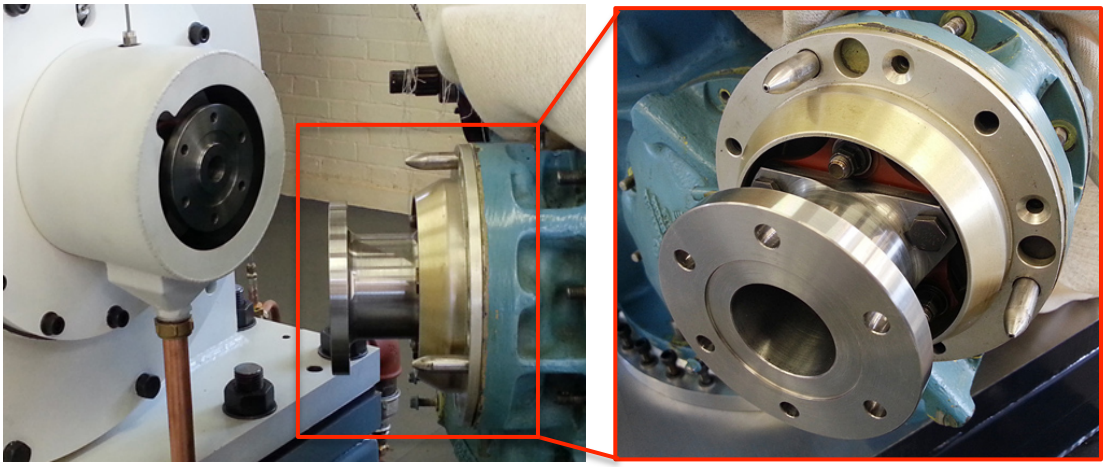

Figure B.18 Coupling Flange for Mating Speed-Increasing Gearbox to MGB (Source: Author)

B.2.2 MGB Load System

The loading system for the MGB experiment comprises an absorption dynamometer, which creates a level of resistance proportional to the desired loading on the MGB. The Wichita AquaMakks™ (P/N: 7-325AM-B-1300) is a clutch and brake system selected for the task. It is a pneumatically controlled, dynamic brake system that is designed for continuous slip torque production. It uses air pressure to generate a clamping force between the rotating drive plates

that are driven by a splined hub mated to the output drive shaft of the MGB. The drive plates have friction disks that slide against copper alloy wear plates to generate a torque[3] that is proportional to the air pressured introduced. The heat generated by the frictional torque is removed using cooling water that flows through water jackets in the assembly (Figure B.19). Air pressure and flowing water are delivered to the assembly using flexible external tubes. The operating specifications of the clutch and brake system are summarised in Table B.4.

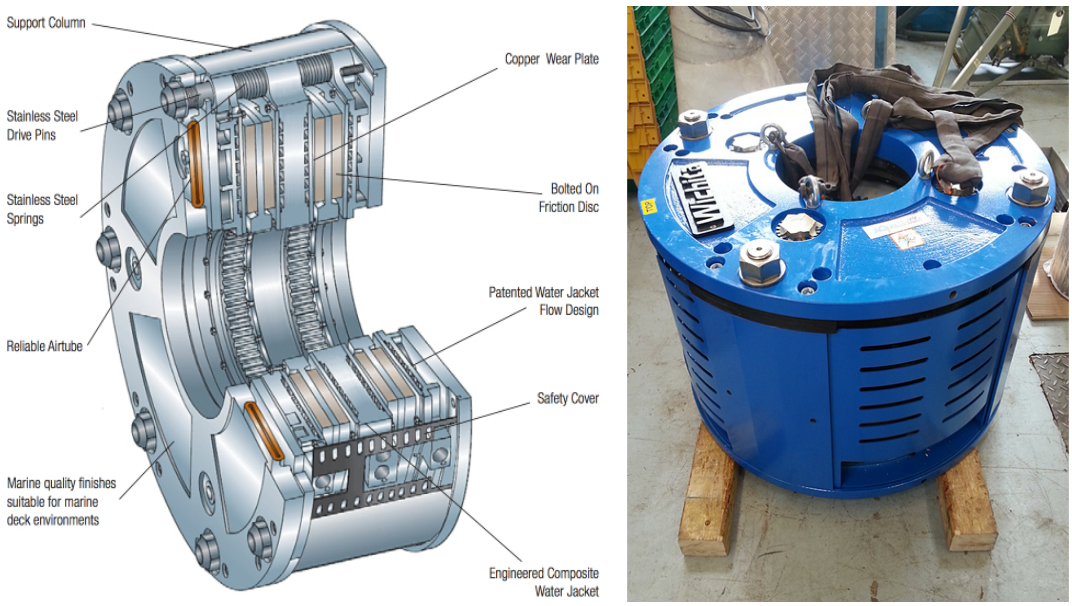

Figure B.19 Wichita Clutch and Brake Cutaway (Left) and Assembly (Right) (Sources: www.wichita.com and author)

Absorption Dynamometer – Wichita Clutch and Brake System (P/N: 7-325AM-B-1300)	
Description	**Value (unit)**
Maximum Rotational Speed	935 (RPM)
Torque at Air Pressure of 0.24 bars	3224 (Nm)[4]
Torque at Air Pressure of 7.0 bars	55950 (Nm)
Maximum Air Tube Pressure	9.0 (bars)
Maximum Water Supply Temperature	49 (°C)
Maximum Water Return Temperature	77 (°C)
Maximum Water Supply Pressure	2.7 (bars)
Minimum Water Flow Rate for 895 kW of Frictional Heat	454 (LPM)

Table B.3 Absorption Dynamometer Operating Characteristics (Source: Author)

[3] According to the OEM, the frictional torque is affected by the wear of the brake lining, as well as the operating temperature and speed of the dynamometer.

[4] This frictional torque of the dynamometer is obtained following its installation onto the test rig and the conduct of an operational checkout with an air pressure of 0.24 bars. This enables the determination of a pressure-torque curve, which is used to determine the air pressure necessary to load the MGB at a specific power setting.

The helicopter manufacturer has also informed that with a sum of input power of 750 kW to the MGB, the expected frictional heat generation is 40 kW. Hence for a single drive input power of 293 kW, the expected frictional heat generation would be approximately 16 kW[5] (Equation B.3). This implies that the available power at the MGB output drive would be 277 kW (Equation B.4), assuming no other power losses.

$$Friction_2 = Friction_1 * \frac{Power_2}{Power_1} = 40 * \frac{293}{750} = 15.63\ kW \quad \text{Equation B.3}$$

$$Power\ Out = Power\ In - Friction = 293 - 15.63 = 277.37kW \quad \text{Equation B.4}$$

With an overall speed ratio of (1: 86.19), the output drive speed of the MGB would be 207 RPM for an input drive speed of 17,842 RPM (Equation B.5). Therefore to absorb the available power of 277 kW at the MGB output shaft, the dynamometer has to generate up to 12,778Nm at 207 RPM (Equation B.6).

$$Output\ Speed = Input\ Speed * Speed\ Ratio = 17{,}842 * \frac{1}{86.19} = 207\ RPM \quad \text{Equation B.5}$$

$$Torque = Power * \frac{60}{RPM * 2\pi} = 277.37x10^3 * \frac{60}{207 * 2\pi} = 12{,}795.60\ Nm \quad \text{Equation B.6}$$

From the pressure-torque curve obtained during the operational checkout of the dynamometer and the rule of similar triangles (Figure B.20), the approximate air pressure required to generate a resisting torque value of 12,796 Nm was 1.47 bars (Equation B.7). This resisting torque would produce a frictional heat value equivalent to the available power at the MGB output shaft and would require at least 141 LPM (Equation B.8) of water to remove.

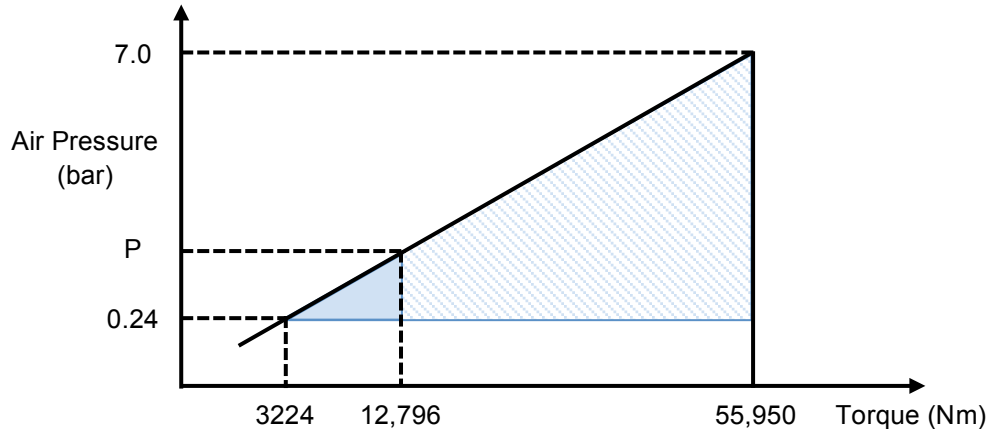

Figure B.20 Air Pressure – Torque Relationship of Dynamometer (Source: Author)

[5] The actual heat generation would be lower due to that fact that the reduction gears in the RH Fwd Reduction Gear Module would not be turning as the RH freewheel intermediate shaft was removed to facilitate instrumentation wiring

$$\frac{P - 0.24}{12796 - 3224} = \frac{7.0 - 0.24}{55{,}950 - 3224} \quad Hence\ P = 1.47\ bars$$ Equation B.7

$$Water\ Flow\ Rate = \frac{277}{895} * 454 = 140.51\ LPM$$ Equation B.8

The coupling of the MGB output drive to the dynamometer involved several mechanical components. An original helicopter rotor mast that is splined to the MGB output drive was modified to couple with the splined hub of the dynamometer (Figure B.21). The rotor mast was first cut off along a section from the splined end. This section was then installed to a steel hollow shaft using an interference fit assembly. The steel hollow shaft had a keyway to facilitate assembly onto the splined hub of the dynamometer. To strengthen the inner walls of the rotor mast splined end, a steel plug was installed (Figure B.22).

Figure B.21 Modified Rotor Shaft Assembly (Source: Author)

The dynamometer is mounted on a support structure that is fixed to the base plate of the assembly mounting structure. The base plate is inclined with the same angle as the MGB output drive in order for the proper alignment and coupling of the modified rotor mast to the splined hub of the dynamometer. The weight of the dynamometer and the coupling assembly is borne by the support structure. In particular, a thrust bearing on the support structure allows free swivel of the coupling assembly, while bearing its weight. This configuration ensures that the MGB bears no loads from the dynamometer or the coupling assembly, similar to its installation on the helicopter (Figures B.22 and B.23). A radial bearing sits at the top of the dynamometer and takes radial loads from the steel hollow shaft. This also ensures a proper alignment of the coupling assembly to the MGB output drive.

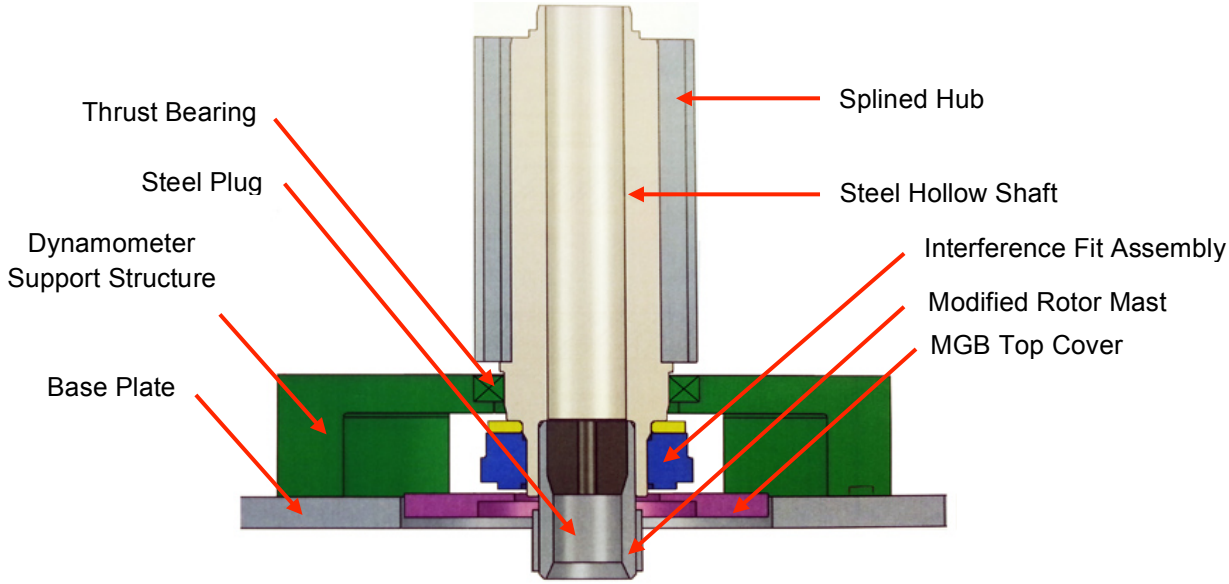

Figure B.22 Modified Rotor Mast to Splined Hub Coupling (Source: Author)

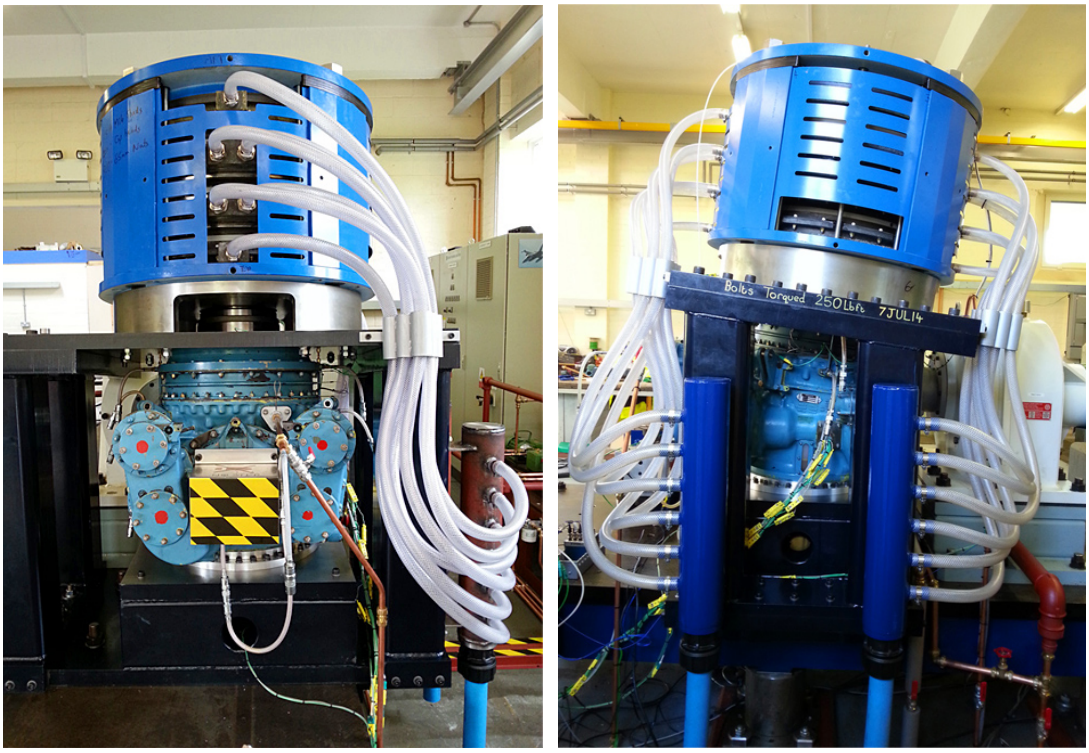

Figure B.23 Dynamometer Mounting Structure: Front View (Left) and Side View (Right) (Source: Author)

B.3 Test Rig Lubrication and Cooling System

The MGB test rig has various rotating systems that demand different lubrication and cooling requirements. It is important that such requirements are met in order to ensure proper operation of the test rig and consistency in the MGB test results.

The DC electric motor uses forced air ventilation to cool the armature windings and Grade 3 lithium grease for its drive shaft bearings. The greasing interval for the each of the bearings is 1800 operational hours.

The speed-increasing gearbox uses Aeroshell 500 (NATO O-156[6]) lubricating oil, supplied at 2.8 bars and 40°C to cool its internal gears and bearings. To achieve this, an external lubrication system comprising a supply tank, feed and suction (return) pumps, filter assembly, display gauges and a pressure regulator was set up (Figures B.24 and B.25). The supply tank can house up to 25 Litres of the lubricant oil, while the feed and suction pumps are each capable of generating a differential pressure of 3.0 bars and at a flow rate of 30 LPM. Display gauges are used to monitor both the feed and return pressure values of the lubrication system. A 25μm filter assembly keeps the lubrication oil system free from debris and contaminants.

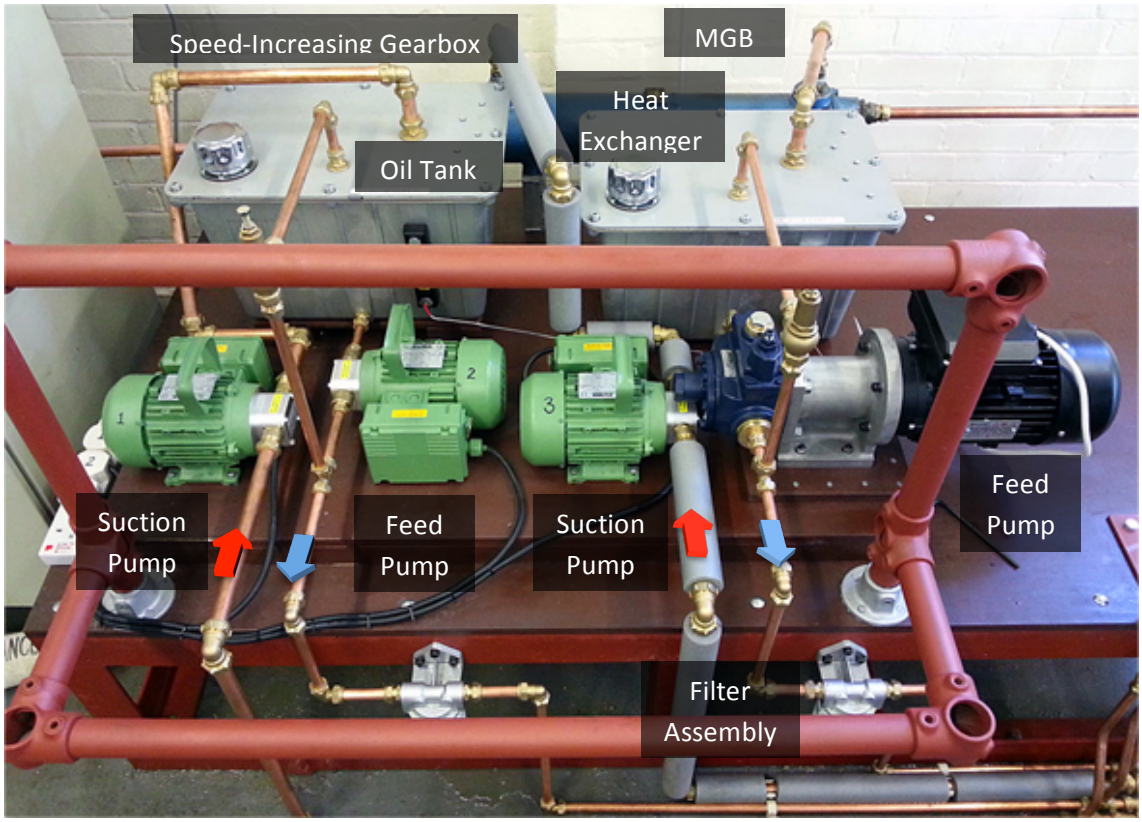

Figure B.24 Lubrication System for MGB Test Rig (Source: Author)

[6] Equivalent specifications to the US MIL-PRF-23699F and the Joint Service Designation OX-27.

The lubrication system for the MGB consists of the same components as those of the speed-increasing gearbox, except that the lubrication oil used is Aeroshell 5M-A (NATO O-155) and the supply pressure is between 1.5 to 1.7 bars. It also involves a heat changer that utilises water supplied from an external water-cooling system to cool the lubricating oil and a feed pump with an improved flowrate of 60 LPM (Figure 3.25). The helicopter manufacturer has advised that an oil flow rate of 4000 LPH (67 LPM) is necessary to remove a frictional heat generation of 40 kW with a sum of input power of 750 kW. Based on the computed frictional heat generation of 16kW from a de-rated power input of 293 kW to the MGB (Equation B.3), the revised flow rate would be 27 LPM (Equation B.9), which is within the operating parameters of the selected oil pumps. However, it is important to note that an upgrade of the oil pumps to handle flow rates of up to 67 LPM would be necessary if future testing involved frictional heat generation of 40 kW. The configuration of both feed and suction pumps allows the fast removal of lubrication oil from the MGB sump, which supports the efficacious testing of the MGB under "oil-off" and thioether mist lubrication conditions.

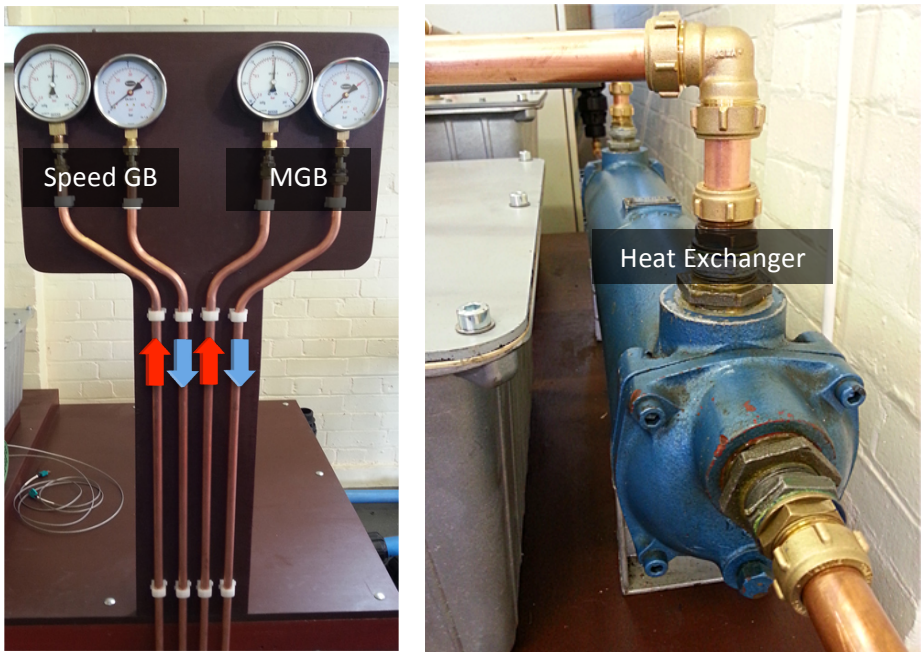

Figure B.25 Lubrication System for MGB Test Rig: Gauges (Left) and MGB Heat Exchanger (Right) (Source: Author)

$$MGB\ Oil\ Flow\ Rate = \frac{16}{40} * 67 = \ 26.8\ LPM \qquad \text{Equation B.9}$$

The dynamometer uses water flowing through its water jackets to extract the heat generated by the frictional torque. The lubrication system involves an external water-cooling system (complete with a water tower, pumps and pipework to the MGB test rig), a water flow meter and a manifold for the distribution of water to and from the dynamometer water jackets (Figure B.26). From Section B.2, the computed water flow rate to the dynamometer was 141 LPM (Equation B.8) for the de-rated power input to the MGB.

The lubrication and cooling requirements for the MGB test rig are summarised in Table B.4.

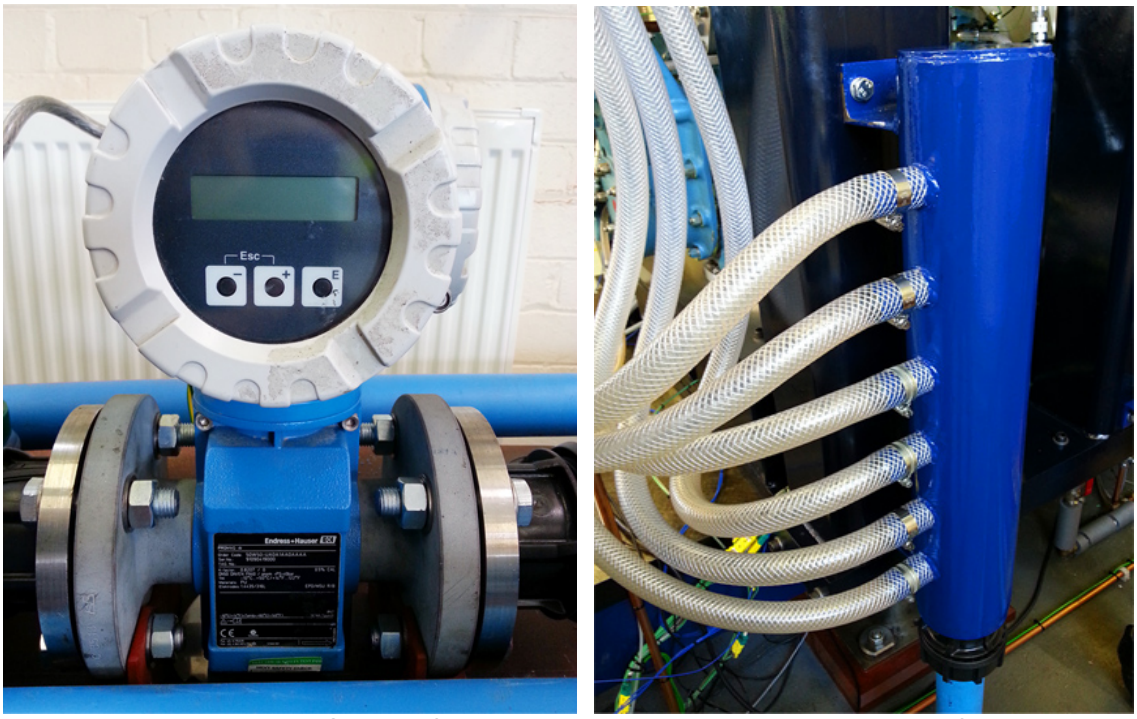

Figure B.26 Lubrication System for Dynamometer: Water Flow Meter (Left) and Water Manifold (Right) (Source: Author)

MGB Test Rig Lubrication and Cooling Requirements				
Description	**DC Electric Motor**	**Speed-Increasing GB**	**Main Gear Box**	**Dynamometer**
Lubricant / Coolant Type	Grease & Force Ventilation	Oil	Oil	Water
Material	Grade 3 Lithium Grease & Air	Aeroshell 500 (NATO O-156)	Aeroshell 5MA (NATO O-155)	Water
Required Flow Rate	NA	NA	27 LPM	141 LPM
Available Flow Rate		30 LPM	60 LPM	383 LPM
Supply Pressure		2.8 bars	1.5 to 1.7 bars	NA
Capacity		25 Litres	25 Litres	NA

Table B.4 Lubrication and Cooling Requirements of MGB Test Rig (Source: Author)

B.4 Nozzle Configuration for Thioether Mist Lubrication

B.4.1 Thioether Mist Lubrication Nozzle Design

In the experiments by NASA and the US Army Research Laboratory [4] and [5], a thioether misting unit was set up external to the spur gears test rig. Not much information was available on this misting unit except that it utilises dried and filtered compressed air to deliver the thioether liquid as a fine mist. As mentioned in Appendix A.5, the regulated flow rates for the thioether lubricant and the pressurised air were 15 mL/hr and 400 L/hr respectively for the lubrication of a pair of spur gears.

With the limited information on the NASA thioether misting unit, an initial plan to incorporate commercially available atomising or misting nozzles[7] directly within the helicopter MGB for the thioether mist lubrication was considered. Having internally located misting nozzles directed at critical gears and bearings would resolve the problem of thioether coalescing along the mist delivery tubes as it would for an external misting unit. This was however found to be non-feasible due to the limited internal space within the MGB. One of the smallest identified hydraulic misting nozzles, with a housing diameter of 11.2 mm[8], was assessed to physically interfere with the internal gears and bearings of the MGB. To overcome this limitation of available space within the MGB, the fabrication of the misting nozzles using thin metal pipes of less than 6 mm in outer diameter was conceived.

B.4.1.1 Flowrate and Sizing of Fabricated Nozzles

The flow rate calculation of the nozzle design was based on the standard pipe flow rate formula for orifices and nozzles as shown in Equation B.10. The flow diagram is shown in Figure B.27.

$$Q = C\pi \frac{{D_2}^2}{4} \sqrt{\left({2\Delta \mathrm{P}}/{\rho}\right)} \qquad \text{Equation B.10}$$

Where $C = \frac{C_d}{\sqrt{1-\beta^4}}$, $\beta = \frac{D_2}{D_1}$ and C_d = discharge coefficient that is interpolated from Table B.5.

[7] These include water atomising nozzles, hydraulic atomising nozzles, fuel-oil atomising nozzles, air-assisted atomising nozzles and ultrasonic atomising nozzles.
[8] Part Number 1/8PJ6 from BETE Nozzles Limited, UK

Discharge Coefficients (C_d) for Nozzles				
Diameter Ratio, $\beta = D_2/D_1$	Reynolds Number - Re			
	10^4	10^5	10^6	10^7
0.2	0.968	0.988	0.994	0.995
0.4	0.957	0.984	0.993	0.995
0.6	0.950	0.981	0.992	0.995
0.8	0.940	0.978	0.991	0.995

Table B.5 Discharge Coefficients for Orifices / Nozzles
(Source: BS EN ISO 5167:2 [22])

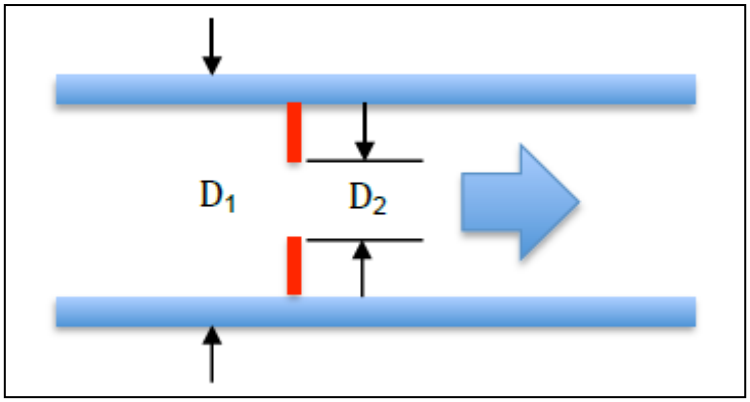

Figure B.27 Orifice / Nozzle Flow Diagram (Source: Author)

Table B.6 summarises the parameters for computing the expected volumetric flow rate, Q, for a standard copper pipe of 3.18 mm inner diameter. For a start, a nozzle diameter, D_2, of 0.15 mm was chosen based on the same dimension of the smallest identified commercial nozzle. Calculations have shown that with such a nozzle size, a pressure differential of 30 bars coupled with a thioether fluid density of 1200 kgm^{-3}, would have an expected flow rate of approximately 0.1 LPM, which is similar to that of the referenced commercial nozzle.

Parameters for Flow Rate Computation		
S/N	**Parameter**	**Value**
1	Pipe Inner Diameter, D_1	3.18 mm (1/8")
2	Nozzle Diameter, D_2	0.15 mm
3	Diameter Ratio, $\beta = D_2/D_1$	0.0472
4	Hydraulic Diameter, $d_h = D_1$	3.18 mm
5	Fluid Density, ρ	1200 kgm^{-3}
6	Dynamic Viscosity, μ	0.03 Nms^{-2}
7	Reynolds Number, $Re = \rho u d_h/\mu$	27 (Laminar)
8	Discharge Coefficient, C_D	0.976 (Table 3.5)
9	Pressure Difference, ΔP	3×10^6 Pa (30 bars)
10	Computed Flow Rate, Q	1.22×10^{-6} m^3s^{-1} (0.07 LPM)

Table B.6 Parameters to Compute Flow Rate (Source: Author)

B.4.1.2 Stress Analysis of Fabricated Nozzles

An analysis of the stresses present in a thin metal pipe with a nozzle diameter of 0.15 mm, which was subjected to a fluid supply pressure of 30 bars, was performed to determine the safety factors against burst pressure. According to the IACS[9] 2011, "Requirements Concerning Pipes and Pressure Vessels" [23], the thioether lubrication piping shall withstand a minimum burst pressure of 1.5 times the working pressure.

With this information, the Safety Factors (S.F.) of the fabricated nozzle against the material yield strength were calculated using the Von Mises yield criterion. Table B.7 summaries the computed S.F. for both a copper (C110 O60) pipe and a 304 stainless steel pipe. The calculations took into account the radial and hoop (tangential) stresses in each pipe due to the burst pressure (1.5 times the working pressure) and the nozzle hole on the wall of the pipe. Equations B.11 and B.12 represent the radial (σ_R) and hoop (σ_T) stresses at a given radial location, R, in a cylindrical metal pipe due to the presence of an internal pressure, P_i.

$$\sigma_R = P_i \frac{{R_1}^2}{{R_2}^2 - {R_1}^2}\left[\frac{{R_2}^2}{R^2} - 1\right] \qquad \text{Equation B.11}$$

$$\sigma_T = P_i \frac{{R_1}^2}{{R_2}^2 - {R_1}^2}\left[1 + \frac{{R_2}^2}{R^2}\right] \qquad \text{Equation B.12}$$

Where R_1 and R_2 denote the inner and outer radius of the metal pipe respectively.

These stresses were the highest at the inner walls of the pipes. With a nozzle hole, there was an increase in the hoop stress value within the pipe material. This increase was taken into account with the use of a Stress Concentration Factor, K_t, which is dependent on both the ratio of the inner and outer wall diameters as well as that of the nozzle hole diameter and the inner wall diameter. See Figure B.28 for the graph of K_t against the geometric ratios. Results have shown a minimum S.F. of 1.9 for the copper pipe, and 7.4 for the stainless steel pipe, both of which are deemed acceptable to proceed with the next phase of the nozzle design: spray testing.

[9] International Association of Classification of Societies

Safety Factors			
Property	**Copper (Soft, Annealed)**	**304 Stainless Steel**	**Remarks**
Yield Stress (MPa)	70	275	S.F. includes Nozzle Stress Concentration Factor, K_t = 3.2
Safety Factor Against (1.5 x Internal Press = 45 bars)	1.9	7.4	

Table B.7 Safety Factors of Fabricated Nozzles (Source: Author)

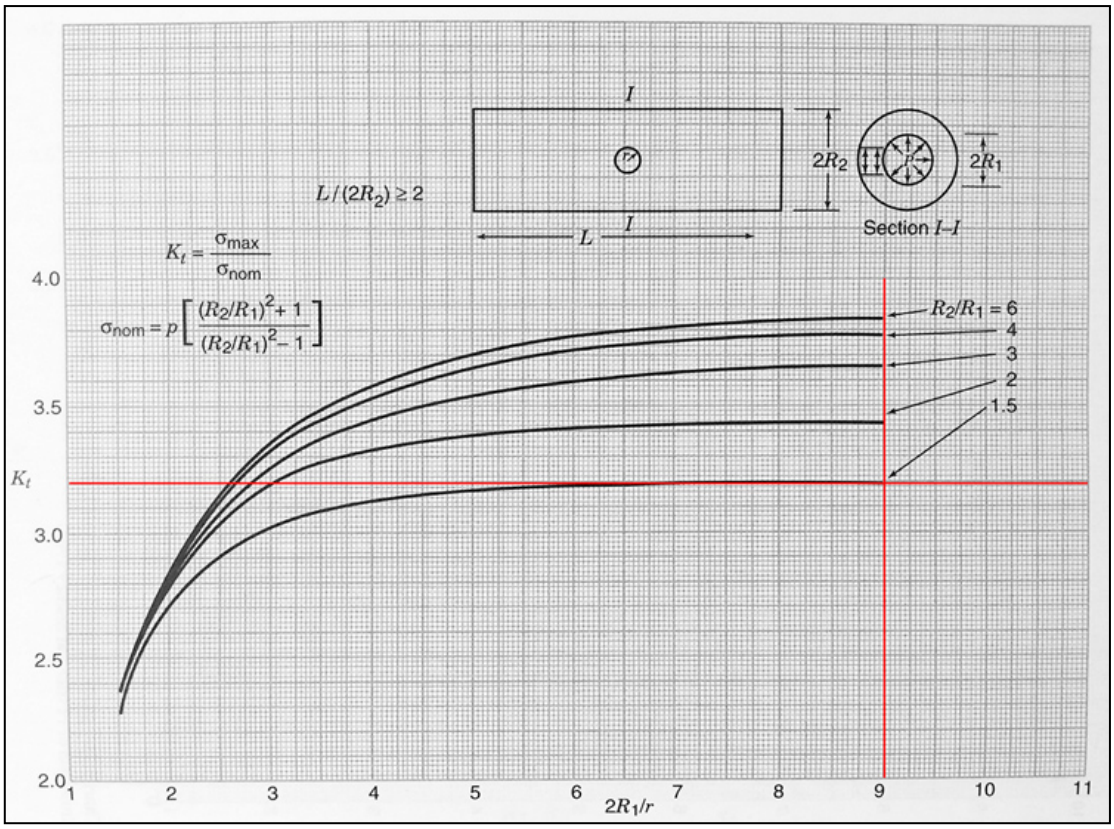

Figure B.28 Stress Concentration Factors for Hole in Pressurised Thick Cylinder (Source: Peterson's Stress Concentration Factors, Second Edition, 1997 [24])

B.4.1.3 Spray Test of Fabricated Nozzles

With satisfactory results from the calculations of the thioether flow rate and material safety factors for the chosen nozzle size diameter and fluid supply pressure, the next phase involved a spray test to demonstrate the feasibility of thioether mist generation. Two metal pipe sections, one of copper and the other of stainless steel material, were each drilled with the hole of diameter 0.15 mm as shown in Figure B.29.

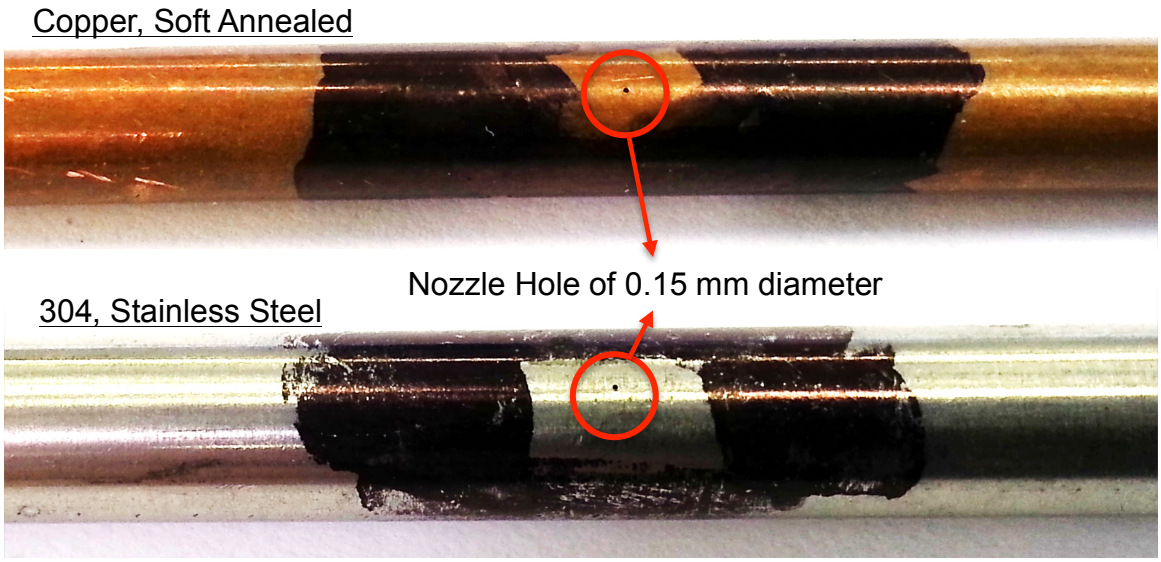

Figure B.29 Nozzles Holes on Metal Pipes (Source: Author)

A schematic representing a rig to test the feasibility of mist lubrication using the drilled pipe sections is shown in Figure B.30. The test rig uses a compressed gas (nitrogen) to pressurise a chamber containing a test fluid in order for to force the test fluid through the nozzle hole at the required pressure. A flow regulator regulates the pressure of the compress gas to 30 bars, to generate the same fluid pressure in the pipe. Figure B.31 shows the actual set up of the test rig. The pressure chamber that contains the test fluid is in the form of a steel pipe section with two shut-off valves that allow easy filling of the fluid into the chamber.

In the spray tests, Vulkanol OT[10] was used as the test fluid given its availability in the test lab and the high cost of the actual thioether lubricant, MCS-293^{TM}. The differences in physical properties between the test fluid and thioether MCS-293^{TM} are captured in Table B.8. Compared to thioether, the test fluid has a lower fluid density and viscosity. Table B.9 summarises the effects on nozzle spray characteristics when test parameters such as operating pressure, fluid specific gravity or density, fluid viscosity, as well as fluid surface tension are varied. It provides the necessary information to assess the spray characteristics of the nozzles using Vulkanol OT as an available and affordable test fluid. For example, spray tests using the fluid test, which has lower specific gravity and fluid viscosity as thioether, would imply droplets of smaller sizes and a higher volumetric flow rate for the given operating pressure.

[10] Product of LANXESS Energizing Company

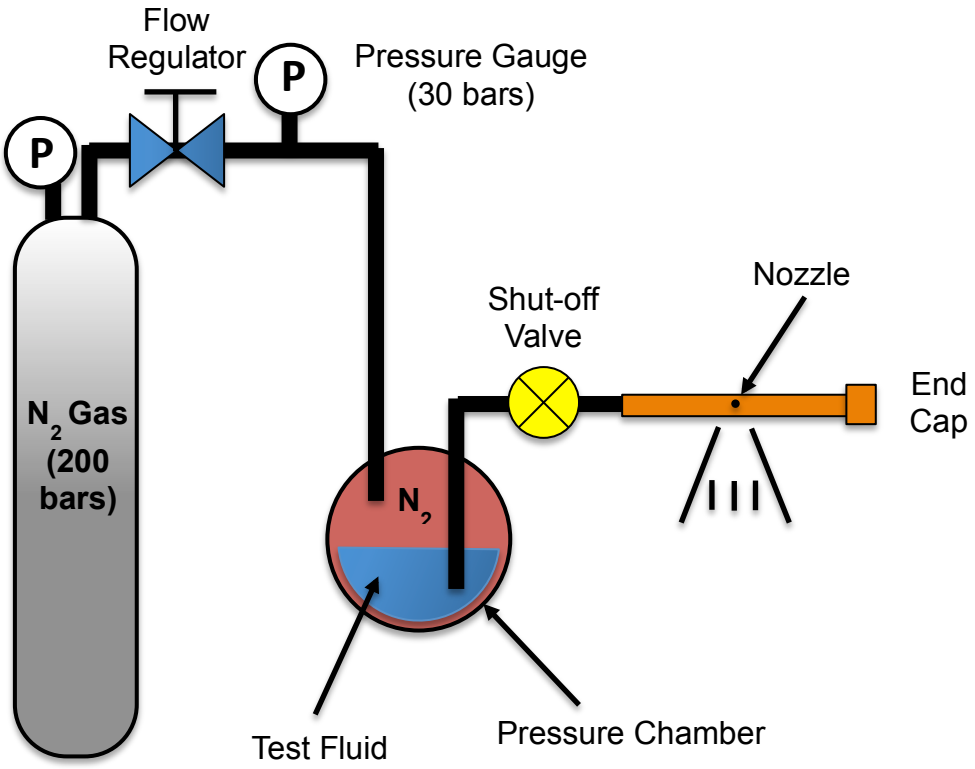

Figure B.30 Schematic of Fabricated Nozzle Spray Test (Source: Author)

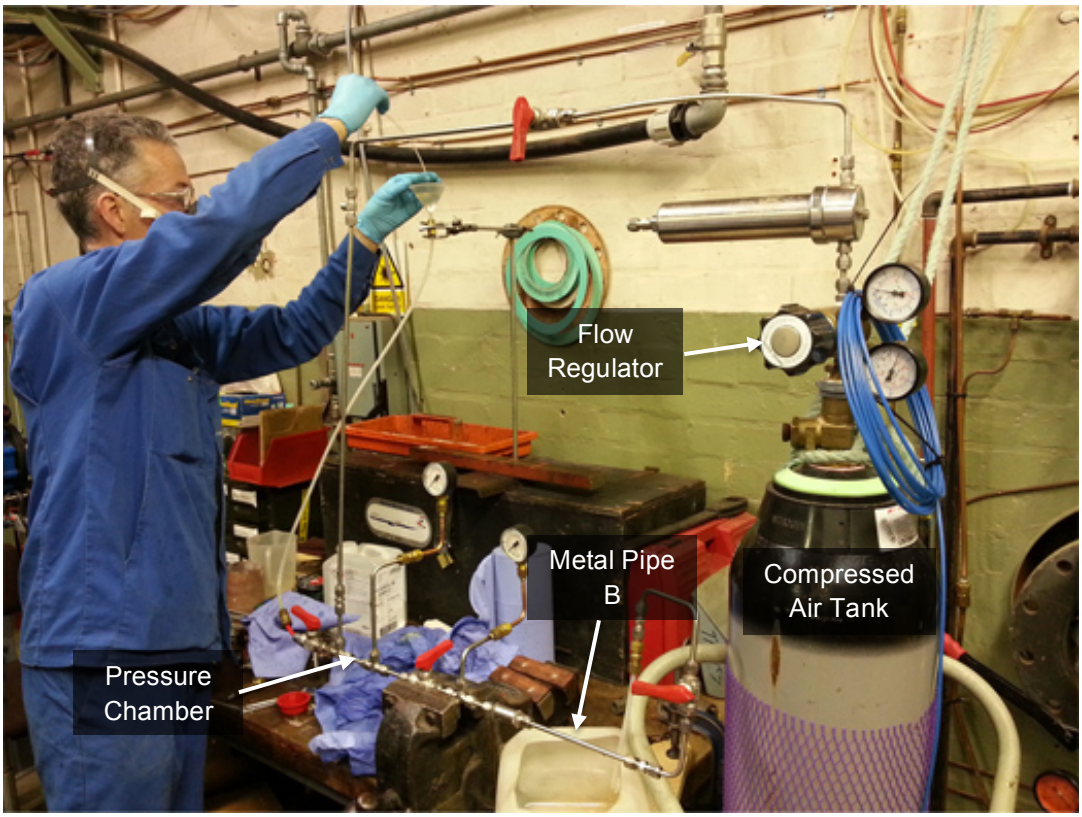

Figure B.31 Test Rig for Fabricated Nozzle Spray Test (Source: Author)

Comparison of Thioether with Test Liquid & Water				
S/N	**Property (Unit)**	**Thioether MCS-293™**	**Vulkanol OT**	**Water**
1	Physical Appearance	Clear, light yellow liquid	Colourless, yellow liquid	Clear
2	Fluid Density (kgm^{-3})	1200	960	1000
3	Dynamic Viscosity (cP)	30.2 (40°C)	24.0 (20°C)	1.0 (20°C)
4	Kinematic Viscosity (cSt)	25.2 (40°C)	25.0 (20°C)	1.0 (20°C)
5	Melting Point (°C)	-29 (Pour Point)	-60	0
6	Boiling Point (°C)	413	230	100
7	Thermal Stability (°C)	329	> 230	NA
8	Surface Tension (dyne/cm)	50	NA	70

Table B.8 Physical Properties of Test Fluid against Thioether and Water
(Source: Author)

Nozzle Characteristics	Increase in Operating Pressure	Increase in Specific Gravity	Increase in Viscosity	Increase in Fluid Temperature	Increase in Surface Tension
Pattern Quality	Improves	Negligible	Deteriorates	Improves	Negligible
Drop Size	Decreases	Negligible	Increases	Decreases	Increases
Spray Angle	Increases then decreases	Negligible	Decreases	Increases	Decreases
Capacity	Increases	Decreases	Full/hollow cone – increases Flat – decreases	Depends on fluid sprayed and nozzle used	No effect
Impact	Increases	Negligible	Decreases	Increases	Negligible
Velocity	Increases	Decreases	Decreases	Increases	Negligible
Wear	Increases	Negligible	Decreases	Depends on fluid sprayed and nozzle used	No effect

Table B.9 Summary of Nozzle Spray Performance
(Source: Nozzle Technical Reference [25])

In preliminary spray tests using Vulkanol OT, the fabricated nozzle successfully generated a fine mist spray with a cone angle of approximately 30° as shown in Figure B.32. The tests demonstrated the feasibility of thioether mist lubrication using a hole of diameter 0.15 mm and under an operating pressure of 30 bars. Unfortunately, the fabricated nozzle had a drawback. There were occasions in which the fabricated nozzle was clogged by the test fluid at the fine hole and required purging with compressed air to clear. This prompted the study of alternative nozzle configurations in order to select one that can be effectively deployed in the confined spaces of the helicopter MGB for thioether mist lubrication.

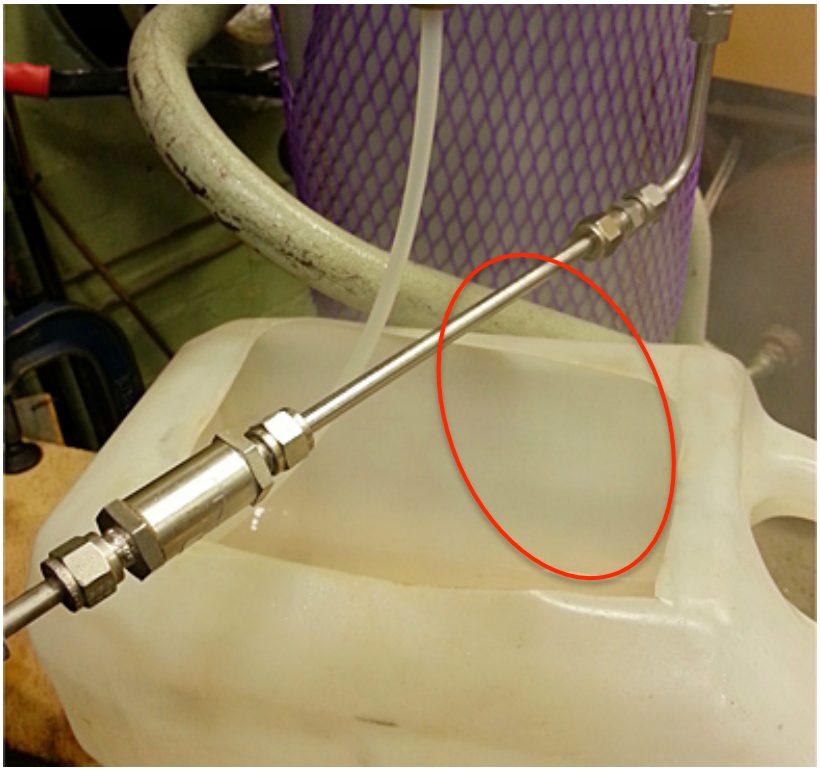

Figure B.32 Mist Generation from the Fabricated Nozzle (Source: Author)

B.4.1.4 Spray Tests with Alternative Nozzle Configurations

Two alternative nozzle configurations were set up to evaluate the spray characteristics of mist generation, with the aims of achieving a fine spray pattern at a low volumetric flow rate. In particular, the desired thioether flow rate from the nozzle configuration should be comparable to 15 mL/hr used by NASA and the US Army Research Laboratory in their earlier experiments. Figure B.33 depicts a schematic of test rig used for combining mist lubricant with an air stream. In this first configuration, the test liquid was kept in an accumulator that is pressurised to 30 bars. A commercial atomiser was used to generate the mist in a plenum, which has an inlet port to allow an air stream at approximately 7 bars to mix with the mist before flowing into the routing pipe. A drain port at the bottom of the plenum allows the draining of the test fluid that coalesces from the mixing. Multiple holes of 0.7 to 0.9 mm diameter were made along the pipe as shown in Figure B.34 to assess the spray characteristic across the pipe, which if successful, would be routed within the MGB to the internal gears and bearings.

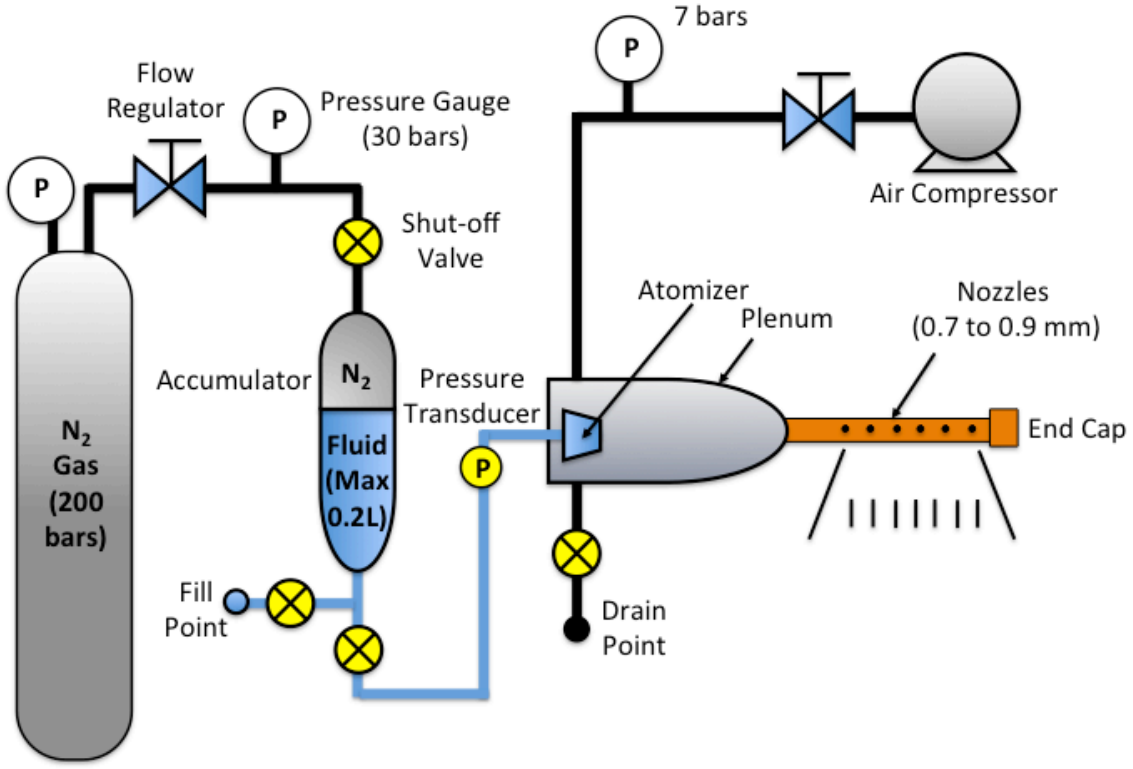

Figure B.33 Schematic of Spray Test Using an Air Stream (Source: Author)

Figure B.34 Routing pipe with Multiple Holes (Source: Author)

A second configuration, shown in Figure B.35, comprises a 5 mm diameter commercial nozzle[11] with a passage width of 0.3 mm that is attached to the end of a routing pipe. In this set up, the test fluid is piped directly to the nozzle at 30 bars through the routing pipe to generate the lubricant mist. An image of the nozzle is shown in Figure B.36, while that of the spray test is captured in Figure B.37. Owing to the relatively larger size of the passage width as compared to that of the fabricated nozzle, the resulting mist was more of a wet spray instead of a fine mist. This meant a high flow rate from the commercial nozzle, which is undesirable for the intended application.

[11] Part Number NZSA1801600D from Lee Products Limited, UK

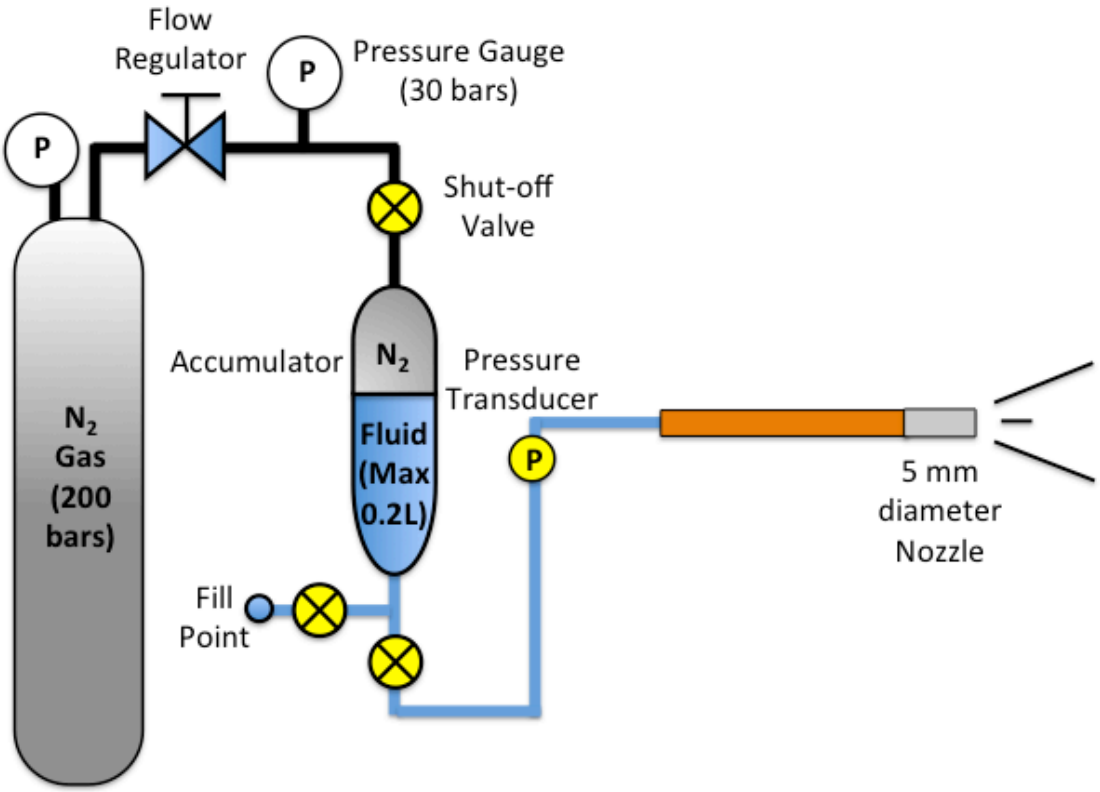

Figure B.35 Schematic of Spray Test Using a 5 mm Diameter Nozzle (Source: Author)

Figure B.36 Commercial Nozzle with 5 mm Housing Diameter and 0.3 mm Passage Width (Source: Author)

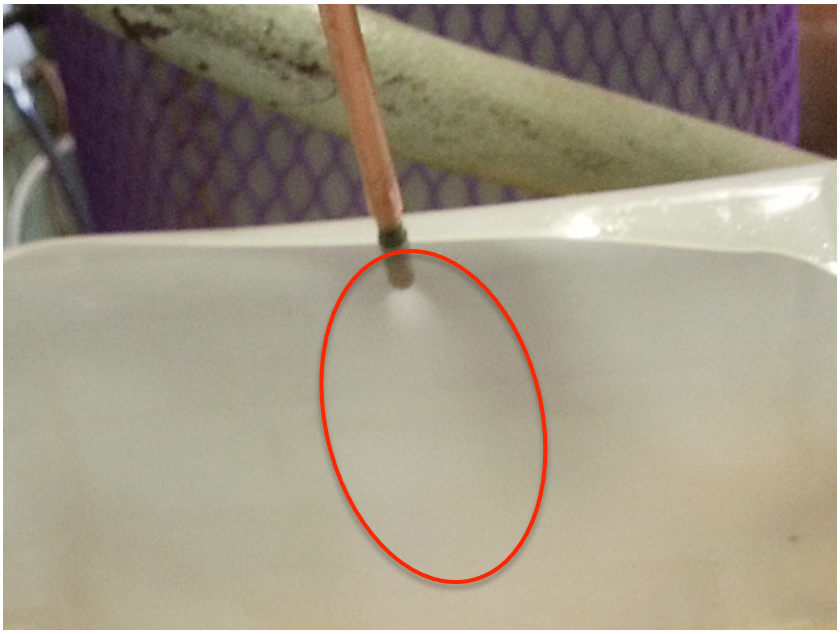

Figure B.37 Spray Test with Commercial Nozzle (Source: Author)

Amongst the three nozzle configurations that were subjected to the spray tests, the configuration involving the mixing of an air stream to deliver thioether in mist form was assessed to be the most feasible for an application within the confined spaces of the MGB. However, before the nozzle configuration could be fielded in the MGB lubrication experiments, the problem of coalescing along the routing pipe must be resolved.

The solution was a hybrid nozzle configuration that features a delivery air stream as well as the 5 mm commercial nozzle as shown in Figure B.38. It would deliver thioether lubricant in a controlled manner and at a low flow rate, while avoiding the drawback of thioether coalescing along the pipe. A controlled rate of thioether delivery is achieved via a piston chamber that is operated through mechanical means (such as an electric stepper motor). Thioether lubricant from the piston chamber gets channeled through a hypodermic needle, where it mixes with an incoming air stream and is carried towards the nozzle at the end of the pipe for atomisation (Figure B.39). This hybrid nozzle configuration could achieve a very low flow rate as compared to the configuration involving only the commercial nozzle. An air filter and dryer are used to ensure a clean and dry delivery air stream. A comparison between the hybrid nozzle and the other three nozzle configurations is summarised in Table B.10.

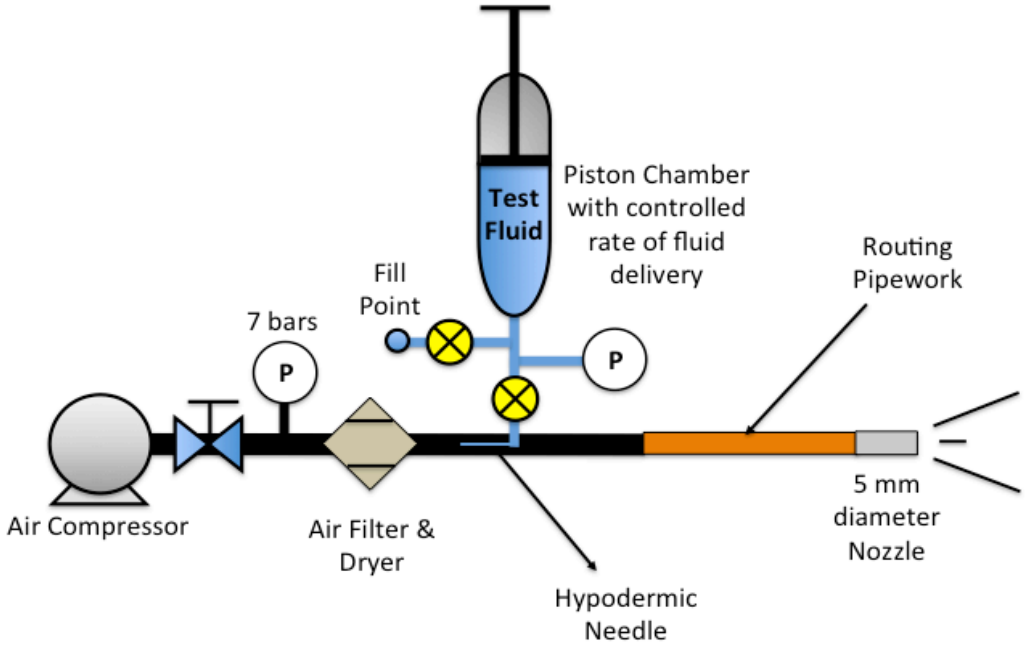

Figure B.38. Schematic of Spray Testing Using Hybrid Nozzle (Source: Author)

Figure B.39 Spray Test with Hybrid Nozzle (Source: Author)

Comparison of Nozzle Configurations					
S/N	**Description**	**Nozzle 1**	**Nozzle 2**	**Nozzle 3**	**Hybrid Nozzle**
1	Construction	Fabricated	Fabricated + Commercial	Commercial	Fabricated + Commercial
2	Air Stream	No	Yes	No	Yes
3	Plenum Mixing	No	Yes	No	Yes (Needle)
4	Passage Diameter	0.15 mm	0.7 to 0.9 mm	0.3 mm	0.3 mm
5	Flow Rate	Low	Very Low	Very High	Very Low
6	Fluid Coalescing	No (Clogging)	Yes	No	No

Table B.10 Comparison between Nozzle Configurations (Source: Author)

B.5 Thioether Routing within Main Gearbox

Following the selection of the hybrid nozzle for the thioether mist lubrication of the MGB, the next stage of the test rig design involved the routing of the thioether pipes and nozzles within the main gearbox. The routing pipework with the hybrid misting nozzles may gain access into the confined spaces of the MGB through four identified entry points (Figure B.40):

1. Access port each located on the LH and RH of the MGB main casing
2. Hole(s) drilled at the MGB sump plate
3. Hole(s) drilled at the MGB top cover

Figure B.40 Entry Points for Thioether Lubrication: Access Ports (Left) and Sump Plate (Right) (Source: Author)

The access ports at the sides of the MGB casing and holes drilled at the sump plate would facilitate the routing of thioether pipework to the gears and bearings located in the Fwd, Aft and Main Reduction Gear Modules, as well as the first stage Epicyclic Reduction Gear Module. The MGB top cover would provide lubrication access to the second stage of the Epicyclic Reduction Gear Module. The pipework and nozzles should be positioned in a way that does not hinder the operation of the existing oil jets and yet be able to provide effective thioether mist lubrication to the gears and bearings.

Unfortunately, given the limited internal spaces within the MGB, the routing of the thioether pipework and nozzles via the above mentioned entry points to all critical gear meshings and bearings could not be fully achieved. Under such circumstance, there was a need drill additional access holes on the MGB casing and to route the pipework and nozzles from the exterior. Examples of areas that require such alternative routing include one of the bearings for the Fwd Reduction Gear Module as well as the gear meshings at the Aft Reduction Module.

An added challenge to the routing of the thioether nozzles was the limited units of the selected commercial nozzles. There were only a total of 11 units available from the supplier within the timeframe of the MGB lubrication project. Therefore, the routing of the thioether pipework and nozzles took into consideration the availability of the nozzles and priority was given to critical areas of the MGB during normal operation (Fwd and Epicyclic Reduction Gear Modules as advised by the Helicopter Manufacturer). The initial proposed routing of thioether pipework and nozzles within the MGB are captured in Figures B.41 to B.45.

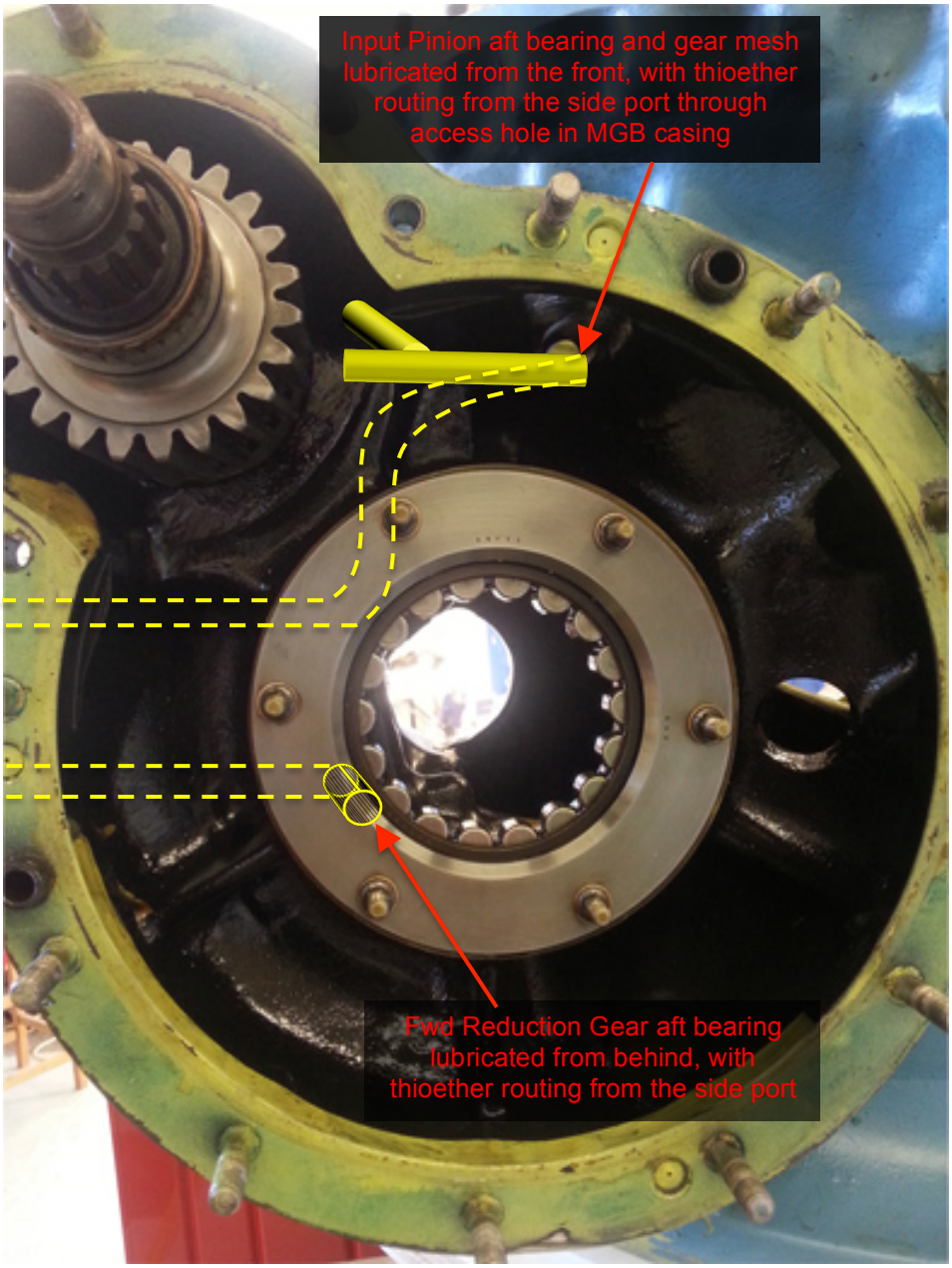

Figure B.41 Thioether Routing for Forward Reduction Module (Part 1) (Source: Author)

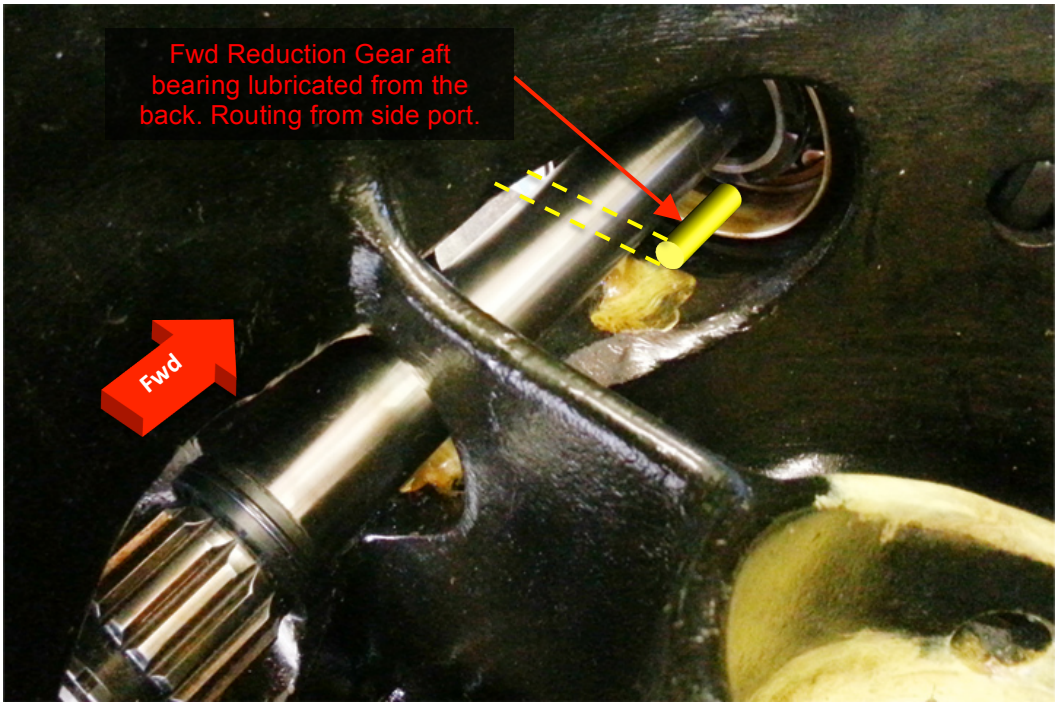

Figure B.42 Thioether Routing for Forward Reduction Module (Part 2) (Source: Author)

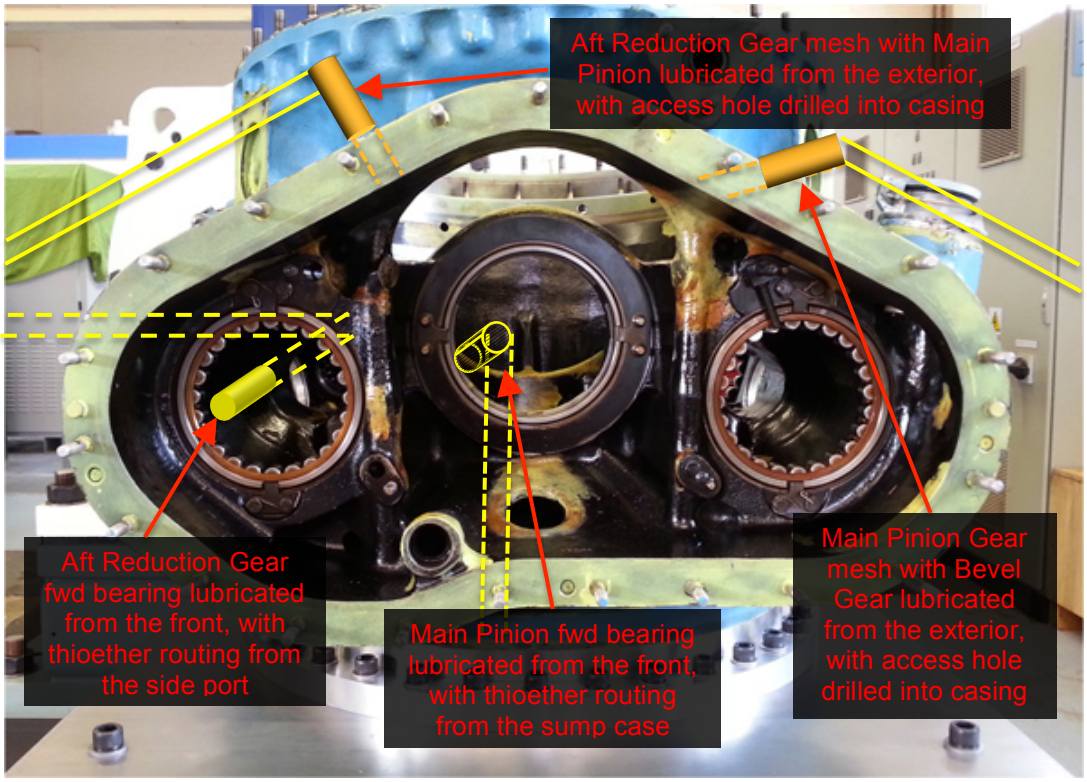

Figure B.43 Thioether Routing for Aft Reduction Module (Source: Author)

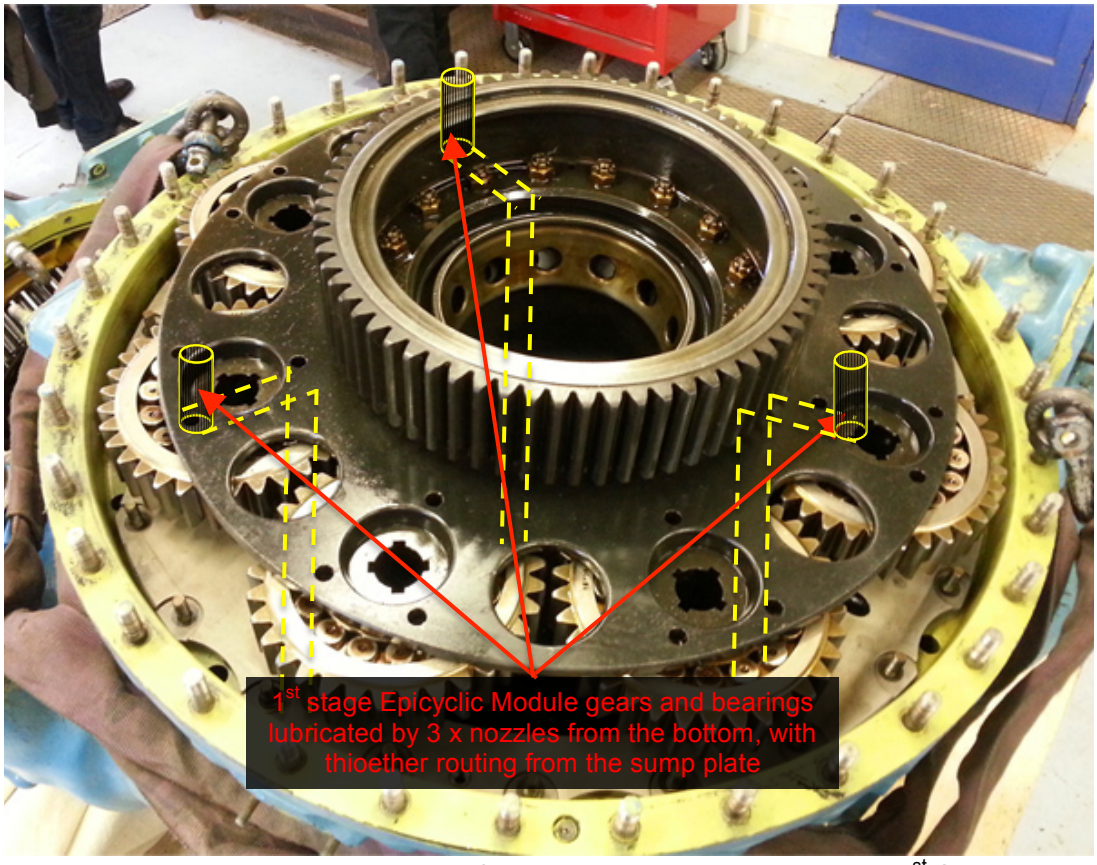

Figure B.44 Thioether Routing for Epicyclic Reduction Module (1st Stage)
(Source: Author)

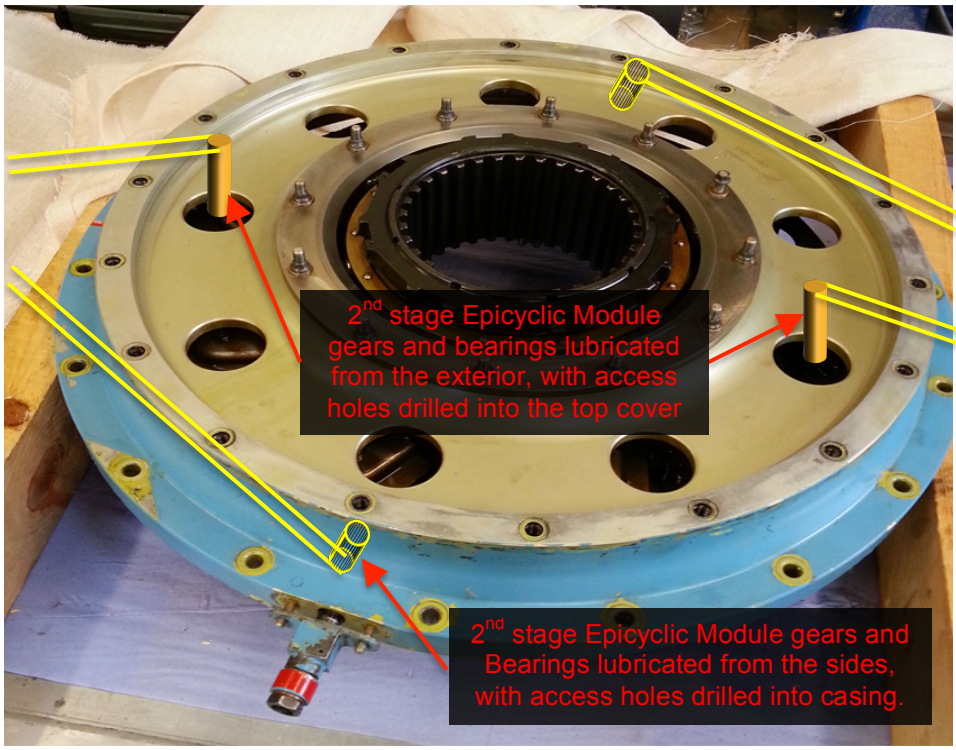

Figure B.45 Thioether Routing for Epicyclic Reduction Module (2nd Stage)
(Source: Author)

The initial proposal for the routing of the thioether pipework and nozzles was time consuming. It was also risky as it involved routing the metal pipes close to high speed rotating components that would damage the internal gears and bearings if they were not properly secured.

The alternative proposal was to route the thioether through the existing oil lubrication port and internal galleries and there were several advantages to this approach. It would allow the delivery of thioether mist lubricant to all the MGB gears and bearings through the existing oil nozzles, thus ensuring a complete coverage of the MGB rotating components. There would be no damage risk to the rotating components since no metal pipes were introduced. The approach required no additional time and effort, as no pipework was necessary. Lastly, because only one commercial nozzle would be utilised to generate the thioether mist at the inlet oil lubrication port of the MGB, the remaining nozzles could be employed to supplement mist generation through other access ports. This would provide improved coverage of the thioether mist within the MGB. One drawback with the solution was the possible clogging of the existing oil nozzles and the coalescing of thioether liquid within the internal galleries, which would affect the performance of the MGB oil lubrication system. This could be tackled by flushing the MGB with lubrication oil following each MGB experiment with thioether mist. The locations of the access ports for thioether mist lubrication together with the existing inlet port are depicted in Figure B.46. Figures B.47 to B.52 provide details of these access ports.

As the thioether mist access ports connect directly to the MGB internal oil galleries, there was a need to introduce check valves (Figure B.53) to prevent the outflow of lubrication oil during normal operation. The check valves have quick release connectors that allow the efficient coupling of thioether flexible hoses to the MGB.

The schematic of the finalised thioether mist lubrication system is depicted in Figure B.54. It comprises a piston chamber that is driven by a stepper motor (Figure B.55). The motor speed has been set to deliver thioether from the chamber at a flow rate of 165 mL/hr based on the usage of 11 commercial nozzles for mist generation. A spring-loaded check valve downstream of the chamber allows passage of the thioether only when the pressure has reached about 7.6 bars. Pressurised thioether liquid is then passed through a hypodermic needle, where it will mix with dry and clean compressed air at 7 bars before flowing towards the nozzle manifold (Figure B.56). At the manifold the mixture of air and thioether is split into 11 chambers, each with a 5 mm commercial nozzle to atomise the mixture into a fine mist. The mist is channelled to the 11 access ports of the MGB using flexible tubes and check valves (Figure B.57).

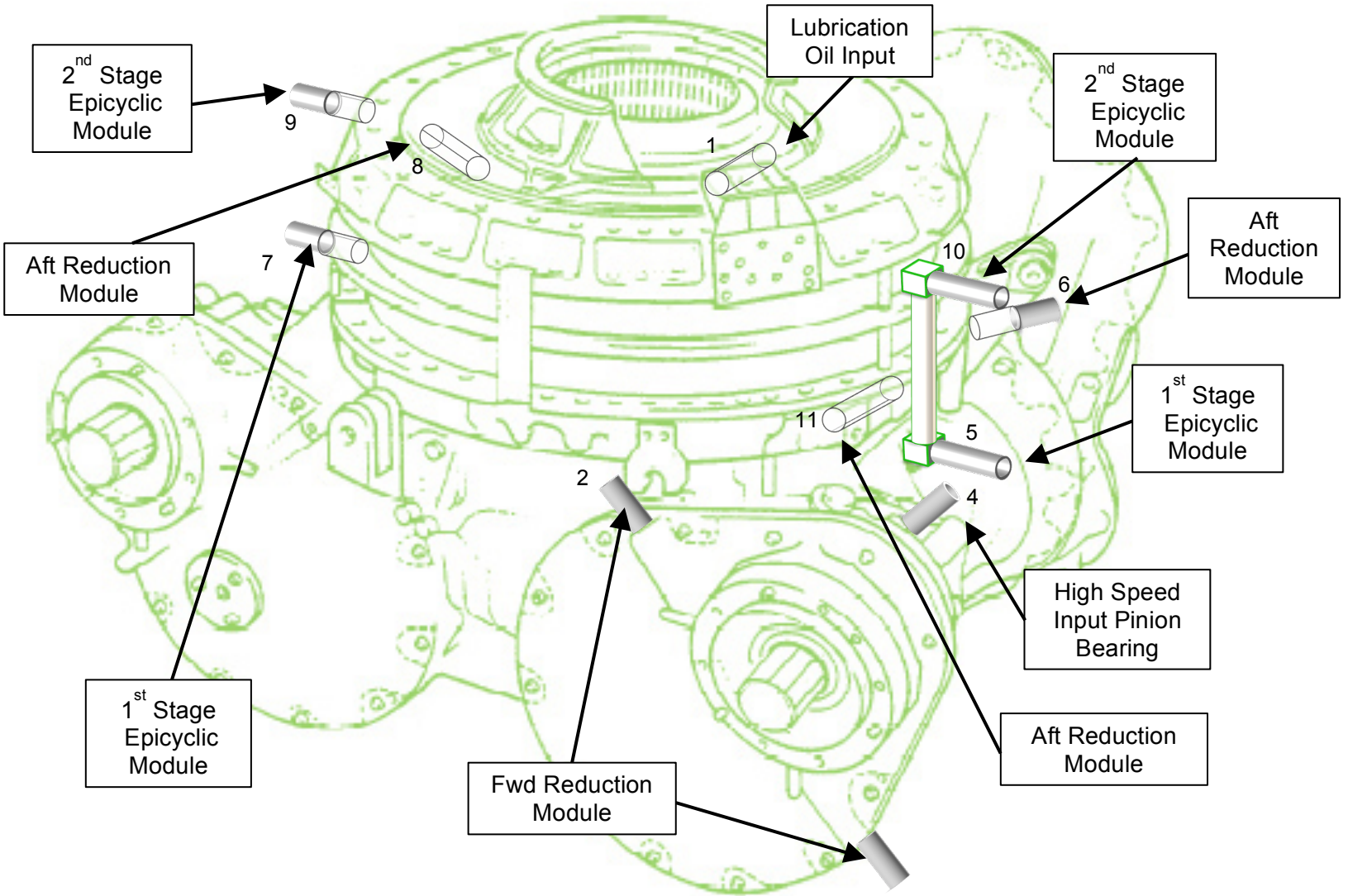

Figure B.46 Location of Thioether Mist Lubrication Access Ports (Source: Author)

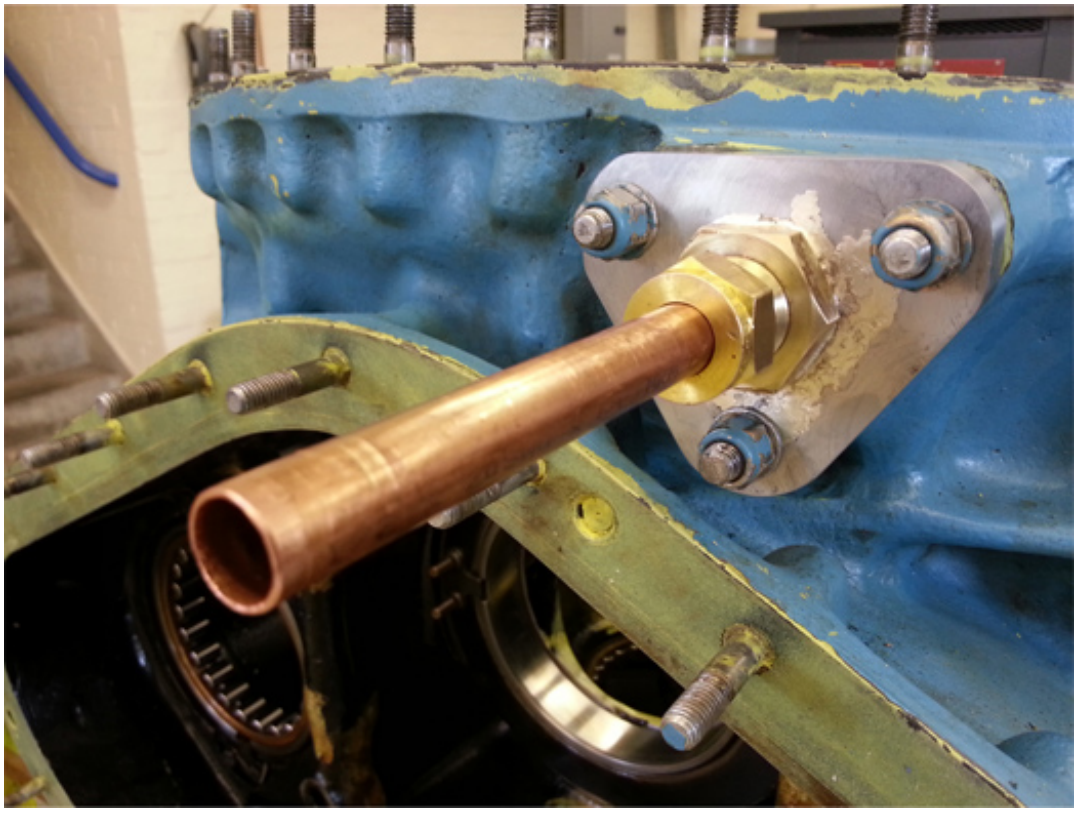

Figure B.47 Main Inlet Port (Source: Author)

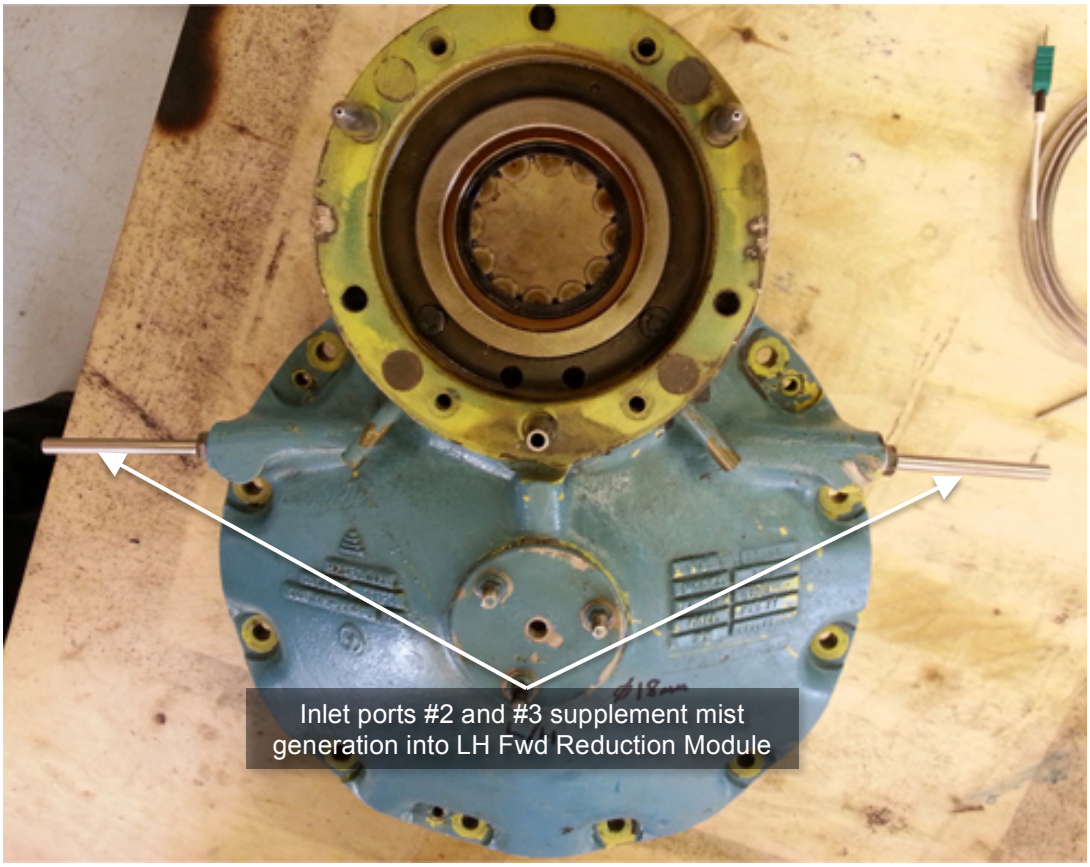

Figure B.48 Access Ports to LH Fwd Reduction Module (Source: Author)

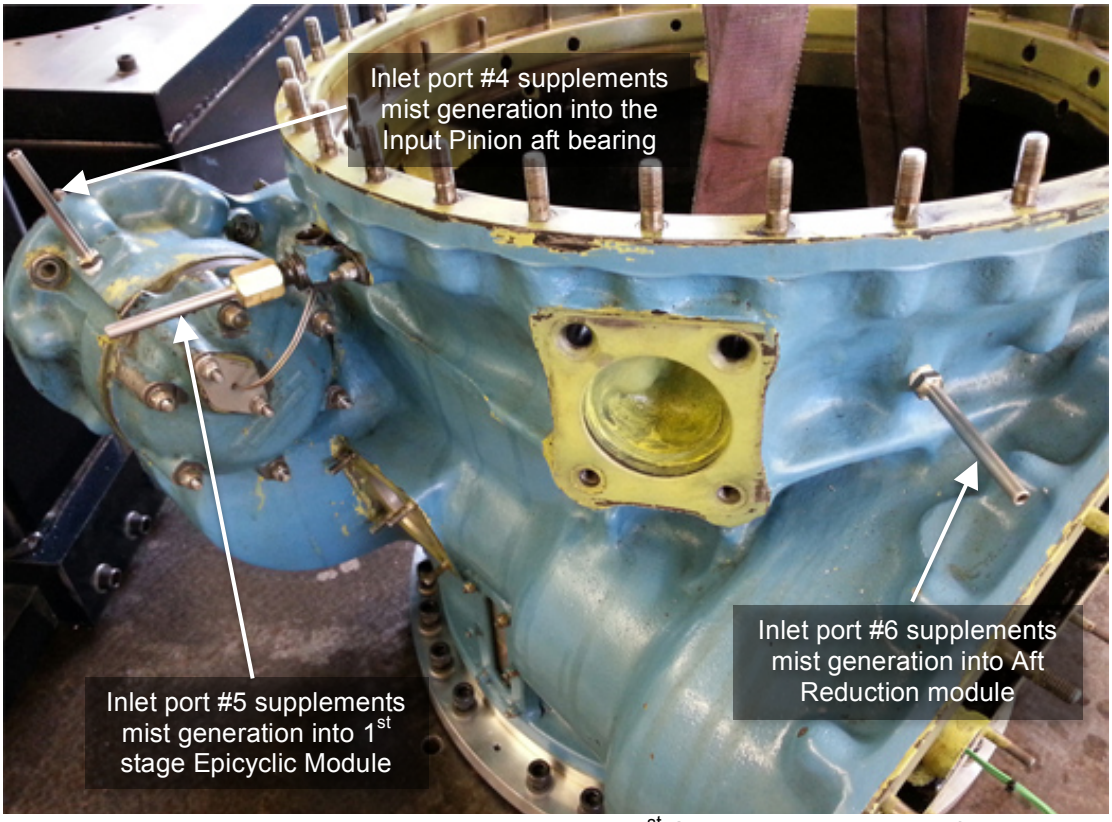

Figure B.49 Access Ports to LH Fwd Reduction, 1st Stage Epicyclic and Aft Reduction Modules (Source: Author)

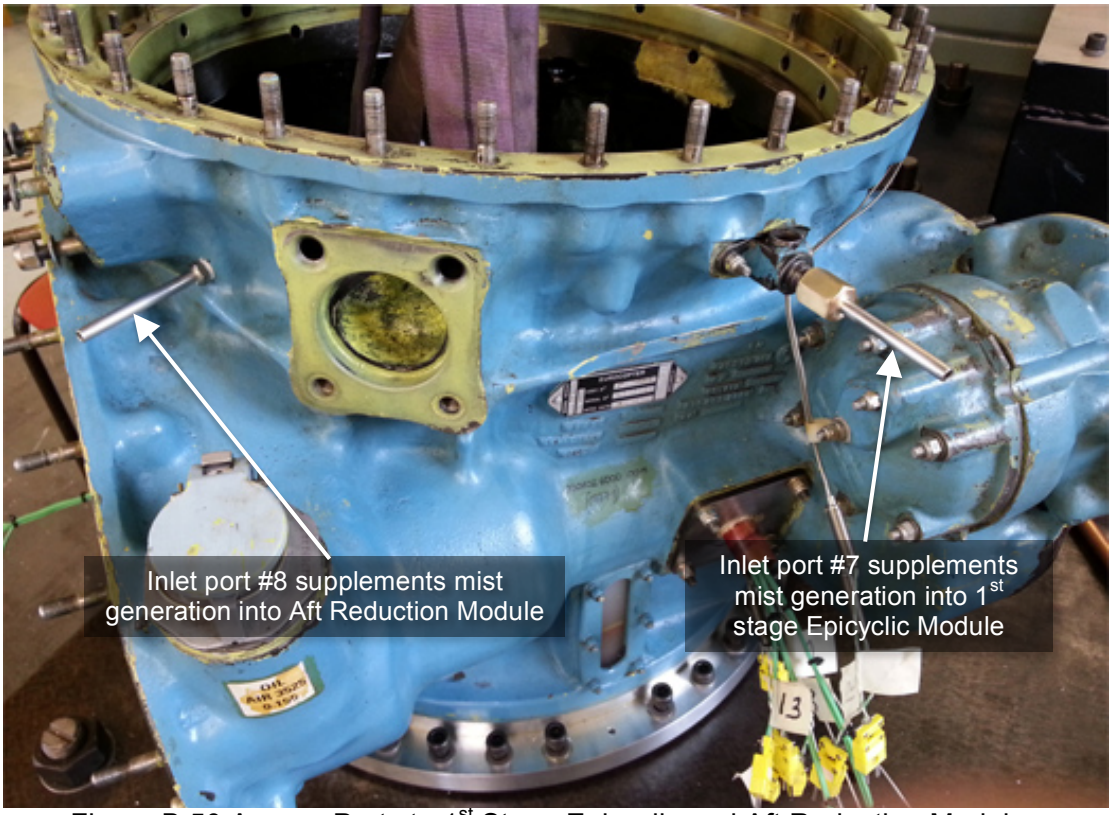

Figure B.50 Access Ports to 1st Stage Epicyclic and Aft Reduction Modules (Source: Author)

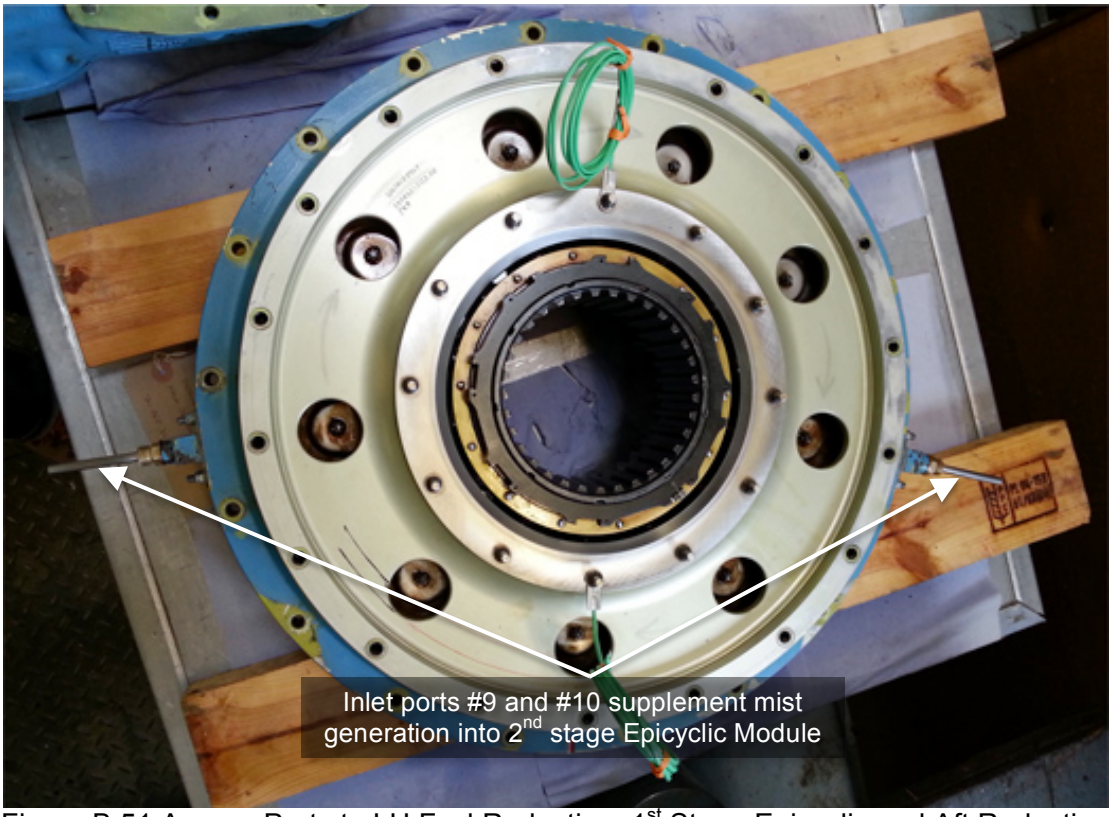

Figure B.51 Access Ports to LH Fwd Reduction, 1st Stage Epicyclic and Aft Reduction Modules (Source: Author)

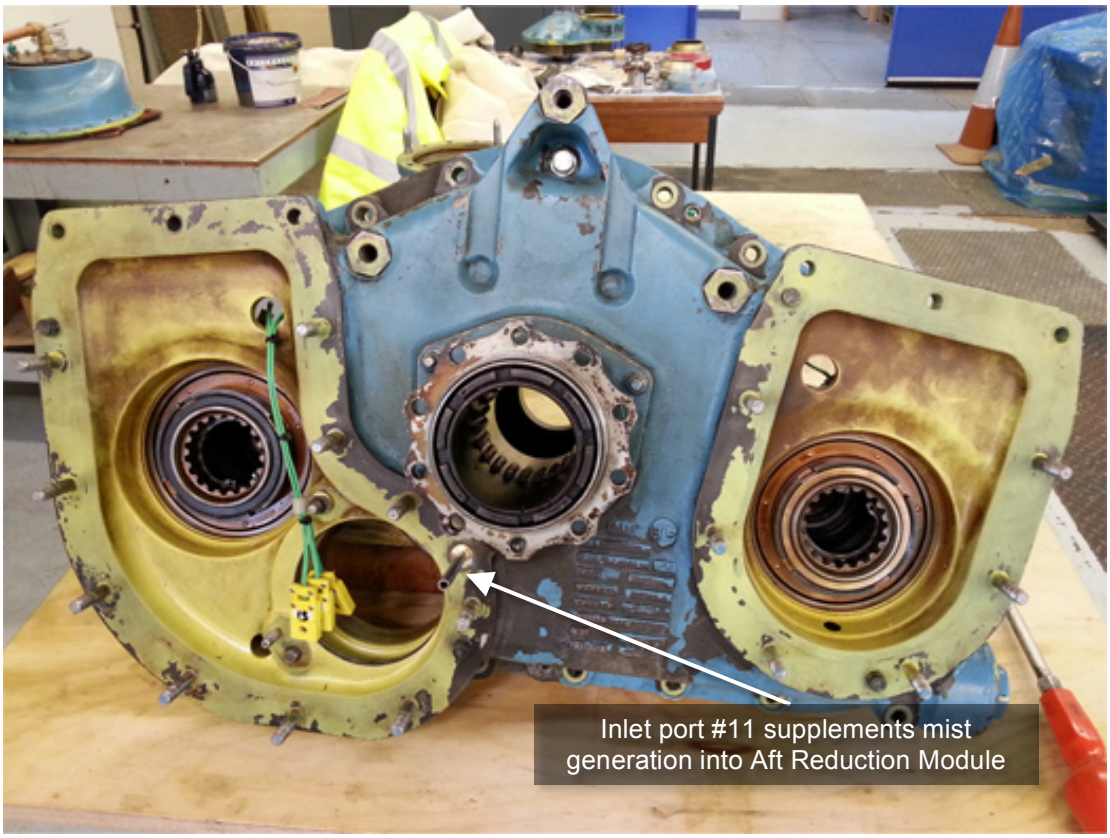

Figure B.52 Access Port to Aft Reduction Module (Source: Author)

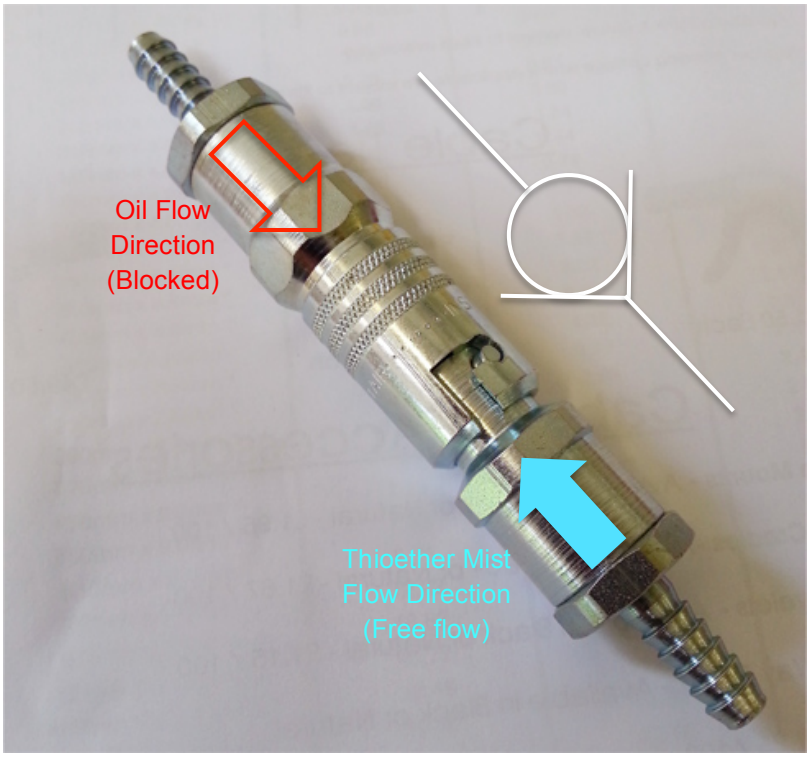

Figure B.53 Check Valve for Thioether Mist Generation (Source: Author)

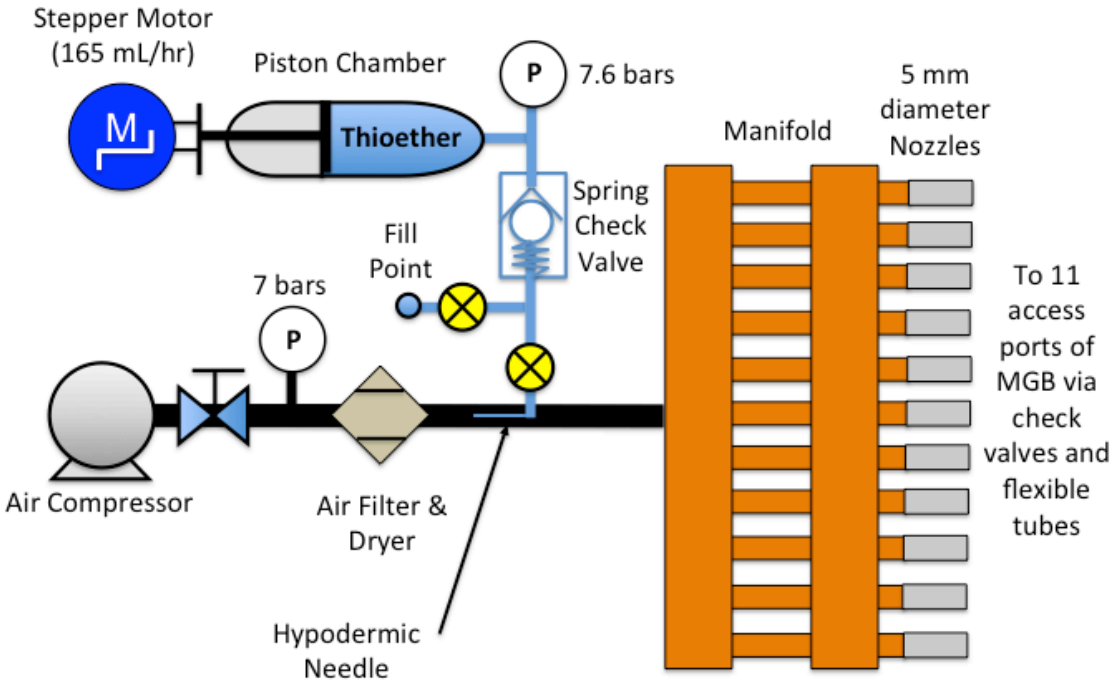

Figure B.54 Schematic for Finalised Thioether Mist Lubrication of MGB (Source: Author)

Figure B.55 Stepper Motor for Controlled Delivery of Thioether
(Source: Author)

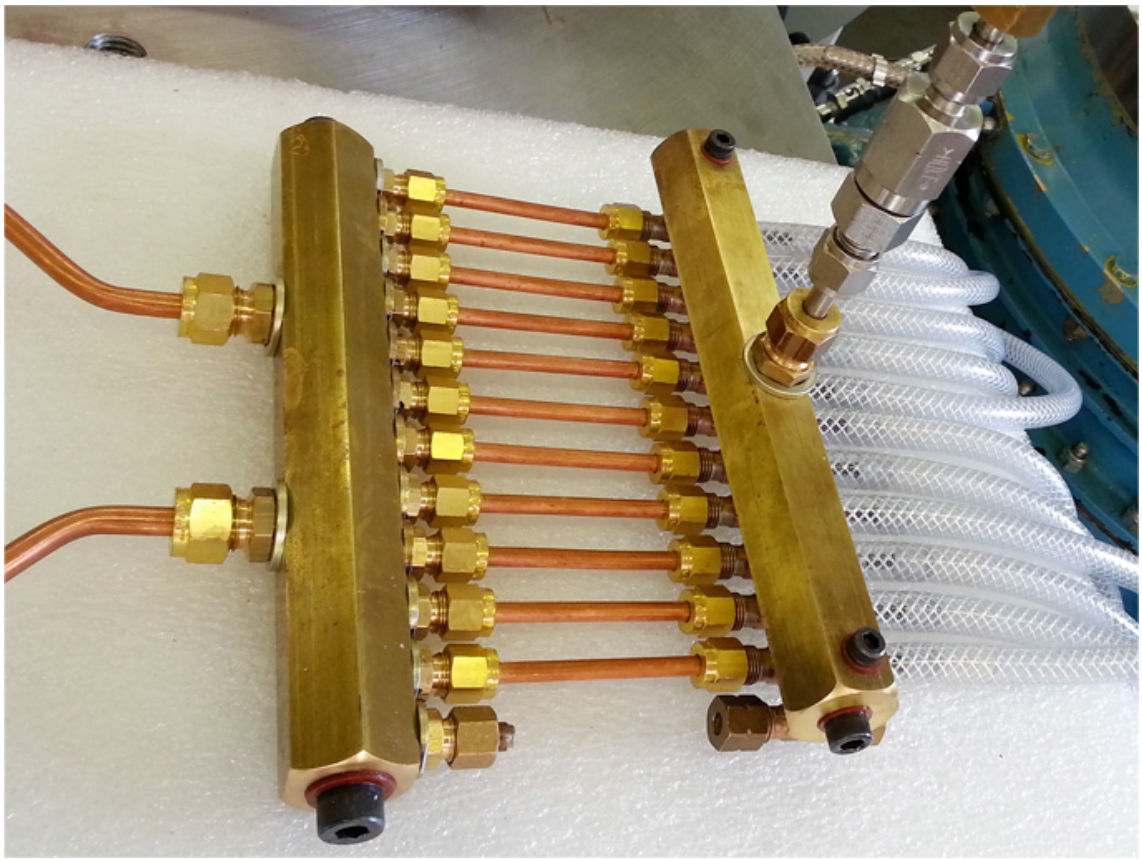
Figure B.56 Nozzle Manifold for Thioether Mist Generation
(Source: Author)

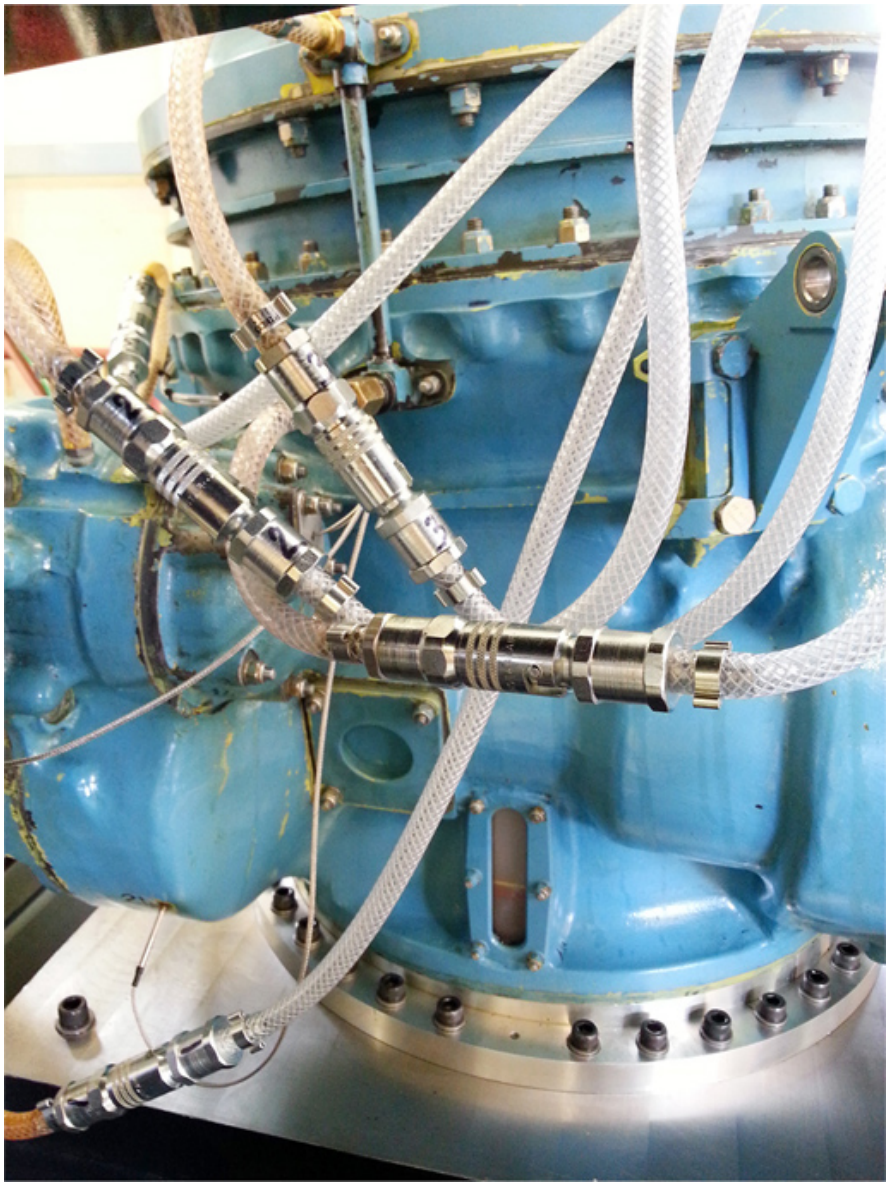

Figure B.57 Flexible Tubes and Check Valves for Thioether Mist Generation (Source: Author)

The inert properties of MCS-293^{TM} are listed clearly in the corresponding Technical Data Sheet (TDS) from Santolubes®, which states that the chemical "is compatible with most metals, plastics, and elastomers and is essentially nontoxic, especially when proper hygienic practices are employed"[26]. This implies a good chemical compatibility between the thioether lubricant and the elastomeric seals, bearings and gears within the MGB. In this regard, no leaks from the gearbox seals as well as damage to the bearings and gears are expected following the thioether mist lubrication tests. There is also no need for special protective equipment when handling the thioether lubricant.

B.6 Instrumentation and Data Acquisition

B.6.1 Temperature Measurement

As the temperature profile of the internal gears and bearings within the MGB is one of the important performance measurements for the lubrication experiment, the selection of the appropriate temperature sensors is critical to the success of the project. Table B.11 compares the properties of common sensors used in temperature measurements.

Comparison of Temperature Sensors				
S/N	**Property**	**Thermocouple**	**Resistance Temperature Detector (RTD)**	**Thermistor**
1	Temperature Range	-267 to 2316°C	-240 to 649°C	-100 to 500°C
2	Accuracy	Good	Best	Good
3	Linearity	Better	Best	Good
4	Sensitivity	Good	Better	Best
5	Response	Best	Good	Best
6	Cost	Best	Good	Better
7	Signal Conditioning Requirements	- Amplification - Filtering - Cold-Junction Compensation	- Amplification - Filtering - Current Excitation	- Amplification - Filtering - Voltage Excitation

Table B.11 Comparison between Temperature Sensors (Source: National Instruments)

The thermocouple was selected as the preferred choice of temperature sensor for the MGB test rig given its low cost and fast response time. In particular, its quick reaction to temperature variation allows the temperature of the MGB gears and bearings be monitored closely during an “oil-off” lubrication condition. Thermocouples, which are rugged in design, are also more suitable for operating environments subjected to shocks and vibrations such as a MGB. They also come in various physical forms, such as washer, sheath and probe, to suit the installation within the MGB test rig.

The type “K” thermocouple with nickel-chromium alloy and nickel-aluminium alloy as the materials of the conductors (Table B.12) are used for the MGB test rig given its low cost, relatively good voltage response and a wide range of operating temperatures (Figure B.58).

Three forms of type “K” thermocouples are used to instrument the MGB test rig. The grounded washer form thermocouples (Figure B.59) are installed on the studs of the bearing housing retainer plates found in the Fwd Reduction Gear Module, the Aft Reduction Gear Module and the Epicyclic Reduction Gear Module. Simply mounted on the studs and secured via stop nuts, they allow easy measurement of a bearing temperature through the housing and the retainer plate.

The mineral insulated sheath form thermocouples (Figure B.60) are used for measuring the temperature of the bearings in the Aft Reduction Gear Module and the Main Reduction Gear Module, where retainer taps are used to secure the bearings. They are welded to the retainer taps at the tips to measure the temperature of the bearings. The Inconel® Alloy 600 metal sheath, which is 1.5 mm in outer diameter and 1000 mm in length, is flexible to allow the forming of the sheath to suit the routing of the thermocouple leads.

Lastly, the grounded probe form thermocouples (Figure B.61) are installed through access holes drilled into the casings of the Fwd Reduction Gear Module, the Aft Reduction Gear Module and the Epicyclic Reduction Gear Module. The rigid probe tips are place in direct contact with the bearing housings to allow temperature measurements not accessible by the other forms of thermocouples. Measuring 3 mm in outer diameter, they allow unobtrusive holes to be made on the casings. The access holes are sealed to prevent the leakage of lubricant oil during operation of the MGB.

Composition of Thermocouple Types			
S/N	**Thermocouple Type**	**Conductor (Positive)**	**Conductor (Negative)**
1	B	Platinum – 30% Rhodium	Platinum – 6% Rhodium
2	E	Nickel-Chromium Alloy	Copper-Nickel Alloy
3	J	Iron	Copper-Nickel Alloy
4	K	Nickel-Chromium Alloy	Nickel-Aluminum Alloy
5	N	Nickel-Chromium-Silicon Alloy	Nickel-Silicon-Magnesium Alloy
6	R	Platinum – 13% Rhodium	Platinum
7	S	Platinum – 10% Rhodium	Platinum
8	T	Copper	Copper-Nickel Alloy

Table B.12 Letter Designations and Composition of Thermocouples
(Source: National Instruments)

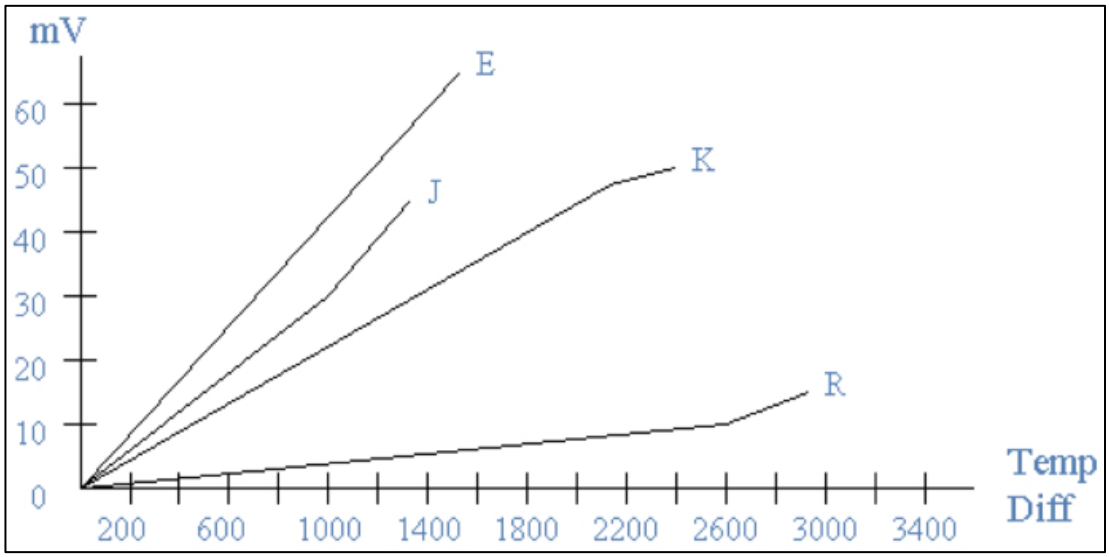

Figure B.58 Electrical Response for Type “E, J, K and R” Thermocouples
(Source: National Instruments)

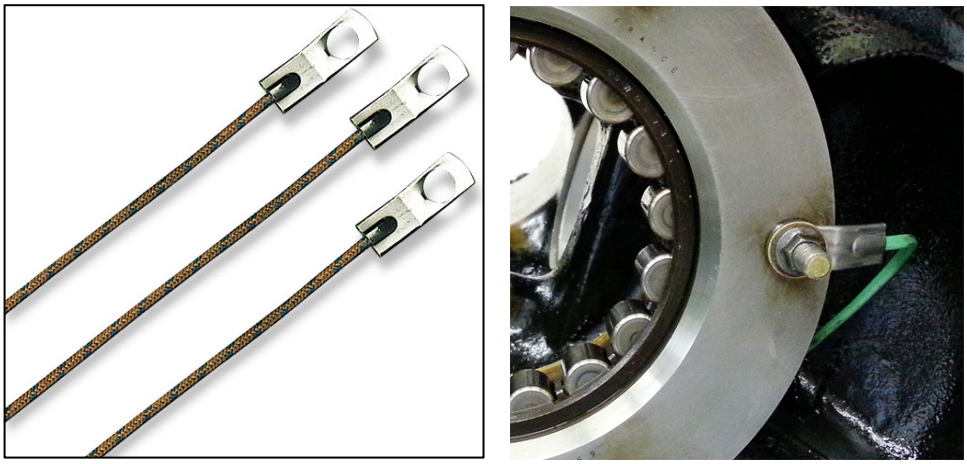

Figure B.59 Washer Form Type “K” Thermocouples (Left) and Installation (Right)
(Sources: www.omega.co.uk and Author)

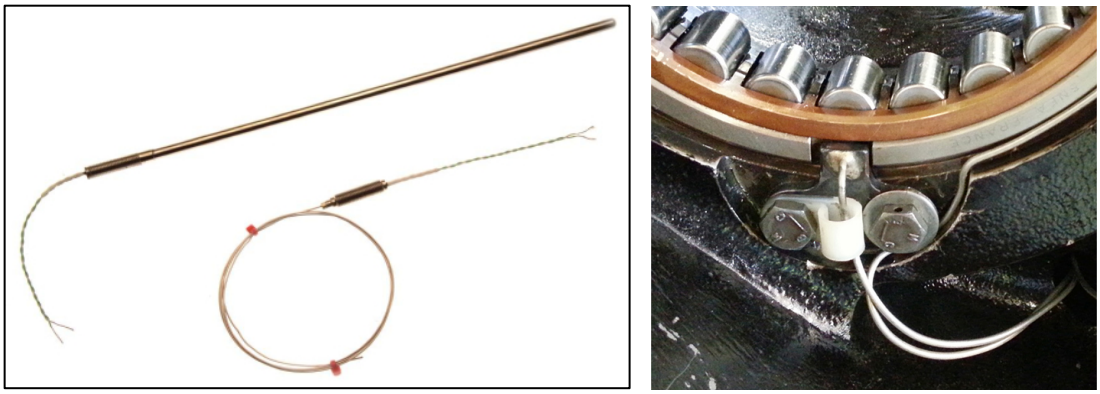

Figure B.60 Sheath Form Type “K” Thermocouple (Left) and Installation (Right)
(Source: www.uk.rs-online.com and Author)

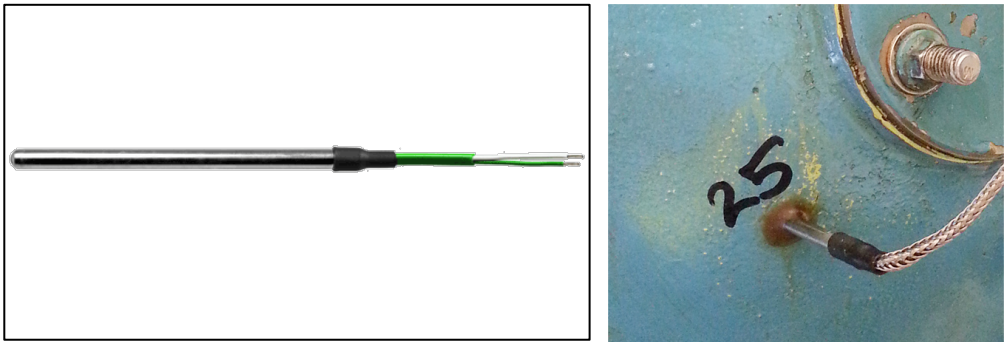

Figure B.61 Probe Form Type “K” Thermocouple (Left) and Installation (Right)
(Source: www.thermosense.co.uk and Author)

Besides the MGB gears and bearings, there are also temperature measurements for the supply and return of the lubrication oil for the MGB and the speed-increasing gearbox, as well as the bearings of the speed-increasing gearbox. These are necessary to ensure proper operation of the MGB test rig. A total of 32 thermocouples are used on the MGB test rig. Their locations are shown in Figures B.62 to B.77, while their label names are listed in Table B.13.

Sensors Summary	
Description	**Number**
Thermocouple (washer form)	10
Thermocouple (sheath form)	10
Thermocouple (probe form)	8

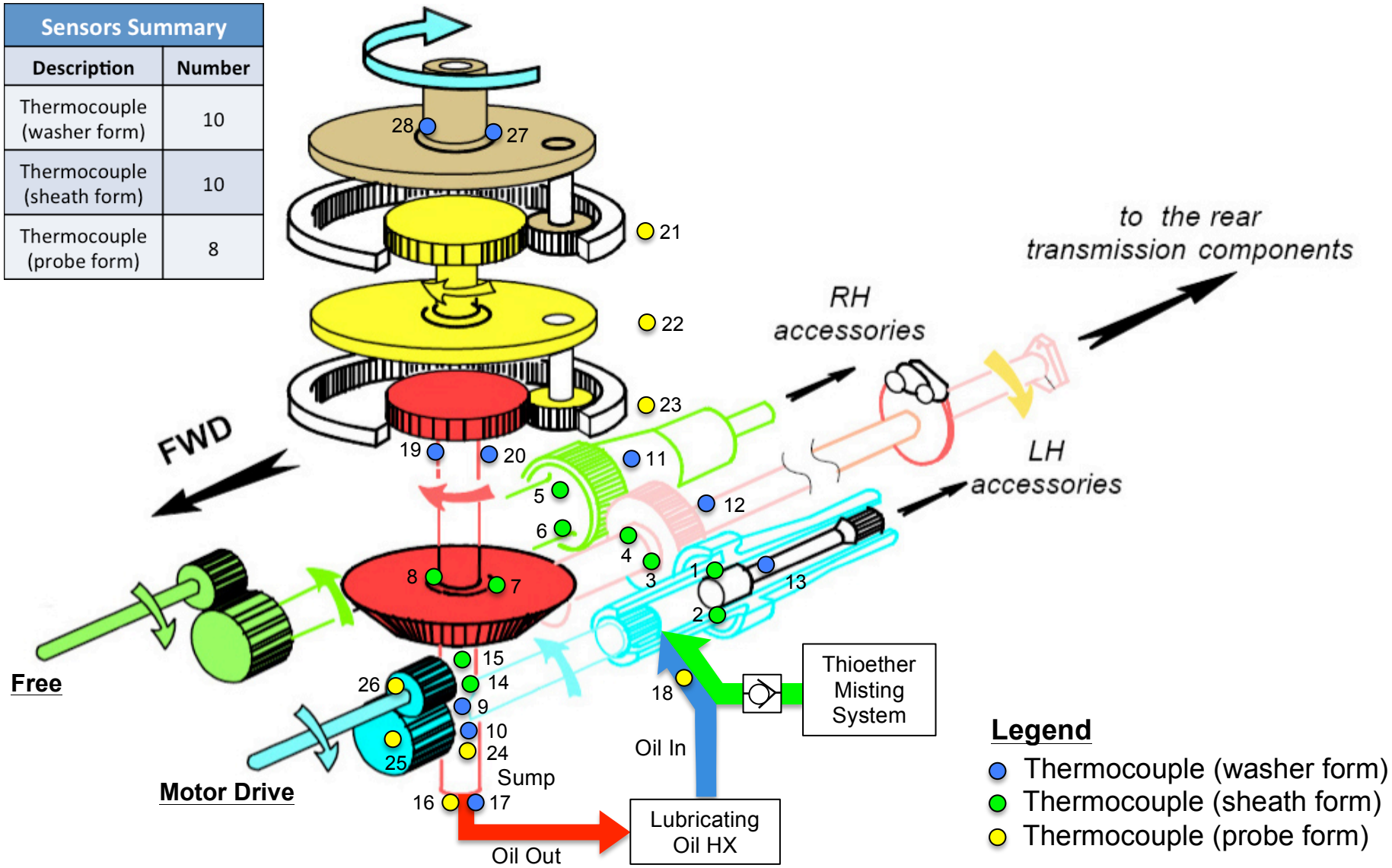

Figure B.62 Thermocouple Locations on MGB (Source: Helicopter Manufacturer and Author)

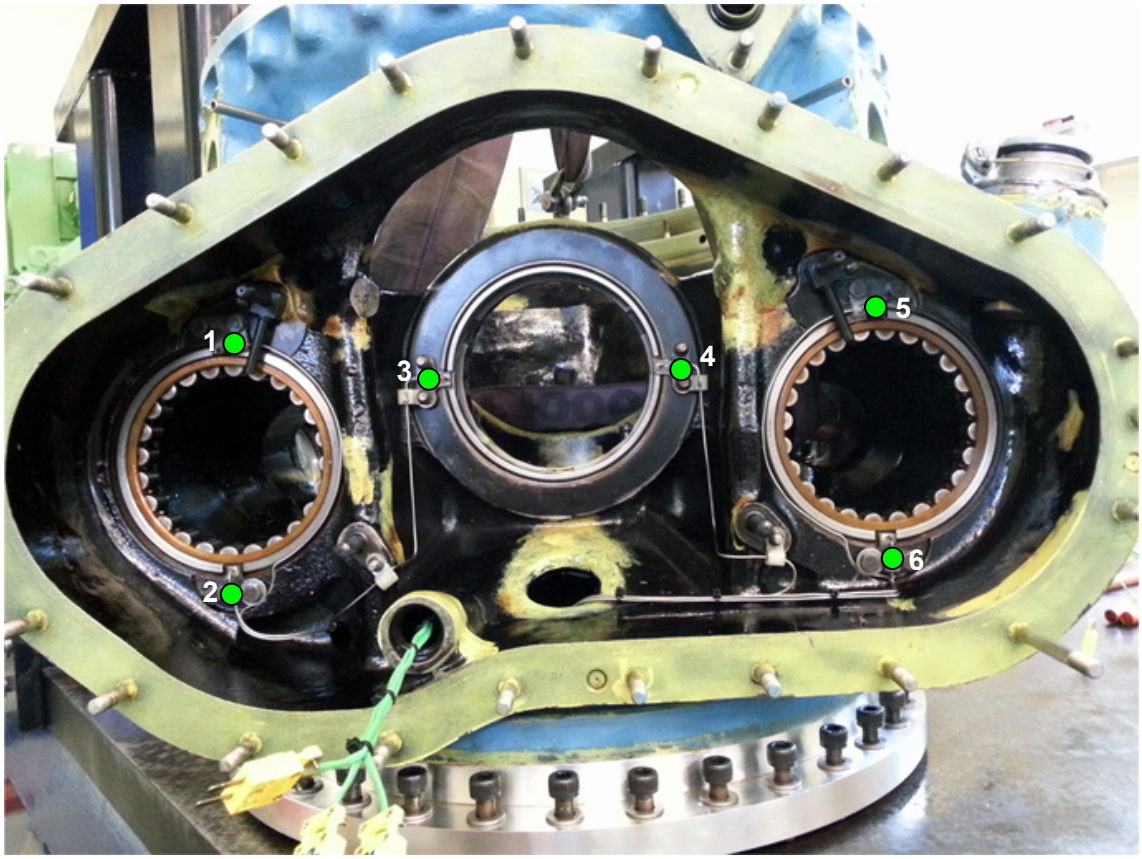

Figure B.63 Thermocouple Locations #1 to 6 (View from Aft) (Source: Author)

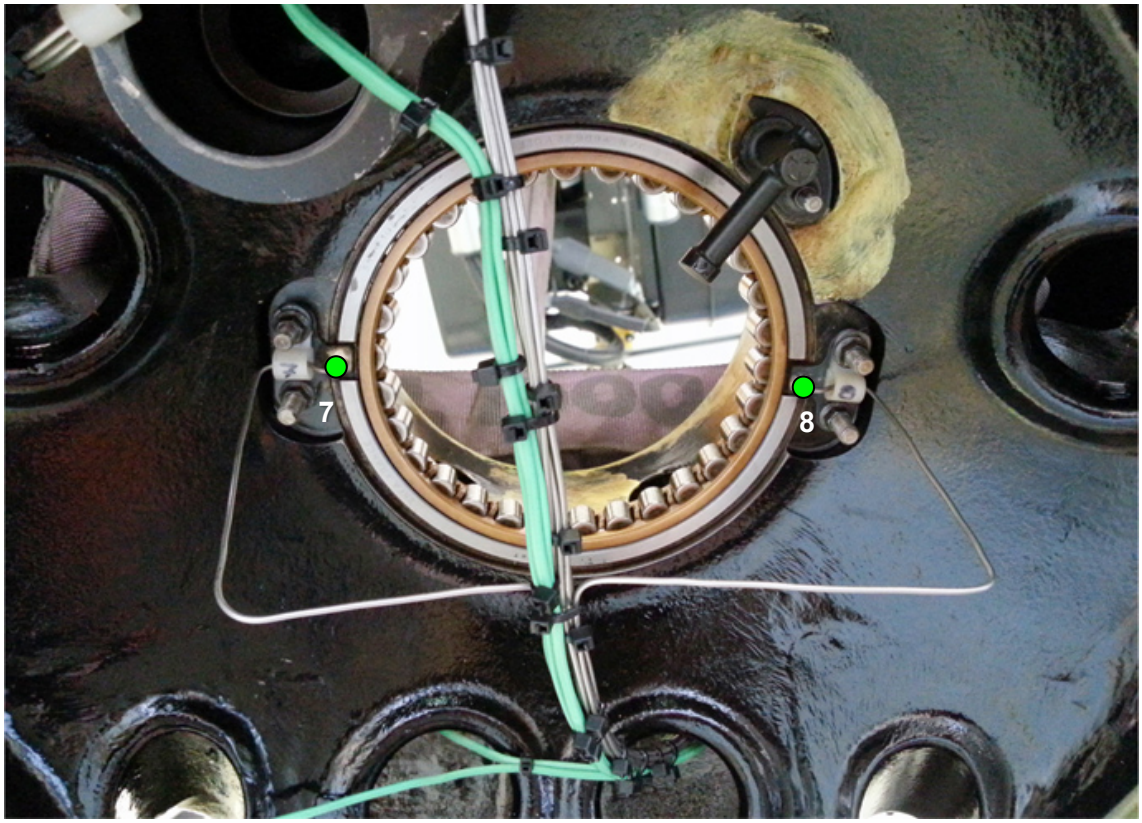

Figure B.64 Thermocouple Locations #7 and 8 (View from Sump) (Source: Author)

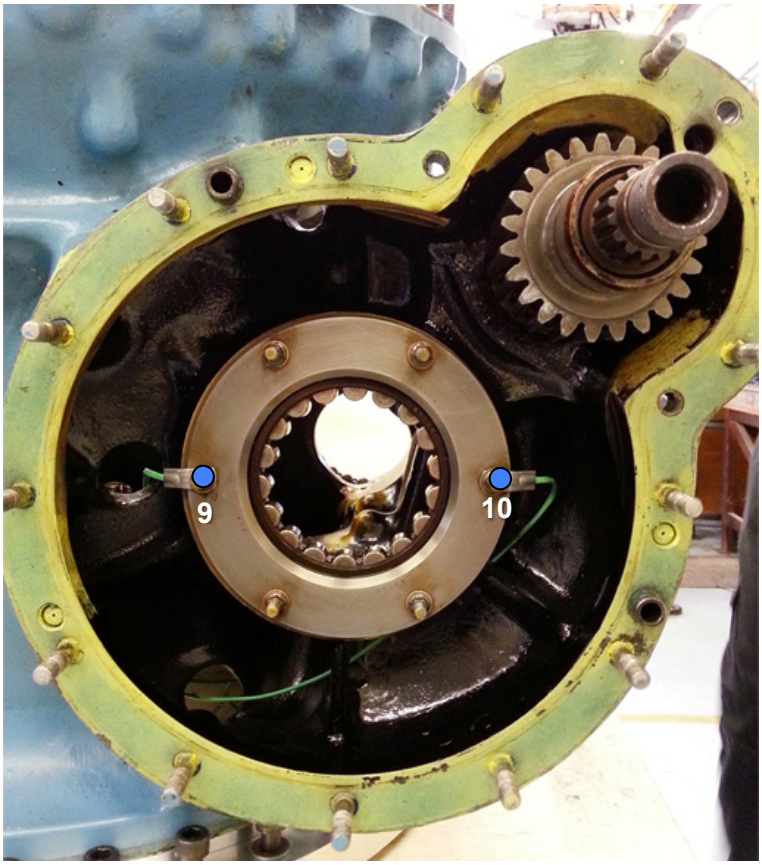

Figure B.65 Thermocouple Locations #9 and 10 (Source: Author)

Figure B.66 Thermocouple Locations #11 to 13 (Source: Author)

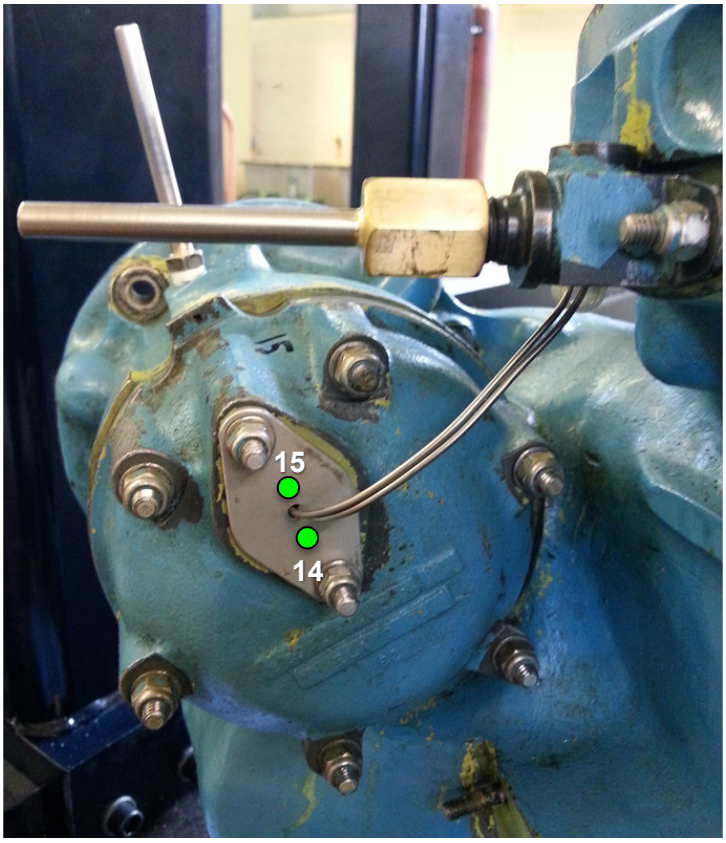

Figure B.67 Thermocouple Locations #14 and 15 (Source: Author)

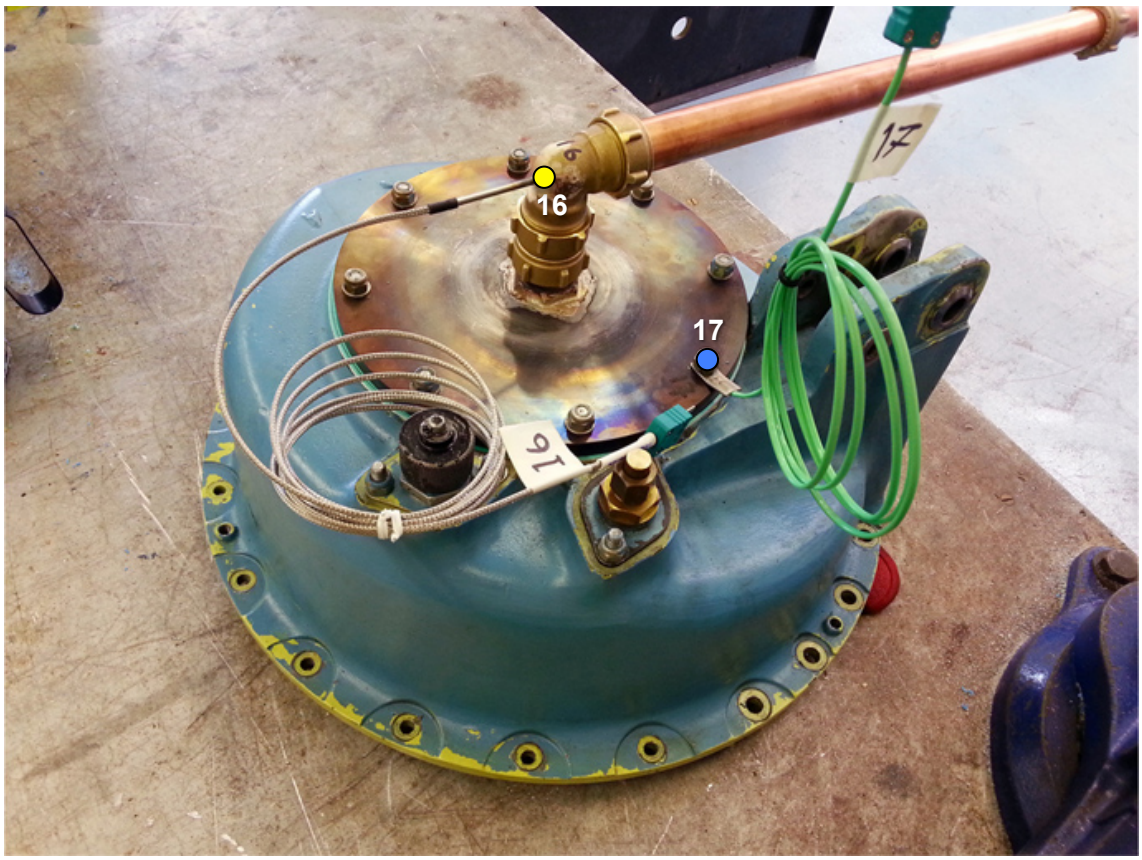

Figure B.68 Thermocouple Locations #16 and 17 (Source: Author)

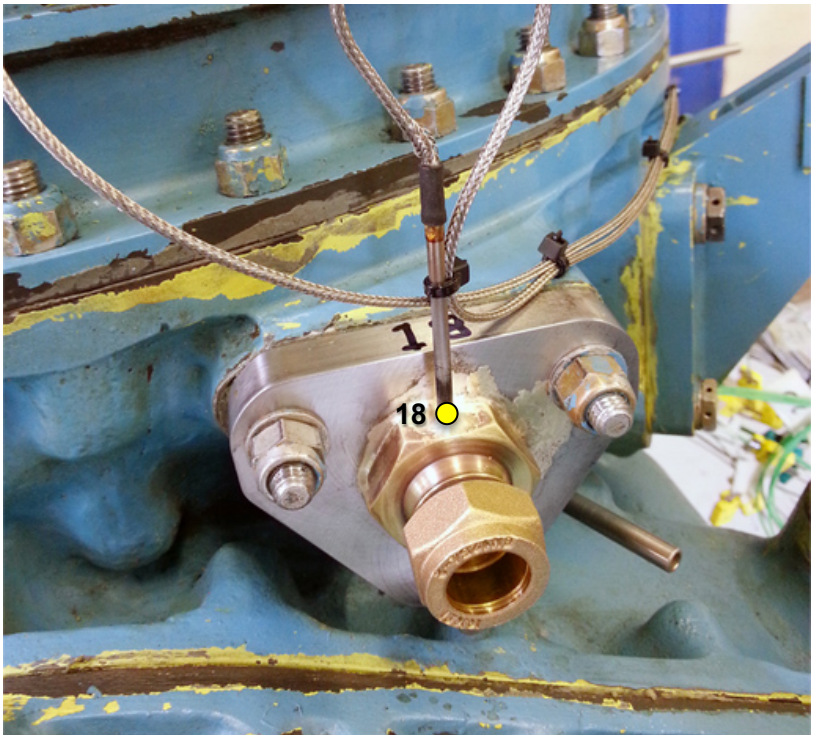

Figure B.69 Thermocouple Location #18 (Source: Author)

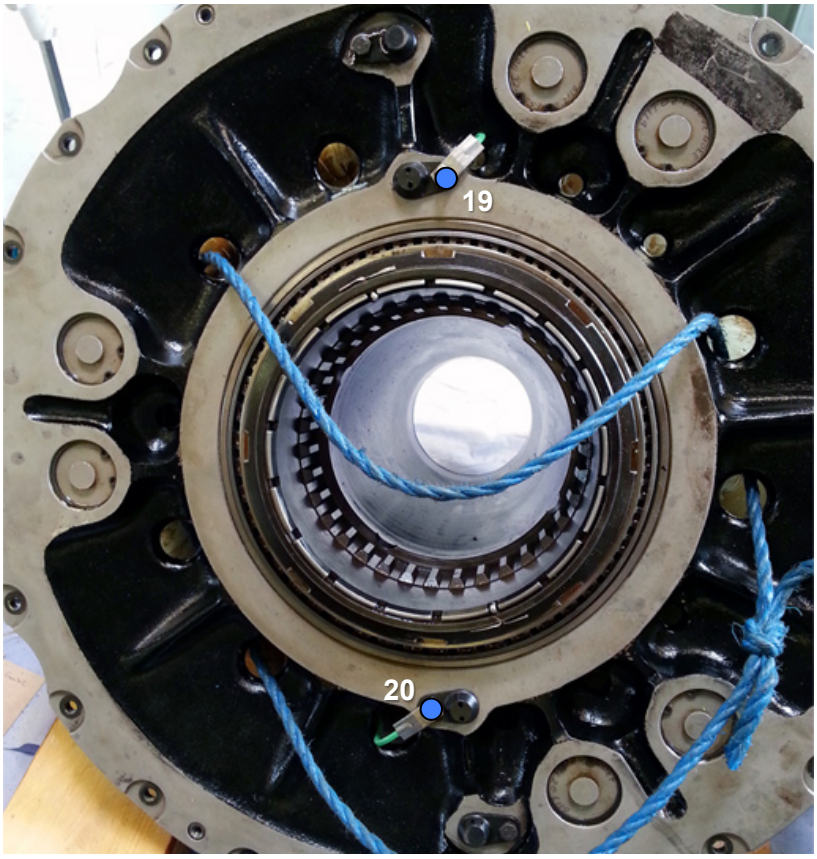

Figure B.70 Thermocouple Locations #19 and 20 (Source: Author)

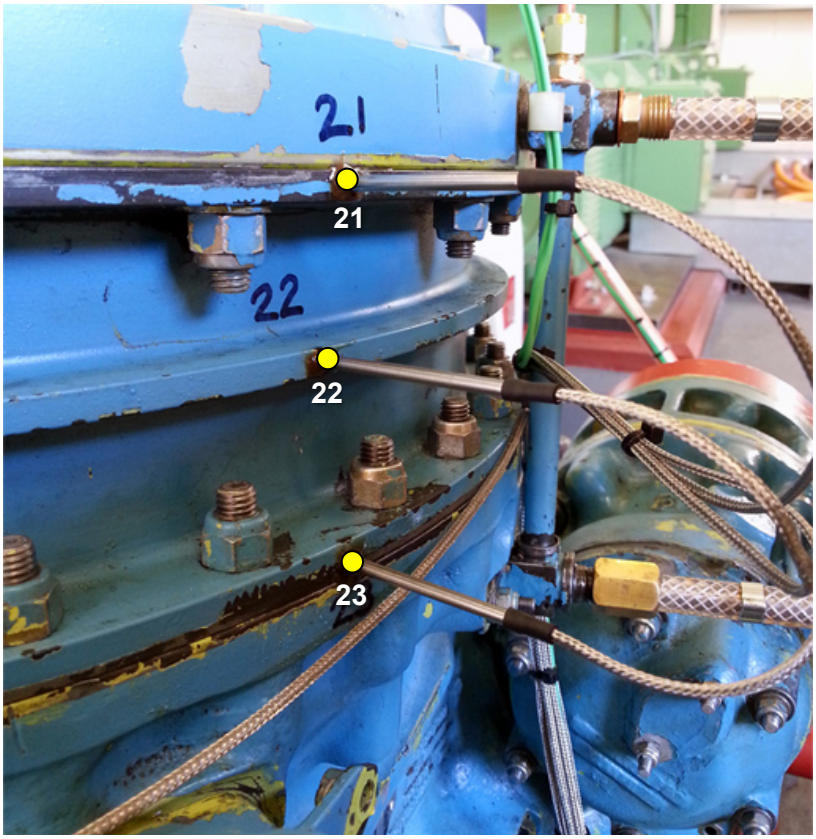

Figure B.71 Thermocouple Locations #21 to 23 (Source: Author)

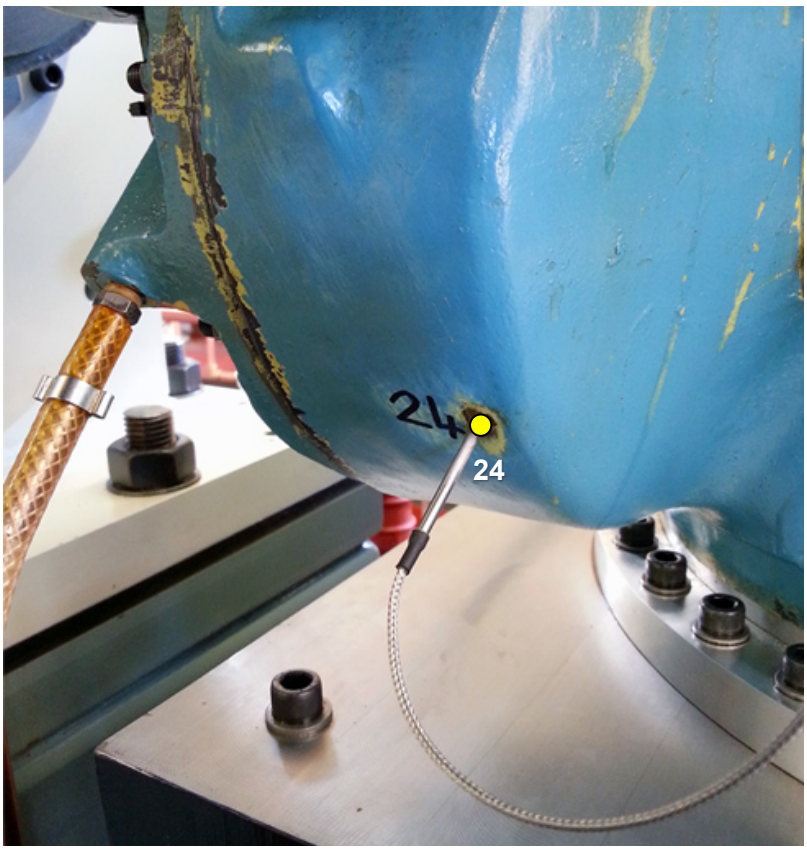

Figure B.72 Thermocouple Location #24 (Source: Author)

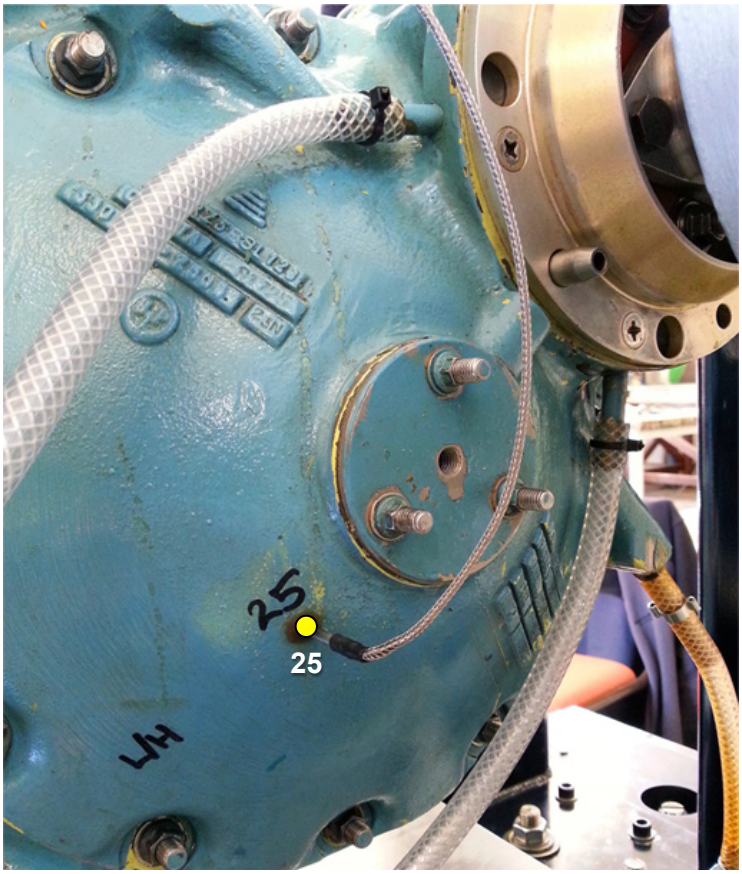

Figure B.73 Thermocouple Location #25 (Source: Author)

Figure B.74 Thermocouple Location #26 (Source: Author)

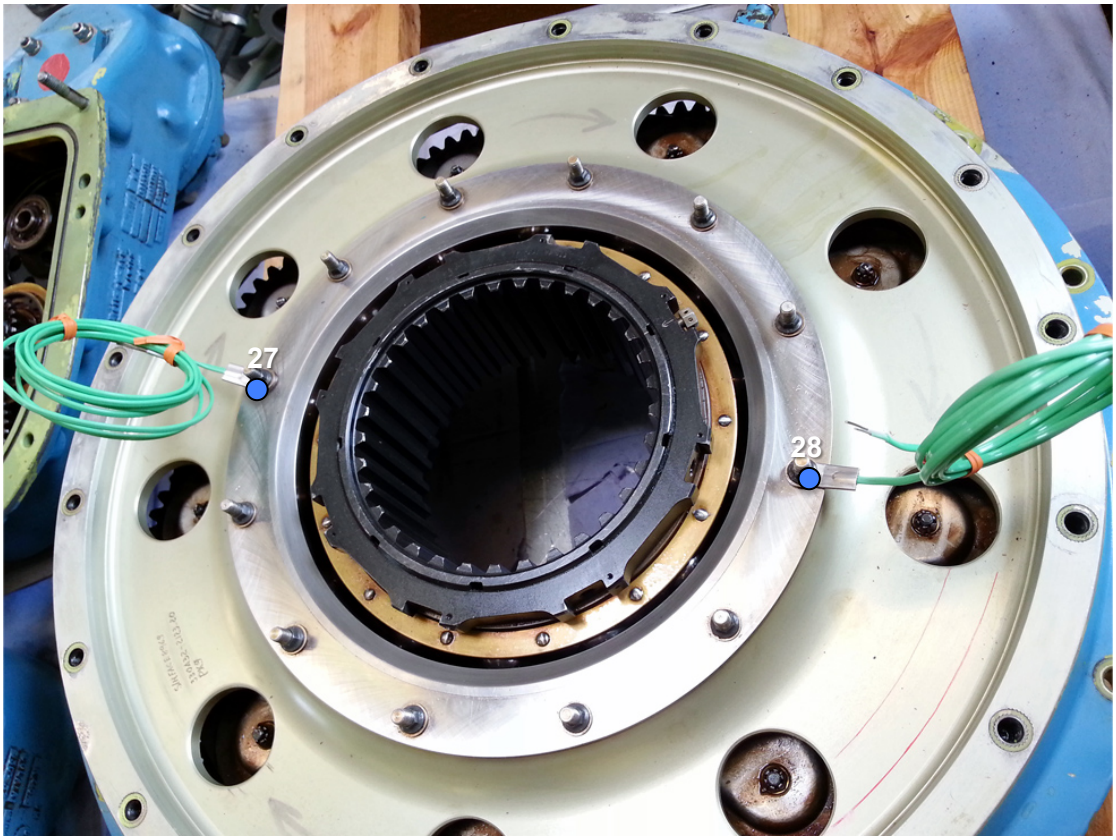

Figure B.75 Thermocouple Locations #27 and 28 (Source: Author)

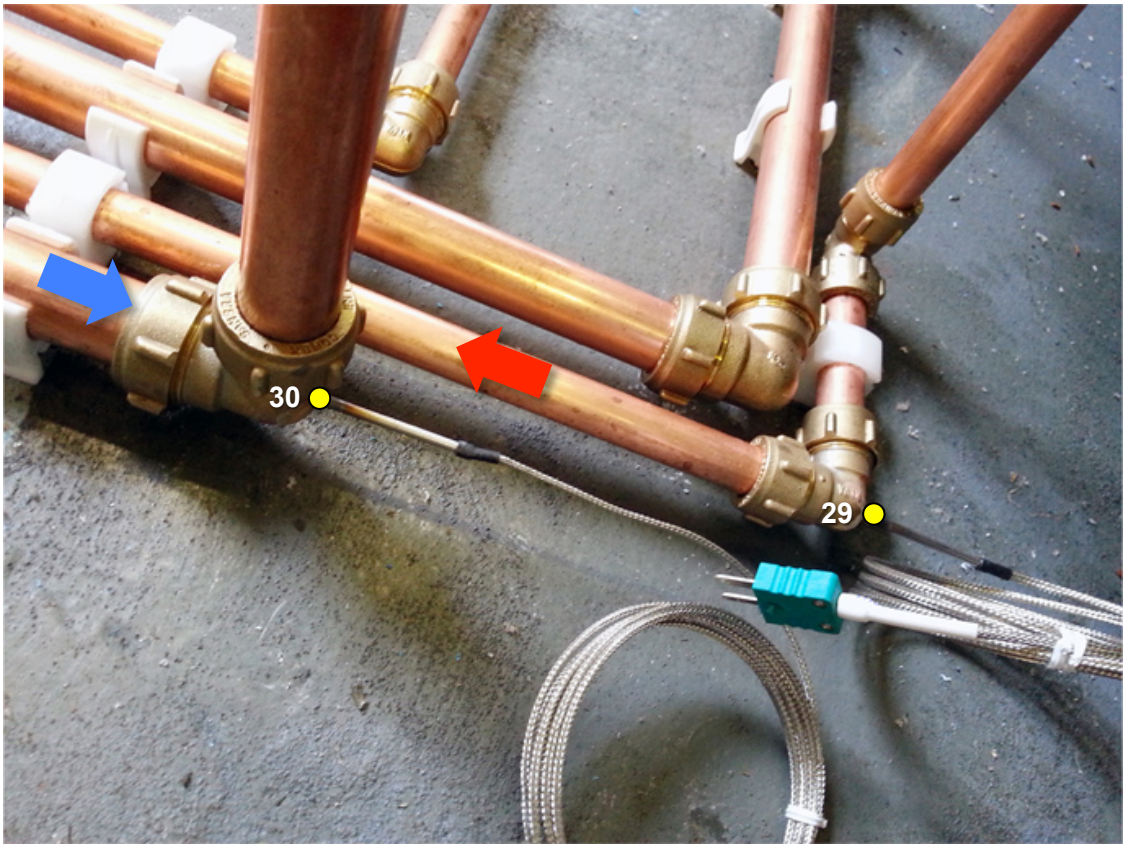

Figure B.76 Thermocouple Locations #29 and 30 (Source: Author)

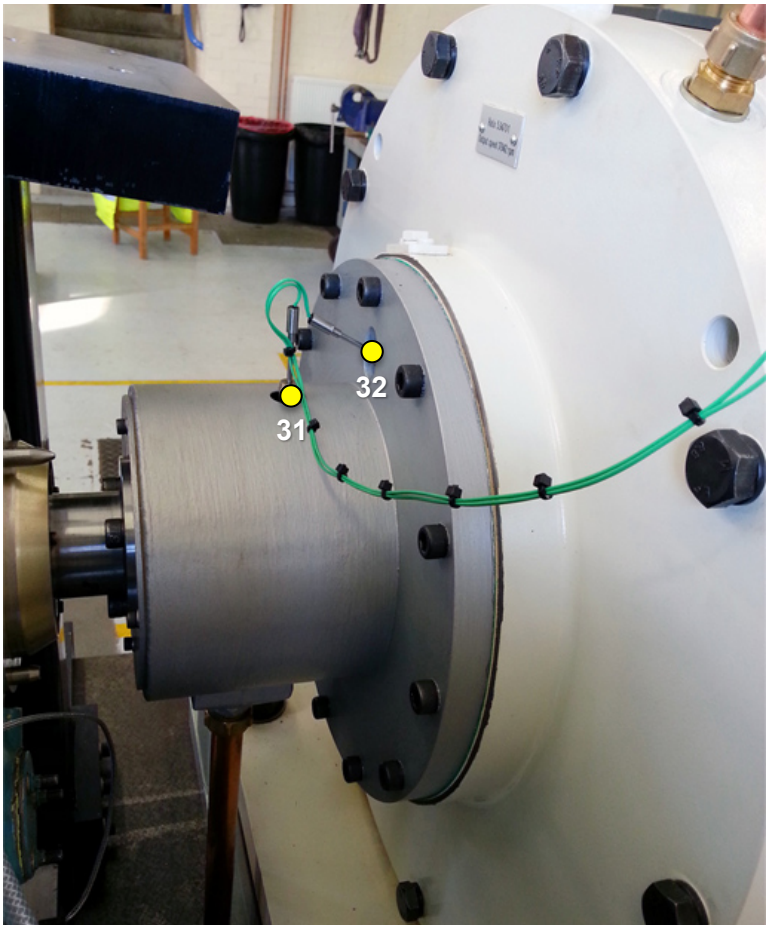

Figure 3.77 Thermocouple Locations #31 and 32 (Source: Author)

Thermocouple #	Description	Thermocouple #	Description
1	Fwd Brg LH Aft Red	17	Sump Plate
2	Fwd Brg LH Aft Red	18	Oil Feed Supply
3	Fwd Brg Cen Aft Red	19	Brg Bevel Plate
4	Fwd Brg Cen Aft Red	20	Brg Bevel Plate
5	Fwd Brg RH Aft Red	21	Epi Case 2nd
6	Fwd Brg RH Aft Red	22	Epi Case Ring
7	Brg Bevel	23	Epi Case 1st
8	Brg Bevel	24	Aft Brg LH Fwd Red
9	Aft Brg LH Fwd Red	25	Fwd Brg LH Fwd Red
10	Aft Brg LH Fwd Red	26	Fwd Brg LH Input
11	Aft Brg RH Aft Red	27	Output Brg
12	Aft Brg Cen Aft Red	28	Output Brg
13	Aft Brg LH Aft Red	29	Oil Out Speed GB
14	Aft Brg LH Input	30	Oil In Speed GB
15	Aft Brg LH Input	31	Brg 2 Speed GB
16	Oil Out Sump	32	Brg 1 Speed GB

Table B.13 Label Names of Thermocouples on MGB Test Rig (Source: Author)

B.6.2 Pressure, Flow and Vibration Measurements

Pressure measurements on the MGB test rig are achieved with the use of dial pressure gauges and pressure transducers. Dial gauges are installed on the lubrication systems of the speed-increasing gearbox and the MGB, the thioether misting system as well as the dynamometer air pressure system (Figures B.78 to B.80). They allow easy feedback on the flow parameters of the test rig, which are essential to the safe and proper conduct of the lubrication experiments.

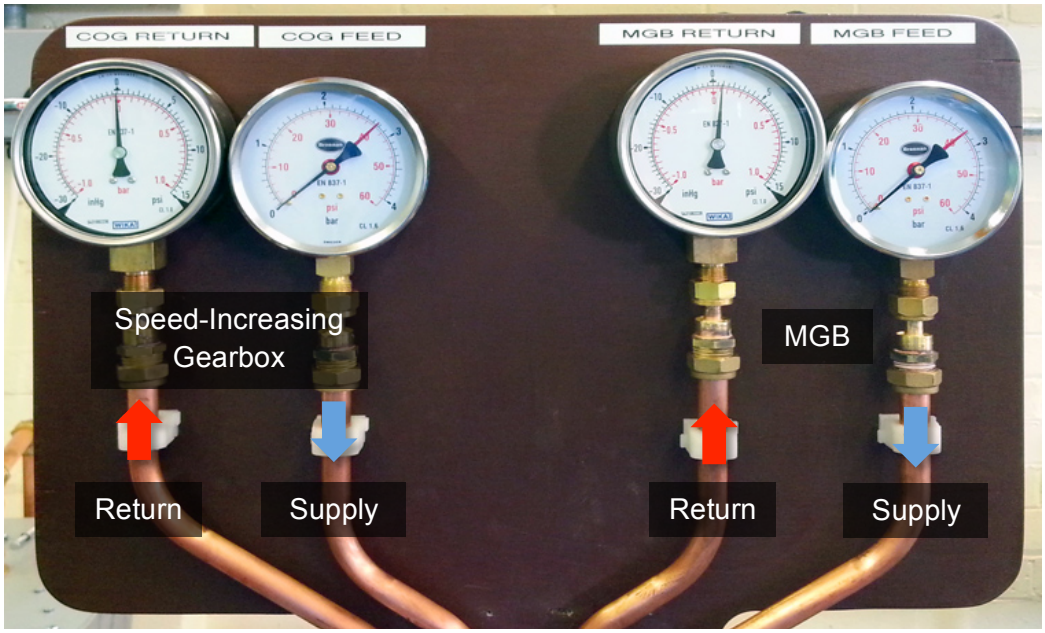

Figure B.78 Dial Pressure Gauges for Speed-Increasing Gearbox and MGB (Source: Author)

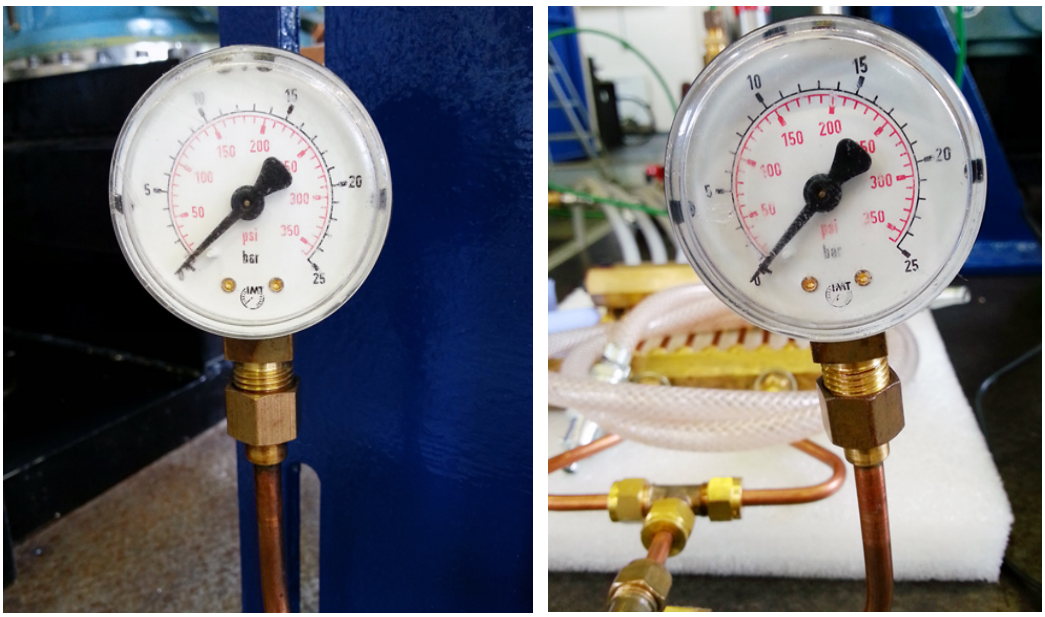

Figure B.79 Dial Pressure Gauges for Thioether Misting System: Piston Chamber (Left) and Air Supply Pressure (Right) (Source: Author)

Figure B.80 Dial Pressure Gauges for Dynamometer Air Pressure System: Accumulator (Left) and Supply Line (Right) (Source: Author)

Supplementing the dial pressure gauges are two pressure transducers (Figure B.81) for the dynamometer air pressure line and the thioether piston chamber. They provide remote monitoring and data logging of the MGB test rig critical pressure parameters in the control room.

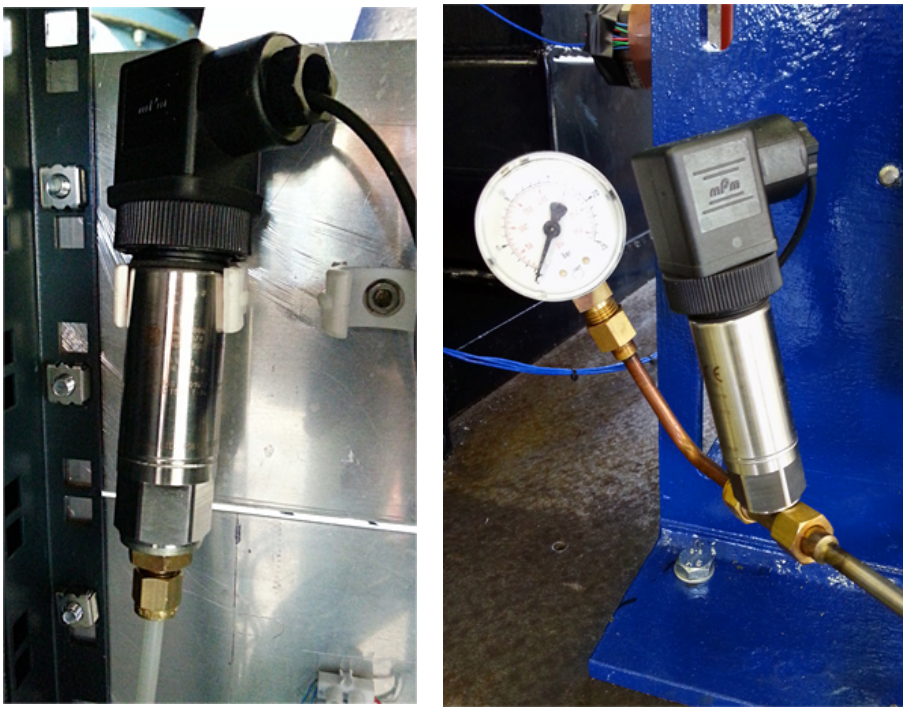

Figure B.81 Pressure Transducer for Dynamometer Air Pressure Line (Left) and Thioether Piston Chamber (Right) (Source: Author)

Flow measurement is made for the dynamometer cooling system using a digital flow meter (Figure B.82). This ensures that adequate water flow is present to remove the heat generated by the frictional torque.

Figure B.82 Digital Flow Meter for Dynamometer Water Cooling System
(Source: Author)

Vibrational measurements are made with the use of single-axis accelerometers at three identified locations on the MGB and one location on the speed-increasing gearbox (Figures B.83 to B.85). The three locations on the MGB include the Fwd Reduction Gear Module, the Aft Reduction Gear Module and the Epicyclic Reduction Gear Module. These MGB vibration signatures would be analysed according to ISO 8579-2:1993 [1], and they allow a comparison of the MGB performance to be made under varying load and lubricating conditions. The vibration signature of the speed-increasing gearbox is monitored to ensure its safe operation throughout the lubrication tests.

[1] This ISO lists the criteria for assessing mechanical vibrations (shaft or housing) of four different ratings of gearboxes.

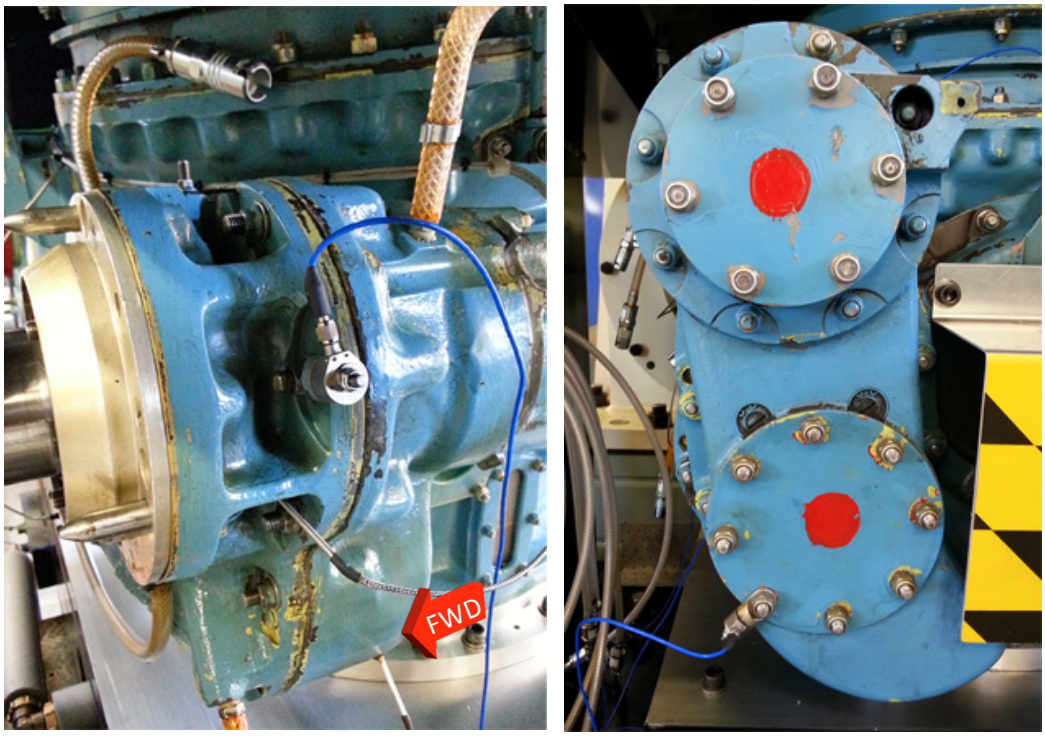

Figure B.83 MGB Vibration Measurement: Fwd Reduction Gear Module (Left) and Aft Reduction Module (Right) (Source: Author)

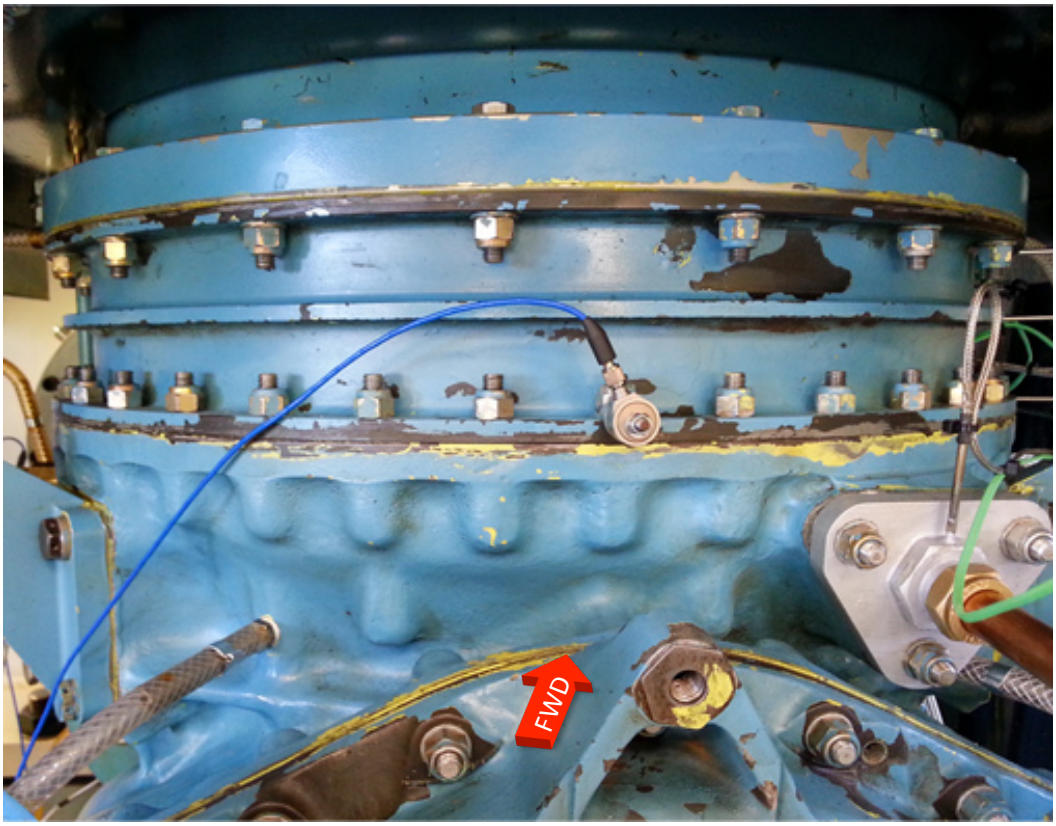

Figure B.84 MGB Vibration Measurement: Epicyclic Reduction Module (Source: Author)

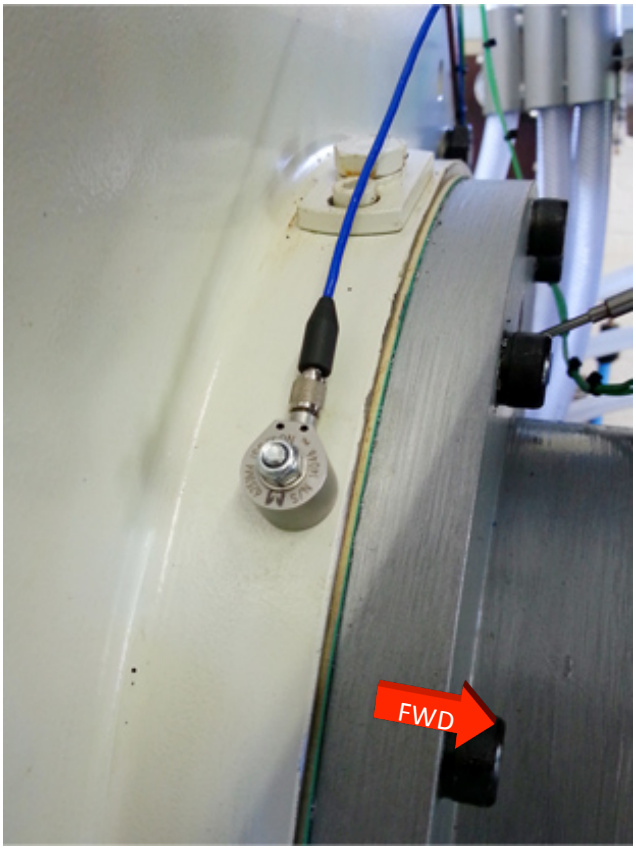

Figure B.85 Speed-Increasing Gearbox Vibration Measurement (Source: Author)

B.6.3 Motor Drive Power Measurement

The required air pressure to be delivered to the dynamometer to generate a frictional torque equivalent to an input power of 293 kW has been determined in Section B.2.2. However, to ensure an accurate delivery of available power by the tandem electric drive system, it is necessary to measure the power drawn by the DC electric motors. From Table B.2, each of the electric motor is capable of delivering up 375 kW and at a maximum continuous torque of 1193 Nm at a maximum rotational speed of 3000 RPM. At this speed and torque setting, the voltage and current drawn would be 605 V and 663 A respectively, which equates to a power drawn of 401 kW (Equation B.13) and a power efficiency of 93.5% (Equation B.14). Since for DC electric drive motors in general, the current drawn through the armature windings is proportional to the torque setting (while voltage is fixed for a specific speed), it is possible to measure the power available to the MGB input drive based on power drawn by each of the electric motor assuming a constant power efficiency for the motor and 97% mechanical efficiency for the speed-increasing gearbox.

$$Power\ Drawn\ =\ V * I\ =\ 605 * 663\ =\ 401.12\ kW \qquad \text{Equation B.13}$$

$$Efficiency\ =\ \frac{Power\ Available}{Power\ Drawn}\ =\ \frac{375}{401.12}\ =\ 93.48\% \qquad \text{Equation B.14}$$

At 293 kW power to the MGB input drive, the power available by the tandem electric drive system would be 302 kW (Equation 3.15). Assuming constant power efficiency, the power drawn by the electric drive system would be 323 kW and with a current of 534 A to the armature windings (Equations 3.16 and 3.17). It is important to note that since each of the electric motor is capable of 375 kW, only one motor would be used for driving the MGB at the required input power.

$$Power\ Available\ =\ \frac{MGB\ Input\ Power}{Mechanical\ Efficiency}\ =\ \frac{293}{0.97}\ =\ 302.06\ kW \qquad \text{Equation B.15}$$

$$Power\ Drawn\ =\ \frac{Power\ Available}{Efficiency}\ =\ \frac{302.06}{0.9348}\ =\ 323.13\ kW \qquad \text{Equation B.16}$$

$$I\ =\ \frac{Power\ Drawn}{V}\ =\ \frac{323.13x10^3}{605}\ =\ 534.10\ A \qquad \text{Equation B.17}$$

Alternatively, at 293 kW power to the MGB input drive, the driving torque at 17,842 rpm would be 156.82 Nm (Equation B.18). Upstream of the speed-increasing gearbox, the driving torque by the electric motor would be 961 Nm (Equation B.19). Since current is proportional to torque setting, the current required in the armature windings of the electric motor would be 534 A (Equation B.20), which is similar to the value calculated using power availability.

$$Torque = Power * \frac{60}{RPM * 2\pi} = 293x10^3 * \frac{60}{17{,}842 * 2\pi} = 156.82\ Nm$$ Equation B.18

$$Torque = Power * \frac{60}{RPM * 2\pi} = 302.06x10^3 * \frac{60}{3000 * 2\pi} = 961.48\ Nm$$ Equation B.19

$$Since\ I \propto Torque,$$
$$I_2 = I_1 * \frac{Torque_2}{Torque_1} = 663 * \frac{(961.48)}{1193} = 534.33\ A$$ Equation B.20

The measurement of the current drawn by each of the DC electric motor thus allows an accurate determination of the power available to the MGB input drive. This is performed with the use of an AC/DC current clamp that operates on the principle of Hall Effect (Figure B.86). A primary current placed in the core of a hall element would result in a hall voltage rise due to the magnetic induction generated at the core. The output voltage from the hall element is proportional to the primary current and allows the indirect measurement of the primary current. Clamps meters have the advantages convenience and safety as they permit current measurements on a live conductor without circuit interruption.

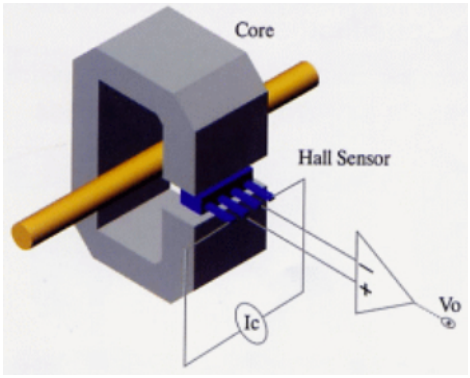

Figure B.86 Hall Effect Schematic (Source: www.hallsensors.de)

The selected AC/DC current clamp for the MGB test rig is the Fluke i410. For added safety, it is paired with the Fluke ac3002 that works with the Fluke Connect™ software to enable wireless monitoring and recording of the current drawn by each of the electric motor. Each of the DC electric motor is configured with two current feed cables due to the high armature current drawn during operation. This implies that the total current drawn for each motor drive would be twice the measured current by the AC/DC current clamp installed on a cable assembly (Figure B.87). At the desired input power of 293 kW the required current would therefore be 267A. The wireless monitoring and recording of the current in each cable assembly is achieved with a laptop (Figure B.88) located in the control room.

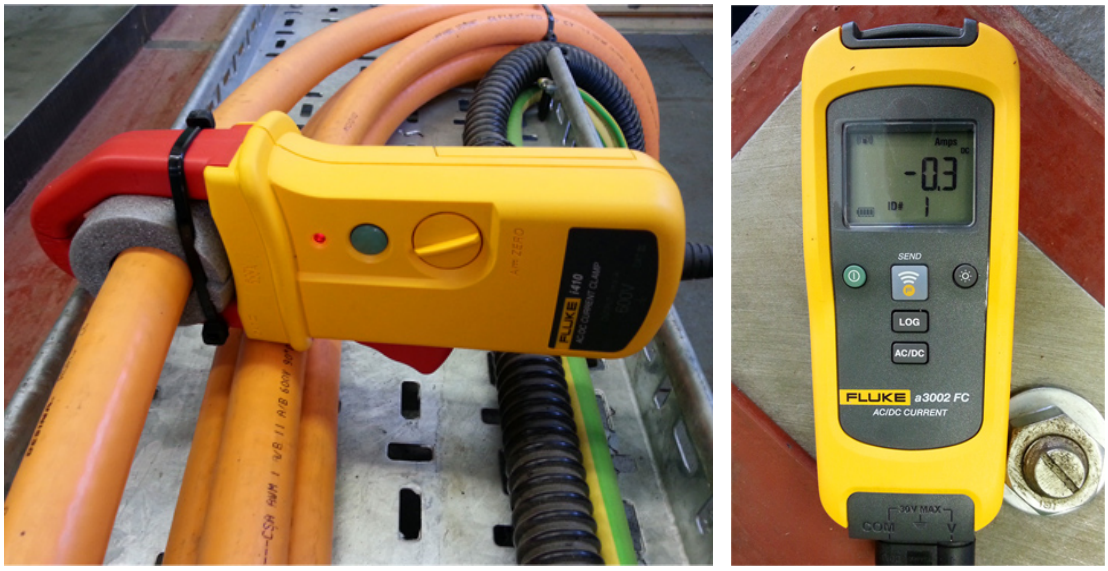

Figure B.87 DC Electric Motor Current Measurement: Fluke i4010 Clamp (Left) and Fluke a3002 Current Module (Right) (Source: Author)

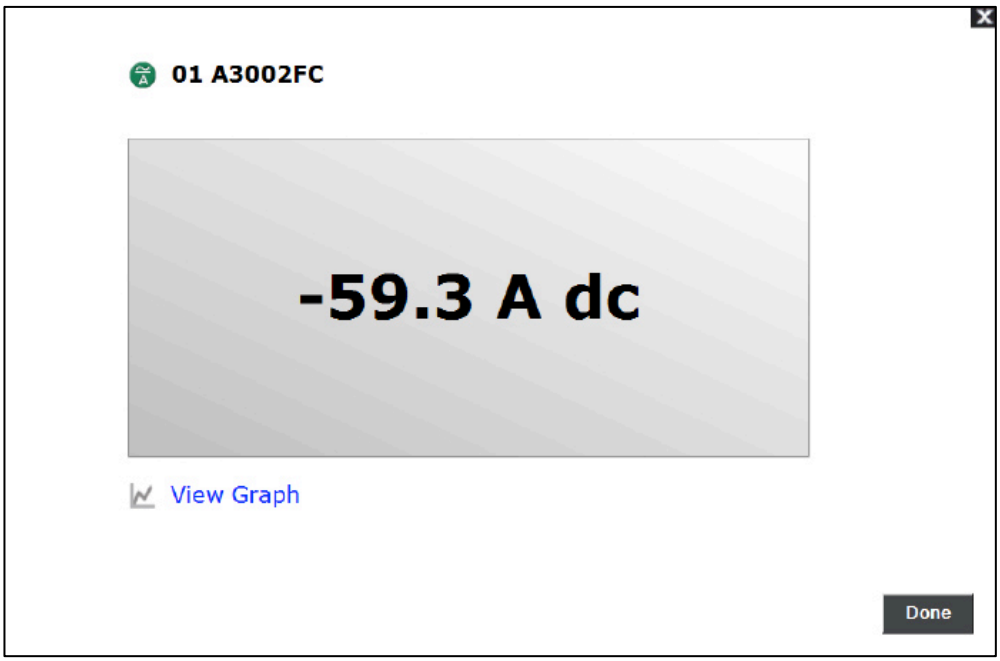

Figure B.88 DC Electric Motor Current Measurement: Current Reading via Laptop (Source: Author)

B.6.4 Motor Drive Speed Measurement

The speed of the tandem motor drive system is another parameter that is critical to the success of MGB lubrication experiments. For a given motor speed, the voltage across the armature windings can be inferred and the available power by the motor computed. The available power of the motor can also be computed using the motor speed and a known torque value that is indicated by the current drawn. The motor speed also determines the driven speed of the dynamometer shaft, which allows the calculation of the power absorbed by the dynamometer for a known torque value indicated by the brake air pressure setting. The power and torque values experienced within the MGB test rig therefore hinges on the accuracy of the motor drive speed.

To measure the speed of the motor, a tachometer is fixed at the drive shaft that connects the motor drive system to the speed-increasing gearbox (Figure B.89). Measurements by the tachometer are feed to the control room and displayed together with the test rig temperature and pressure readings.

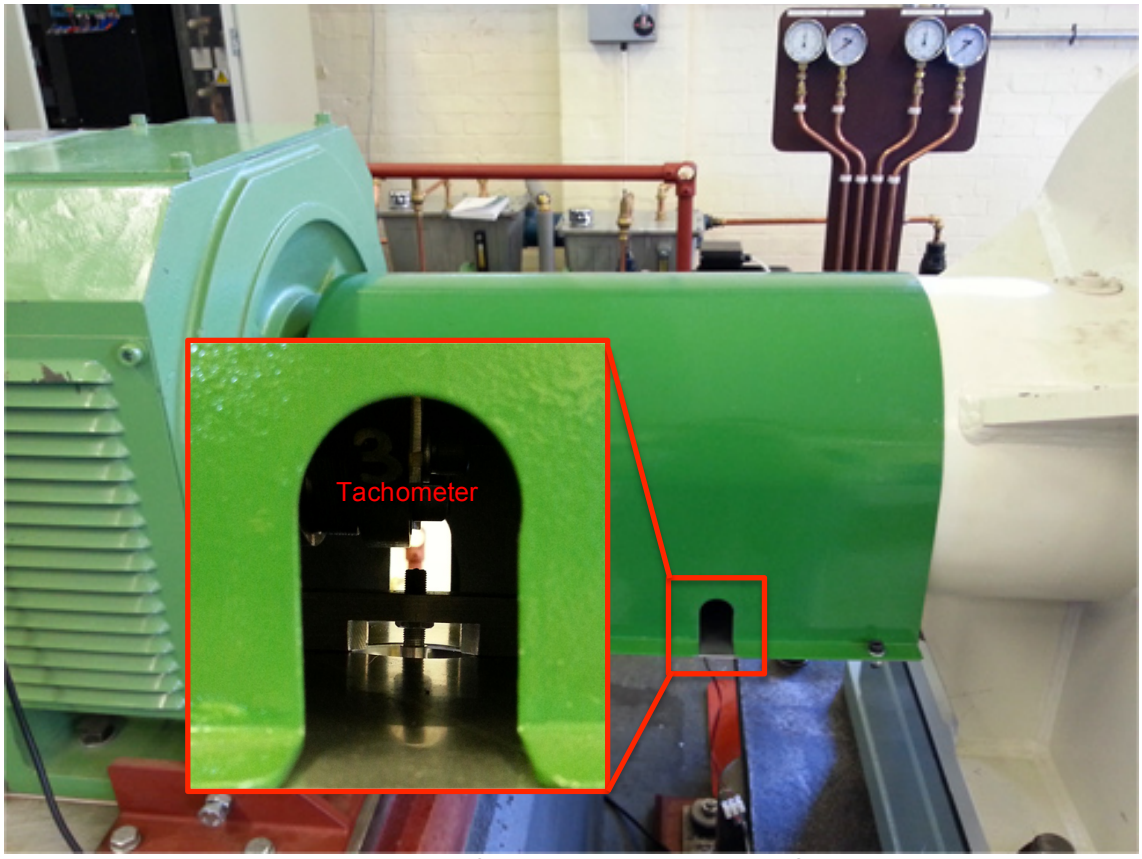

Figure B.89 Tachometer for Electric Motor Drive (Source: Author)

B.6.5 Data Acquisition and Information Display

Temperature measurements from the 32 thermocouples of the MGB test rig are transmitted as voltage signals to a National Instruments (NI) Data Acquisition (DAQ) device for data logging. To facilitate the ease of MGB removal from the test rig and future teardowns, each instrumentation wiring incorporates a connector pair that allows for quick disconnect of the thermocouple leads from the extension wiring to the DAQ. The instrumentation wiring is also labelled for easy identification and bundled together for an organised routing (Figure B.90).

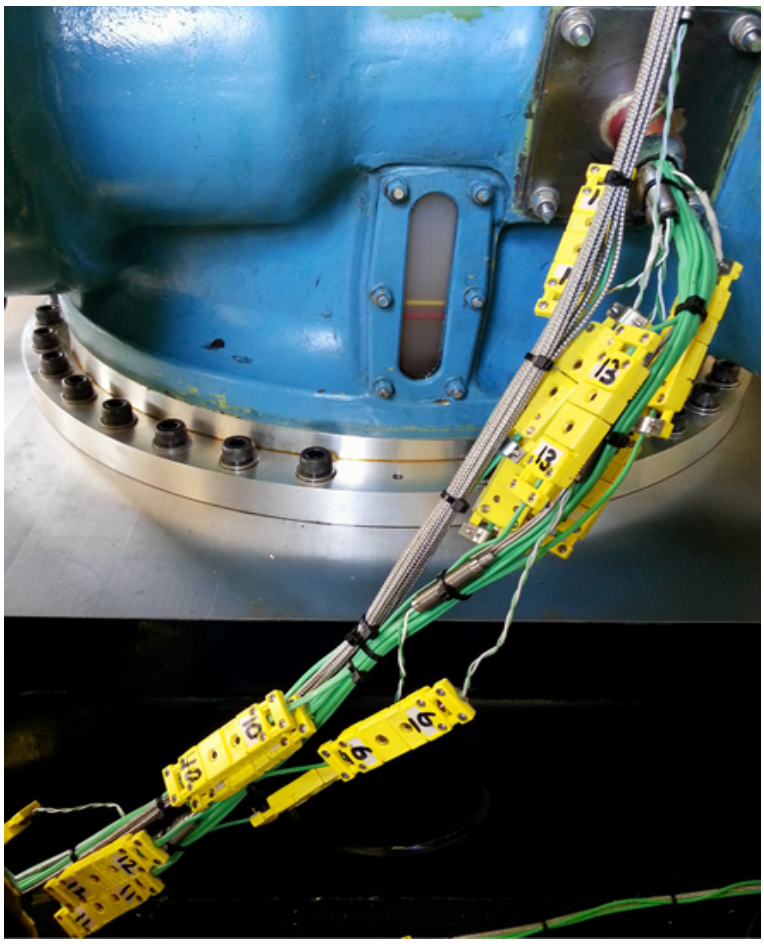

Figure B.90 Instrumentation Wiring for Thermocouples (Source: Author)

An USB-enabled NI compact DAQ (P/N: NI cDAQ-9174) (Figure B.91), complete with three 16-Channel Thermocouple Input Modules (P/N: NI 9213) and a 4-Channal Analogue Input Module (P/N: NI 9215), works in conjunction with a laptop for the data logging of the temperature parameters of the MGB test rig. A total of 32 digital data channels are used to support the thermocouples installed within the MGB test rig, while three analogue data channels are used to support pressure and speed measurements. The data capture rate for each channel is configured as 5 Hz.

Figure B.91 NI cDAQ-9174 for Temperature Data Logging (Source: Author)

Information from the DAQ to the end user involves the use of the NI LabVIEW software that displays measured values through a configurable Graphical User Interface (GUI). This allows critical decisions to be made based on the temperature profiles of the MGB gears and bearings as well as temperature parameters of the test rig. Information is displayed on a wide screen TV in the control room and includes temperature, motor speed and dynamometer air pressure readings (Figure B.92).

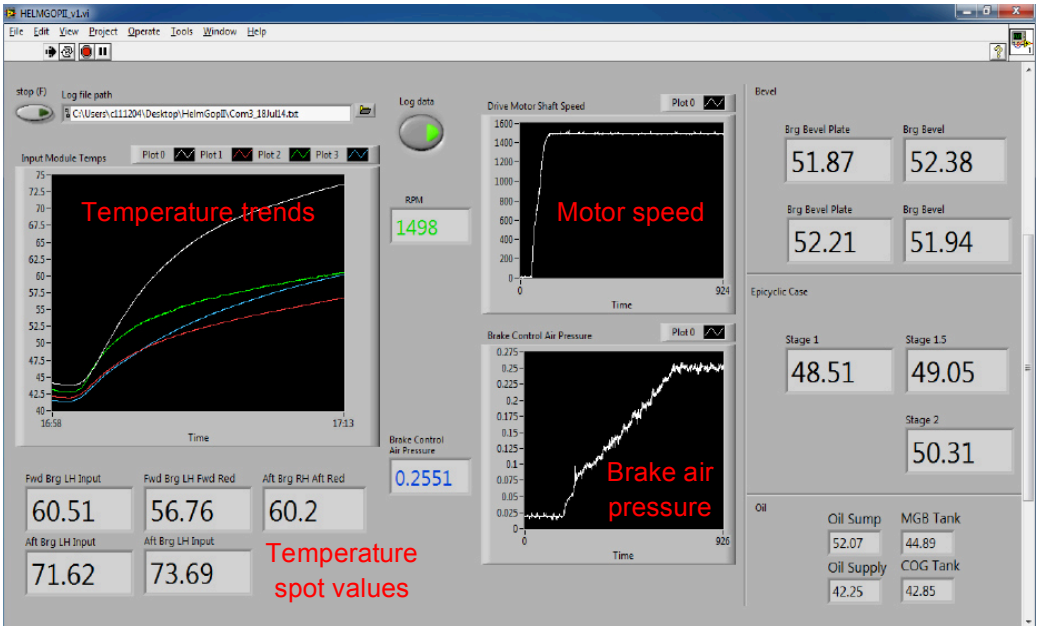

Figure B.92 Temperature Information Display for MGB Test Rig (Source: Author)

Vibration data capturing is achieved using an USB-enabled NI C-Series Single Module Carrier (P/N: NI USB-9162) and the 4-Channel C-Series dynamic signal acquisition module (P/N: NI-9234).

EASA
European Aviation Safety Agency

European Aviation Safety Agency

Postal address
Postfach 10 12 53
50452 Cologne
Germany

Visiting address
Ottoplatz 1
50679 Cologne
Germany

Tel. +49 221 89990 - 000
Fax +49 221 89990 - 999
Mail info@easa.europa.eu
Web www.easa.europa.eu